A paleoenvironmental reconstruction of the Elands Bay area using carbon and nitrogen isotopes in tortoise bone.

By Navashni Naidoo

Supervised by Professor Judith Sealy

Dissertation submitted in fulfilment of the requirements for the degree of Master of Science (MSc) in Archaeology

In the Department of Archaeology

University of Cape Town

July 2017

Plagiarism Declaration

I have used the Harvard convention for citation and referencing. Each contribution from, and quotation in, this thesis from the work(s) of other people has been attributed, and has been cited and referenced. This thesis is my own work.

Abstract

This study explores the utility of stable light isotopes in *Chersina angulata* (angulate or bowsprit tortoise) bone collagen as a paleoenvironmental proxy, to augment the limited range of proxies preserved in Southern Africa. $\delta^{13}C$ and $\delta^{15}N$ were measured in 76 archaeological tortoises from Elands Bay Cave and nearby Tortoise Cave. The samples range in age from the late Holocene to the terminal Pleistocene. $\delta^{15}N$ values are not strongly correlated with $\delta^{13}C$, indicating different drivers of variation in the two isotopes. $\delta^{13}C$ and $\delta^{15}N$ values are lower between 154-487 cal. BP, which spans the Little Ice Age, compared with 744-1 042 cal. BP, which is the period of the Medieval Climate Anomaly (MCA). This implies that conditions were cool and wet during the LIA, and hot and dry during the early MCA. $\delta^{13}C$ and $\delta^{15}N$ values were higher during the early stages of the MCA (744-1 042 cal. BP), indicating drier conditions than in the late MCA (547-669 cal. BP). In the period prior to the MCA (1180-1357 cal. BP), lower $\delta^{13}C$ and $\delta^{15}N$ values indicate cooler, moister conditions. Higher $\delta^{13}C$ values also indicate a temperature increase at the beginning of the Middle Holocene (4005-5 720 cal. BP). These findings are generally consistent with existing paleoenvironmental records from the Cederberg and Elands Bay region. The paleoenvironmental record generated from the tortoise carapace and plastron bone provides the first evidence from the terrestrial archaeological record for the LIA and MCA at Elands Bay. Hence, the tortoise record is able to provide a more detailed climate record than the charcoal and faunal record at EBC. This study shows that the analysis of stable isotopes in *C. angulata* from archaeological sites is a viable option for paleoenvironmental reconstruction.

Acknowledgments

There are many people to whom I owe a great debt of thanks. First and foremost, Prof. Judith Sealy, whose comments and guidance have been invaluable. Thanks must also to go to Dr Ashley Coutu, Mr. John Lanham and especially Mr. Ian Newton for all their assistance in the lab. I thank Dr John Parkington for his advice and comments on this project. I am grateful to Mr. Charles Malherbe, Mr. Jan Smit and Mr. F.C Basson from the Western Cape Government and Department of Agriculture for their willingness to answer questions on agricultural practice. I also wish to thank Dr. Wendy Black and Mrs Wilhelmina Seconna from Iziko Museums for accommodating me during my sample collections. Thanks, must also go to the Iziko Museums for allowing me to work on their collections. Lastly, I wish to express gratitude to the South African Research Chairs Initiative (SARChI) of the Department of Science and Technology (DST) and National Research Foundation (NRF) of South Africa, for providing funding for this thesis.

Contents

List of Figures

List of Tables

Chapter One

1. Introduction:

1.1 Preface

The influence of climate on human behaviour has been a much-debated topic in archaeology since the 1960s (Johnson 2011). Many archaeologists believe that changes in physical environments can accelerate, decelerate or may simply coincide with social change (Dinacauze 2000). That is, humans make behavioural choices suited to their environmental context. As such, paleoenvironmental reconstructions are an integral step in reconstructing past human behaviour.

Unfortunately, many aspects of paleoenvironments are a challenge to reconstruct in southern Africa. This is in part due to the climate of the region. Aridity and strong rainfall seasonality have hindered the preservation of many traditional proxies across much of the country (Chase & Meadows 2007). The dearth of paleoclimatic information has forced archaeologists to generalize information from one or two sites to entire regions. This is problematic for two reasons: first, it ignores the possibility of microclimates and second, it can lump together areas that do not belong in the same ecozone.

The solution to this problem is either to develop new proxy records that are suited for the southern African ecosystem or to seek new applications for classic methods. This dissertation does the latter, using stable carbon and nitrogen isotopic analysis of collagen from tortoise carapace found at archaeological sites to reconstruct past environments. Tortoise remains are abundant within the archaeological record in the Western Cape compared with mammal remains (e.g. Klein & Cruz-Uribe 1987). The study of tortoises will therefore enable isotopic

analysis of a larger number of individuals than is possible with other animals, and in turn allow more meaningful statistical testing.

Tortoise bones (including fragments of carapace and plastron) make up a large component of the faunal assemblages in many sites in the drier parts of the Western and Northern Cape (Klein & Cruz-Uribe 1983, 1987; Steele & Klein 2013). The majority of previous studies on tortoises have used changes in humeral and femoral size through the record as a proxy for predation intensity, and thus human population size (Klein & Cruz-Uribe 1983; Henshilwood *et al.* 2001; Steele & Klein 2013). Studies have also been carried out to determine the nutritional value of tortoise compared to ungulates in human diet (Thompson & Henshilwood 2014a) as well as taphonomic analysis as to how tortoise remains enter the fossil record (Thompson & Henshilwood 2014b). Thus, despite their abundance in the record, tortoises remain relatively under-analysed in terms of providing human behavioural or environmental contextual information.

Therefore, this study seeks to use stable carbon and nitrogen isotopes found within the bone collagen of tortoise carapace to investigate past environments. Tortoise bones were chosen for this analysis as the sheer numbers found in many assemblages means that destructive analysis will not substantially impact on the value of the fossil assemblage for future research.

Carbon isotope ratios of animal tissues reflect the diet of the animals, and as tortoises are predominantly browsers one would expect their collagen to give a C_3 signal (Bocherens & Drucker 2003). A strong C_3 signal is expected from the tortoises in this study as both sites are in the winter rainfall zone in which C_4 grasses account for 5% or less of the vegetation (Vogel *et al*. 1978).

Since the carbon isotope ratios of plants that make use of the Calvin-Benson (C_3) photosynthetic pathway are sensitive to moisture and temperature, one expects fluctuations in temperature and/or moisture to lead to changes in the $\delta^{13}C$ values of the tortoises (Cerling *et al.* 1997). Nitrogen isotopes from tortoise bone will reflect aridity within the region of study, where samples high in ^{15}N will be from more arid time periods than those low in ^{15}N (Murphy & Bowman 2006). There has, however, been relatively little published work on stable isotope values in reptile bones. Thus, this dissertation aims to evaluate how useful the $\delta^{13}C$ and $\delta^{15}N$ values of tortoises are as records of paleoenvironmental information.

Tortoise bone from Elands Bay Cave and Tortoise Cave will be used for this study. These sites were chosen as they boast large amount of tortoise carapace and have been well dated. They are also close together (5 km apart). Anthropological studies of San hunter-gatherers show that people typically gather resources in a 10km radius from their base (Lee 1968). This is important as it means tortoises found at Elands Bay Cave and Tortoise Cave are subsets of the same population. Restricting the study to one area also minimizes the chances of palaeoenvironmental signals being complicated or obscured by small-scale regional variations. One of the most important reasons for using these sites is that the Elands Bay region has a well-documented paleolandscape defined by traditional proxy sources (Klein and Cruz-Uribe 1987; Avery 1990; Cohen *et al*. 1992; Meadows *et al*. 1996, Baxter and Meadows 1999; Meadows and Baxter 1999; Cowling 1999; Meadows and Baxter 2001; Stager *et al*. 2012; Stowe & Sealy 2016; Cartwright *et al*. 2016; Klein and Cruz-Uribe 2016). Finally, a pilot study for this project was performed in this locale by Mr Joshua Weeber (Weeber 2013).

1.2 Aim

This project investigates the utility of $\delta^{13}C$ and $\delta^{15}N$ in collagen from the carapace and plastron of the angulate tortoise (*Chersina angulata*) as proxies for paleoenvironmental reconstruction.

1.3 Research objectives

- First, this dissertation will explore the value of $\delta^{13}C$ and $\delta^{15}N$ in the carapace and plastron as proxies for paleoenvironmental reconstructions.
- Second, this dissertation seeks to contribute to the existing Holocene climate record in the Elands Bay region.

1.4 Thesis outline

The remainder of this thesis is divided into six chapters. Chapter Two introduces proxy records, and provides a review of the use of stable isotopes of carbon and nitrogen as environmental indicators, as well as some background information on angulate tortoises.

Chapter Three provides a critical analysis and review of the literature on the region surrounding Elands Bay Cave and Tortoise Cave, focussing on climate. It summarises relevant aspects of the archaeological sequences at Elands Bay Cave and Tortoise Cave. Chapter Three also provides a summary of previous paleoenvironmental research from the Elands Bay, Langebaan and Cederberg region.

Chapter Four focuses on the methods used in choice of samples, extraction of collagen and measurement of the isotope ratios on the mass spectrometer.

Chapter Five provides the results of this project and statistical analysis.

Chapter Six is a review of the results and their climatic significance, highlighting noteworthy events identified within the record. In addition, it aims to contextualise the results in terms of the literature reviewed in Chapter Three.

Chapter Seven provides an overview of the study and introduces new research direction.

Chapter Two

2. Paleoenvironmental proxies

2.1 Introduction to proxies

In the absence of direct observations and measurements of the past, paleoenvironmental reconstructions rely on the use of proxy records. Proxy data can come from biological, geophysical and/or written records (Luckman 1997). Different proxies provide different environmental information at varying timescales (Jones & Mann 2004). The various records can complement or contradict one another. Thus, it is essential that multiple proxies be used in conjunction with one another to recreate an accurate image of past environments (Jones & Mann 2004). Common natural archives used for proxy records include stalagmites, pollen, faunal remains and tree ring records. However, these records are sparse in many areas of Africa due to poor preservation. A lack of, or too much rainfall, can destroy certain proxies or cause temporal absences in others. For instance, in xeric conditions speleothems are subject to temporal lapses as no carbonate is precipitated (Talma & Vogel 1992), and pollen does not preserve well in humid and moist environments (Meadows *et al*. 2010). Besides preservation factors, certain proxies that have been successfully used in the northern hemisphere are not well established on the African continent. Figure 1.1 demonstrates the gaps in paleoenvironmental records in Africa versus better-studied areas of the northern hemisphere.

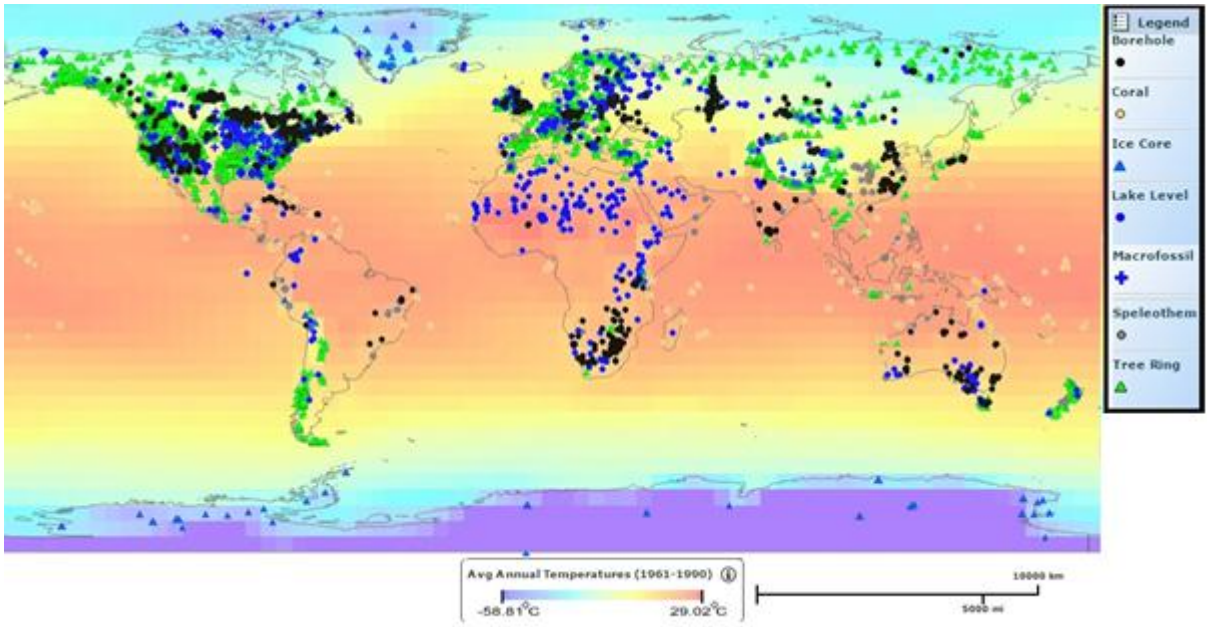

Fig. 1.1: *Map showing different paleoenvironmental archives studied across the globe.* (NOAA 2016)

Thus, the nature of Africa's climate system has led to the paleoenvironmental record for this continent lagging far behind that of Europe and North America (Chase 2007). The spatial lapses in climatic information have caused a blanket effect on paleoreconstructions in much of Africa in which information from one site is used over large areas, ignoring the possibility that there may be regional differences (Meadows & Baxter 1999).

To combat this, researchers working on the African continent need to develop proxy records that are suited to and/or developed for Africa. A large amount of work has gone into this research, with new archives such as hyrax middens and baobab records being explored (Chase *et al.* 2012, Woodborne *et al.* 2015). This dissertation explores the use of stable light isotopes from tortoise carapace as a paleoenvironmental record.

Stable light isotopes are a well-established technique in paleoenvironmental analysis, being used for both geological and biological proxies (e.g. Talma & Vogel 1992, Cerling *et al.* 1998, Bar-Matthews *et al*. 2010). Archaeologists have most commonly used ungulate remains

when performing isotopic analysis on paleo- or archaeofauna (e.g. Cerling *et al*. 2003, Lee-Thorp & Sponheimer 2003). Analysis of carbon, oxygen and nitrogen isotopes in ungulate teeth and bones from archaeological and fossil sites has produced high-quality data on vegetation, rainfall regime and aridity, over timescales varying from millions of years to mere seasons (Luyt *et al*. 2000, Balasse *et al*. 2003, Stowe & Sealy 2016). However, this approach is constrained by the availability of suitable material for analysis. It is rare to be able to sample enough individuals of any one taxon for meaningful statistical analysis i.*e.* twelve or more individuals. Archaeological and fossil bones are often fragmented and teeth may be worn, making it difficult to identify them to species with confidence. This is a problem in isotope studies as isotope signals are reflective of animal diet and behaviour.

Unlike ungulate bones, tortoise carapace is easy to identify and makes up a high percentage of the faunal remains at archaeological sites in the dry western parts of South Africa (Klein & Cruz-Uribe 1989). Tortoises also have much smaller home ranges than ungulates, thus the isotopic signal represents a more localized environment. This is a crucial factor as vegetation communities and rainfall can change dramatically over relatively short distances. Tortoises are also very resilient to environmental changes (e.g. Nagy & Medica 1986), meaning that a species has the potential to persist in an area for extensive periods of time. These factors will allow for the collection of larger datasets and more meaningful statistical testing of patterns through time, allowing for more accurate conclusions.

2.2 Stable light isotopes as a proxy

An element is defined by the number of protons it has. For example, carbon has six protons; if it were to gain another proton, it would become nitrogen. Isotopes are defined by the number of neutrons the atom possesses. For instance, carbon with six neutrons is known as ^{12}C and carbon with seven neutrons is known as ^{13}C, this number represents the atomic weight and is calculated by adding the neutrons and protons together. Stable light isotopes are

non-radioactive isotopes of light elements, usually considered to be those with atomic mass less than 40 (Sulzman 2007). There are over three hundred known stable isotopes (Sulzman 2007); however, this study focuses on the two most abundant isotopes of carbon ($^{13}C/^{12}C$) and nitrogen ($^{15}N/^{14}N$).

The ratios of stable light isotopes are effective natural tracers of biogeochemical processes. In elements with atomic mass less than 40, the mass difference between the isotope pair is sufficiently great that the lighter isotopes are energetically favoured during processes such as evaporation or diffusion (Hoefs 2009). In many enzymatically mediated biological reactions, there is also enzymatic selection, usually for the lighter isotope. A shift in the proportion of the heavy to the light isotope is known as "fractionation". Differences in isotopic composition are expressed as a ratio of the heavier to the lighter isotope in the sample material compared with a standard, using the delta notation:

$$\delta^{13}C = [(^{13}C/^{12}C_{sample} \div {}^{13}C/^{12}C_{std}) - 1)] \times 1000 \text{ ‰}$$

&

$$\delta^{15}N = [(^{15}N/^{14}N_{sample} \div {}^{15}N/^{14}N_{std}) - 1] \times 1000 \text{ ‰}$$ (Sharp 2007)

The internationally accepted standard for carbon isotope measurements is PeeDeeBelemite (PDB), a marine limestone. Since the carbon in most biological materials contains less ^{13}C than the standard, $\delta^{13}C$ values are frequently negative (Ambrose 1993). The accepted standard for nitrogen isotope measurements is atmospheric nitrogen *i.e.* air. If the material analysed contains more ^{15}N than air, the $\delta^{15}N$ value will be positive (Ambrose 1993).

2.2.1 Carbon

The processes driving variations in ^{13}C abundances are perhaps better understood than for any other stable light isotope. They are incorporated into the foodweb by plants, which use

atmospheric CO_2 for photosynthesis. There are three dominant pathways which allow plants to do this, namely, the Calvin-Benson or C_3 pathway, the Hatch-Slack or C_4 pathway and the Crassulacean Acid Metabolism pathway (CAM). All pathways discriminate against ^{13}C, but do so to varying extents. $^{13}C/^{12}C$ in photosynthetic products, or the consumers of those products is used to distinguish between these different photosynthetic pathways and to identify subtle changes in a particular pathway.

The Calvin-Benson pathway is the oldest known and most energy efficient photosynthetic pathway (Cerling *et al.* 1997). It is employed by all trees, woody shrubs, most herbs and temperate grass families and makes up 95% of terrestrial biomass (Still *et al*. 2003). C_3 photosynthesizers incorporate carbon into their system as a molecule containing six carbon atoms, which they then convert into two molecules of 3 phosphoglyceric acid, each containing three carbon atoms (Calvin & Benson 1948). These plants discriminate heavily against the ^{13}C isotope, *i.e*. they incorporate much more ^{12}C and less ^{13}C than is present in atmospheric carbon dioxide. The $\delta^{13}C$ values of C_3 plants range between -30 to -22 ‰ with a mean of 26.7±2.3‰ in C_3 grasses (Cerling *et al*. 1997).

Of the three photosynthetic pathways, C_3 plants demonstrate the greatest fluctuations in their $\delta^{13}C$ values because of environmental pressures. In periods of aridity C_3 plants become more enriched in ^{13}C. This is because the degree of carbon isotope fractionation within plants is dependent on moisture availability and Water Use Efficiency *i.e.* net photosynthesis to transpiration (Marshall *et al.* 2007). In arid periods plants limit moisture loss from transpiration by closing their stomata. This effectively decreases the amount of carbon dioxide available to the plant, so that discrimination against the heavier ^{13}C isotope is reduced, resulting in less fractionation and a less negative $\delta^{13}C$ value (O' Leary 1981). This isotopic response is present to a greater degree in C_3 plants than C_4 (Swap *et al*. 2004). The

overall result is that $\delta^{13}C$ values in C_3 plants are negatively correlated with rainfall (Diefendorf *et al.* 2010).

C_3 plants are known to become ^{13}C-depleted in closed canopy environments, known as the canopy effect. This is due to plants reusing CO_2 that has been produced by leaf decomposition (van der Merwe & Medina 1991). Recycled CO_2 is ^{13}C-depleted as compared with atmospheric CO_2, thus plants using it to photosynthesise will have significantly low $\delta^{13}C$ values.

As mentioned previously the Calvin-Benson pathway is the most energy efficient. However, in situations with elevated temperatures, low partial pressure of CO_2 in the atmosphere and/or aridity, C_3 efficiency can be decreased by up to 40% (Ehleringer *et al.* 1991). This is due to the Rubisco enzyme, which fixes CO_2, preferring under these conditions to bond with O_2 instead (Ehleringer & Cerling 2002). When C_3 photosynthesis first evolved this was not a problem as CO_2 atmospheric concentrations were high and O_2 low (Cerling & Ehleringer 1998). Yet, with increase of temperature and oxygen in the atmosphere oxygenation becomes quite problematic. The products of a Rubisco and oxygen reaction can be toxic to the plant in high concentrations and must be processed using photorespiration (Ehleringer & Cerling 2002). Photorespiration not only requires more energy, but leads to a net loss of CO_2. Arid and hot environments cause stomatal closure, limiting the amount of CO_2 in cells in the same way as low CO_2 atmospheric pressure. In these environments, C_3 plants make increased use of photorespiration (Ehleringer & Cerling 2002).

C_4 photosynthesis is an adaption to avoid this type of loss and has evolved independently in many species across the globe. It is important to note that the C_4 or Hatch-Slack photosynthetic pathway is an adaptation of the Calvin Benson system and not an entirely new system (Iglesias *et al*. 1986). In C_4 plants photosynthesis takes place in both the mesophyll

and bundle sheath cells. As with the Calvin-Benson system CO_2 enters through the stomata, into the mesophyll cells (Sage 2004). However, the first compound produced is a four-carbon atom, which is then converted to malate or aspartate. This moves to the bundle sheath cells and decarboxylating enzymes return it to CO_2. It is here in the bundle sheath cells that Rubisco fixes the carbon into a three-carbon compound, which is sent back to the mesophyll cells (Sage 2004).

Bundle sheath cells act as a carbon trap, allowing C_4 plants to discriminate less against ^{13}C and preventing the loss of CO_2 during photorespiration. The presence of bundle sheath cells allows C_4 plants to dominate in areas with high growing season temperatures and/or low partial pressure of CO_2 in the atmosphere (Ehleringer *et al.* 1997). Thus, C_4 plants are less susceptible to environmental influences when compared to C_3 plants and have a $\delta^{13}C$ range between -10 to -14‰, with a mean value of -12.5±1.1‰ found in C_4 grasses (Cerling *et al*. 1997). However, at low growing temperatures, such as those found in Mediterranean climates and high CO_2 atmospheric pressure, found at low altitudes, C_3 plants will dominate the landscape. Figure 2.1 shows the photosynthetic pathway that is favoured in different environmental conditions.

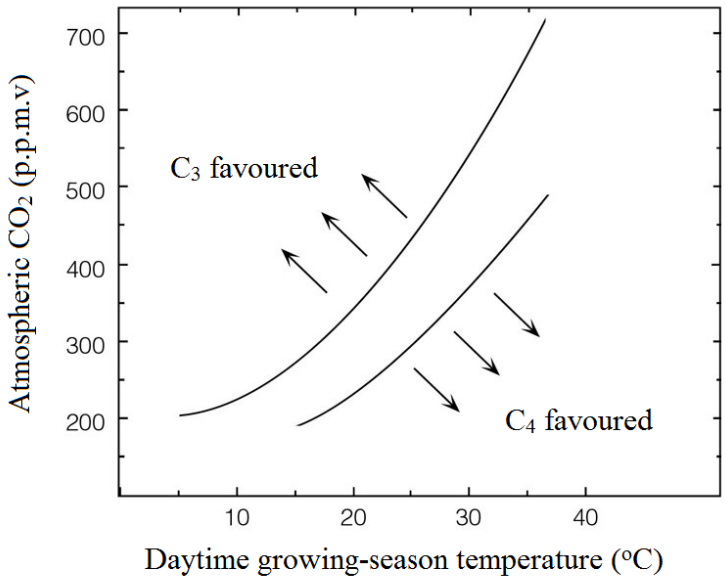

Fig. 2.1: *The modelled dominance of C_3 and C_4 plants for growing temperature vs. CO_2 levels. (Cerling* et al. *1997)*

The third type of photosynthesis is Crassulacean Acid Metabolism (CAM) and is most commonly associated with succulent flora. Unlike C_3 and C_4 photosynthesis which have defined and non-overlapping isotopic ranges, CAM plants have intermediate $\delta^{13}C$ values that may overlap those of both C_3 and C_4 pathways (O'Leary 1981). This is due to CAM plants being able to switch between the Calvin Benson and the Hatch-Slack pathways, depending on the environmental conditions (Ranson & Thomas 1960). This switch may occur seasonally or diurnally.

Herbivore $\delta^{13}C$ values reflect those of the plants they consumed, therefore it is possible to deduce the nature of the food base's photosynthetic pathways from consumer's tissues. However, diet to tissue fractionation must be accounted for when analysing $\delta^{13}C$ variation in consumers. Bone collagen can be in ^{13}C-enriched by 0.5 to 6.1‰ compared to diet (Vogel 1978, Ambrose & Norr 1993). In smaller animals, such as rodents, the difference between diet and bone collagen is usually +3 to 4‰ (Ambrose & Norr 1993; Caut *et al*. 2009).

2.2.2 Nitrogen

Most plants cannot use N_2 directly from the atmosphere. It must first be fixed by bacteria in the soil or plants into ammonium (NH_4^+) and oxidised into nitrites (NO_2^-) and nitrates (NO_3^-), to be used by plants (Pidwirny 2006). Some fixed nitrogen is returned to the atmosphere through a process known as denitrification. The denitrification process discriminates strongly against ^{15}N, releasing N_2 that that is ^{15}N-depleted back to the atmosphere, whilst the soil remains ^{15}N-enriched. Soils can become further ^{15}N-enriched through increased temperature, leaching caused by rainfall, increase in salinity and lack of oxygen (Heaton 1987; Hobbie *et al*. 2000; Pate & Anson 2008). Soils near marine environments are also higher in $\delta^{15}N$ than those further inland due to the deposition of marine nitrate.

Most plants have $\delta^{15}N$ values of approximately 1-4 ‰, however the recorded range extends from -5 to 20 ‰ (Lee-Thorp 2008). This broad range is attributed to variability in precipitation, which has been shown to have an inverse relationship with ^{15}N in plants (Heaton *et al*. 1986; Handley *et al*. 1999; Hartman & Danin 2010). Handley *et al*. (1999) attributes this to soil 'openess', open nitrogen cycles allow for a greater exchange of N_2 with the atmosphere, through nitrogen fixation and denitrification. Dry soils are more open than wet soils, meaning that arid regions will exhibit higher $\delta^{15}N$ values (Murphy & Bowman 2009).

Animals are usually ^{15}N enriched by 3-4 ‰ for each trophic step in a terrestrial food web (Ambrose 1991). A negative relationship between water availability and $\delta^{15}N$ has been reported to exist in herbivore tissues, as in plants (Sealy *et al*. 1987; Heaton *et al*. 1986). Nitrogen enrichment in animals residing in arid areas is believed to be due to diet (Murphy & Bowman 2006). However, some scientists suggest that that $\delta^{15}N$ values in animals are driven not only by diet, but also metabolic processes within the animal.

In arid environments, certain animals are able to recycle their urea in order to conserve water. This process leads to the excretion of concentrated urea, which is ^{15}N-depleted, whilst nutrients and much of the ^{15}N is reabsorbed by the body. It is therefore expected that drought resistant species will have elevated $\delta^{15}N$ values in periods of water stress (e.g. Gröcke *et al.*1997).

However, newer research suggests that metabolic processes do not control animal $\delta^{15}N$ to the extent that was previously thought. Sponheimer *et al*. (2003) showed that llama fecal matter was enriched by 3‰ in ^{15}N compared to diet, whilst urine was depleted by at most 2.3‰. This means that urea recycling would not cause a shift in llama's $\delta^{15}N$ values as fecal matter negates the effect. Studies on kangaroos and their diets in western Australia showed that bone collagen was higher in $\delta^{15}N$ by a constant factor compared to diet, when water availability was factored in (Murphy & Bowman 2006). These authors concluded that, whilst ^{15}N in herbivores is related to water availability, it is a function of diet rather than metabolic processes.

2.3 Bone collagen

Type I collagen is a structural protein found in bone, muscle and tendon. It is made up of three chains of amino acids twisted into a triple helical structure, with extensive cross linking. These cross-links make collagen relatively insoluble, thereby aiding in preservation and combating degradation (Nielsen-Marsh *et al*. 2000). This resistance to degradation made collagen the preferred analytical material for isotope studies on archaeological material, in comparison with bone apatite which is less resistant to changes (Larsen 1997).

On average dry bone is composed of between 60-70% mineral and 30-40% organic matter (Boskey 2013). Collagen accounts for 22% of the weight in living bone. After death, in most depositional environments the collagen in bone begins to decay (Schoeninger *et al*. 1989).

Peptide bonds between amino acids break, followed by loss of some peptide fragments (van Klinken 1999). This process is exacerbated in tropical climates compared with temperate environments (Nielsen-Marsh *et al*. 2000). Tuross *et al.* (1989) have shown that collagen degradation can occur within the first ten years after death, whilst Lee-Thorp *et al.* (1989) have shown that in wet and warm environments there can be little to no collagen after 10 000 years.

Thus, it is essential to ensure the collagen integrity in archaeological material, so that the stable light isotope ratios of bone collagen are reflective of the original bone chemistry. There are three common collagen indicators, namely collagen yield, elemental C: N ratios and the percentages of carbon and nitrogen present in collagen. By comparing these indicators in fresh bone with what is found in the archaeological samples, collagen quality can be assessed.

Collagen makes up 22% of the weight in fresh bone, van Klinken (1999) states that stable isotope measurements on samples yielding less than 1% collagen are unreliable. Removal of contamination from such samples is frequently challenging and $\delta^{15}N$ values can be up to 15‰ too positive (Schwarcz and Schoeninger 1991; Ambrose 1993).

Carbon and nitrogen atomic ratios in collagen are another widely-used method of screening out sub-standard samples. The C: N ratio measured in 'fresh' bone collagen from modern human and animals is between 2.9 and 3.6 (DeNiro 1985). Ratios that fall out of this range are believed to be from compromised specimens.

The third test for collagen integrity is the concentration of carbon and nitrogen present in the combusted extract (Ambrose 1990). These concentrations are expressed as wt % C and wt % N and are calculated from the amount of gas generated in the combustion system attached to the mass spectrometer (van Klinken 1999). van Klinken (1999) states the fresh bone collagen has a carbon concentration of 35 wt % and nitrogen concentration from 11-16 wt % (Van

Klinken 1999). Ambrose (1990) finds that reliable isotope ratios can be measured in collagen with wt % C between 15.3% and 47%, and wt %N from 5.3% to 17.3%. Carbon and nitrogen concentrations that fall out of these ranges are believed to be from degraded or contaminated specimens.

2.4 Angulate tortoises

2.4.1 Physical description

Tortoises first appeared in the fossil record during the Mesozoic era and belong to the Class Reptilia and Order Chelonia (Thompson 1932). South Africa is home to thirteen species of tortoise and is considered the richest location for terrestrial tortoises in the world (Branch *et al.* 1995, Boycott & Bourquin 2000). Three genera are present within the study area, namely *Chersina*, *Psammobates* and *Homopus*, all of which belong to the *Testudinidae* Family (Boycott & Bourquin 2000). However, only *Chersina angulata* – the sole member of the genus – is present at the sites of EBC and TC (Klein & Cruz-Uribe 1987, Robey 1987).

C. angulata is commonly known as the angulate tortoise, for the angular pattern of its scutes. It is endemic to Southern Africa (Branch *et al.* 1995). Angulate tortoises occur in a variety of colours including red, yellow brown and black (Boycott & Bourquinn 2000). They are described as a medium to small tortoise type weighing roughly two kilograms and rarely exceeding 30 centimetres in length (Boycott & Bourquinn 2000). The shells of tortoises are divided into a ventral plastron and dorsal carapace, fused together by a carapical ridge. The plastron consists of nine plates: an undivided gular, a pair of humerals, a pair of abdominals, a pair of femorals and a pair of anals (Boycott & Bourquin 2000) (Figure 2.2). Interestingly *C. angulata* is the only tortoise species on the African continent to possess only one gular plate. The carapace is quite distinctive, being elongated and domed in shape, with no hinges (Hofmeyer 2009). The carapace consists of five pairs of vertebrals, four pairs of costals, eleven left and right marginals, one supracaudal and one nuchal plate (Boycott & Bourquin

2000). The carapace is overlaid with keratinous scutes, which give the animal its colour. It is important to note that scutes do not represent the arrangement of the bony plates in the underlying carapace (Gilbert *et al.* 2007a).

Tortoise shell is quite an interesting feature of evolution. Whilst being a novelty to the tetrapod body plan, it is just a reworking of existing features (Gilbert *et al.* 2007a). The carapace begins to form during incubation and is partially an extension of the animal's ribcage and vertebrae (Thompson 1932). The vertebral plates are fused with the neural spines of the thoracic vertebrae, the ribcage then forms laterally as opposed to ventrally (Gilbert *et al.* 2007a). The costal plates begin formation on the ribcage, whilst, the supracaudal bone overlies the sacrum and pelvis (Gilbert *et al.* 2007a). The above-mentioned plates complete the ossification process through intramembranous ossification and are thus a mix of endochondral axial skeleton and intramembranous dermal bone (Gilbert *et al.* 2007a).

The nuchal, supracaudal and peripheral plates, by contrast, are formed through intramembranous ossification (Gilbert *et al.* 2007a). It is not entirely clear what causes these plates to form; however, Gilbert *et al.* (2007b) suggest that they are formed through neural crest cells.

The nine plates in the plastron are believed to form through intramembranous ossification. As with the nuchal plate, there is debate as to what triggers formation (Gilbert *et al.* 2007a). Clark *et al.* (2001) and Cebra-Thomas *et al.* (2007) have proposed that like nuchal plates, plastron is formed through neural crest cells. This is contentious as trunk neural cells are not known to produce bone, and cranial neural cells, which do, have not been recorded to move more posteriorly than the scapula (Gilbert *et al.* 2007a).

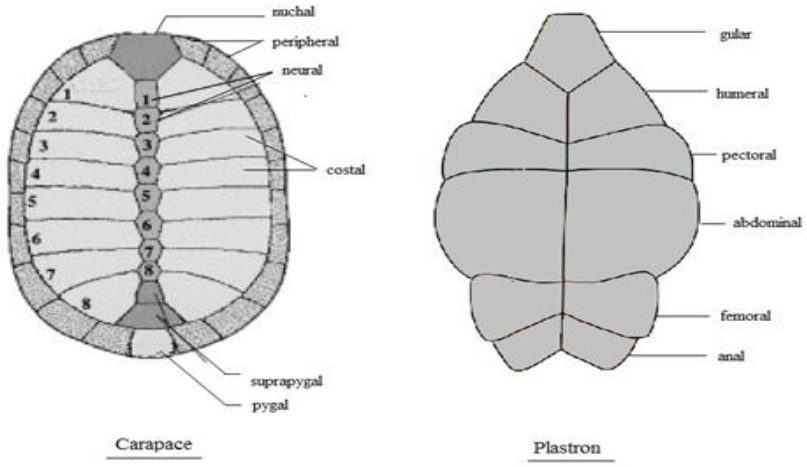

Fig. 2.2: *Schematic of bony plates in an Angulate tortoise: carapace (left) and plastron (right).*

Once the carapace and plastron have formed, some remodelling does take place, but this is mostly restricted to the interior cancellous bone (Scheyer 2007). Unlike mammalian bone, tortoise carapace and plastron is thought not to be fully renewed and homogenised (e.g. Germano 1998). This pattern is common to dermal bone in many reptilian species, both extant (e.g. crocodiles) and extinct (e.g. *Stegosaurus sp.*) (Buffrénil 1982; Scheyer and Sander 2004). However, in the three extant terrestrial species studied there was no evidence of remodelling in the compact outer cortical bone and growth marks could be observed.

It is important to understand the growth and remodelling of bone as it affects the time which is captured by the isotopes in the collagen. It will thereby affect the way the bone is dealt with to extract collagen.

2.4.2 Habitat and diet

As shown in Figure 2.3, the distribution range of *C. angulata* extends from East London to southern Namibia. They are not typically found in the interior, north of the escarpment (Alexander & Marais 2007). These animals prefer open sandy areas to dense bushy

landscapes and tend to live in areas of low rainfall (Hofmeyer 2009). *C. angulata* have a home range of up to two and half hectares (Alexander & Marais 2007) and can be found in densities of up to thirty-eight individuals per hectare (Branch 1984).

Fig. 2.3: *Distribution of* C. angulata *in Southern Africa (from Boycott & Bourquin 2000).*

Thus, this species occupies a variety of habitats ranging from the semi-desert to sub-tropical, and can survive in rainfall conditions varying from 100 to 700mm per annum (Grieg & Burdett 1976, Hofmeyer 2009). Due to its wide range of habitats, it is believed to have a less specialized diet than many other testudines. *C. angulata* are known to be herbivorous, feeding on grasses, annuals and succulents (Alexander & Marais 2007).

Joshua *et al*. (2010) performed a detailed feeding study on angulate tortoises from two different locales within the winter rainfall zone. They studied tortoise diet in the ecologically relatively undisturbed West Coast National Park (WCNP) and the much more altered Dassen Island (DI). Vegetation at WCNP is like that found at Elands Bay: dense scrub vegetation interspersed with restioids (Joshua *et al.* 2005). Vegetation at Dassen Island is sparse and, due to marine influence, temperature fluctuations are smaller, whilst humidity and annual rainfall are higher in comparison to WCNP (Joshua *et al*. 2010). Results of the feeding study showed that angulate tortoise diet changed according to food availability. At the WCNP tortoise diet largely consisted of shrubs and herbs, whilst at DI diet was mostly made up of herbs and seedlings (Joshua *et al*. 2010). During the wet season, more than 50% of diet

comprised herbs and seedlings at both sites. During the dry season, tortoises at WCNP continued to consume herbs, but also included tiny amounts of succulents and almost 20% of dry grass into their diet (Joshua *et al*. 2010). Likewise, tortoises at DI still consumed herbs during the dry season, yet also included a large amount of rabbit faeces into their diet, around 30% of their seasonal diet (Joshua *et al*. 2010). Whilst the inclusion of animal faeces is seen at WCNP, the intake is far less significant, making up less than 5% of annual tortoise diet compared with 15% of the annual diet at DI (Joshua *et al*. 2010).

These observations show that *C. angulata* generally prefer herbaceous and annual plants. Tortoises may be selecting these 'soft' plants to eat as they lack teeth and are thus unable to tear tougher plants (Balsamo *et al.* 2004). It may also be that softer plants are easier to digest and tend to have more protein than fibrous plants (Balsamo *et al.* 2004). Lastly grass may not be a favoured food as its protein content decreases more rapidly with age than that of dicotyledonous plants (Caughley and Sinclair *et al.* 1994). An explanation for *C. angulata* consuming dry grass during summer and autumn at WCNP is that it may be higher in energy than fresh plants as well as high in nitrogen relative to potassium, which favours growth in desert tortoises. Faecal matter may be consumed as a last resort when vegetation is sparse. The rabbit faeces found on Dassen Island are high in energy and may add extra microflora to the tortoises' guts, which could assist in the breakdown of cellulose (Joshua *et al*. 2010). This would make faeces a valuable resource when plants are scarce, such as in the dry season at DI. It should be noted that *C.angulata* are not the only tortoise species to consume faecal matter; rabbit, tortoise, rodent and hyena faeces are known to be eaten by other tortoise species such as *Stigmochelys pardalis* and *Gopherus berlandieri* (Branch 1998; Auffenberg and Weaver, 1969).

Given that the study area falls in a predominantly C_3 zone and that angulate tortoises prefer to eat herbs and annual plants and that current understanding is that these animals do not

consume a lot of succulents *i.e.* CAM plants (Rebelo *et al*. 2006, Joshua *et al*. 2010). One would expect their carapace collagen to show a strong C_3 signal. Furthermore, one might expect that collagen $\delta^{13}C$ should show shifts over time in response to variations in temperature and aridity because it will track $\delta^{13}C$ in the plant food base. It must be noted that angulate tortoises may also eat small quantities of grass, and are known to consume small quantities of succulents, which are CAM photosynthesizers (Joshua *et al*. 2010). If the species of grasses selected are C_4 and/or the succulents use the C_4 pathway, then these foods will lead to an increase of ^{13}C within the carapace. Angulate tortoises are known to drink water through their nostrils and have been seen drinking condensed fog (Joshua *et al.* 2010). In the dry season, they have been noted to collect rainwater in their carapace. This is achieved by withdrawing the head into the shell and standing on the hind legs, allowing the water to collect around the head and then drinking it through the nostrils (Hofmeyer 2009). Thus, it is important to consider $\delta^{15}N_{collagen}$ as well when making paleoclimatic deductions.

2.5 Previous archaeological work on Angulate tortoises

Modern angulate tortoises are a food source for hyenas, jackals, black eagles, crows, kelp gulls, owls, baboons and humans (Alexander & Marais 2007). Hence, the first step in an archaeological investigation is to determine who/what was the bone accumulator. To identify the accumulator, researchers have primarily looked at bone damage. If there is evidence of cut marks and fire use, humans are held responsible, whilst gnaw and claw marks are an indication of animal accumulation (Avery *et al.* 2004, Thompson & Henshilwood 2014a, Klein & Cruz-Uribe 2016). The types of tortoise bone found at the site are also indicative of accumulator. At sites where humans are accumulators there is an absence of vertebrae and sizable proportion of intact carapacial and plastral bone, the opposite of which is seen at raptor sites (Sampson 2000). It is crucial to understand the agent/s of bone accumulation when using changes in tortoise size as a proxy for human behaviour and diet.

Most studies on angulate tortoises accumulated by humans have used the species as a proxy for human population size and resource intensification. Klein & Cruz Uribe (1983) reason that larger tortoises would be preferentially collected over smaller tortoises as they are easier to spot and are the better food resource. However, when populations increased, collection would intensify, leading to the collection of smaller tortoises. Thus, changes in tortoise size over time will indicate changes in human population size and collection strategy. This hypothesis was used to argue for differences in population size and behaviour between Later Stone Age (LSA) and Middle Stone Age (MSA) populations along the Western Cape of South Africa. Measurements on the mediolateral distal humerus showed that tortoises from the LSA were smaller in size to those from the MSA (Klein & Cruz-Uribe 2000). The difference in tortoise size between the two periods were interpreted as indicating that LSA populations were larger than their MSA counterparts and increased their demands on the land (Klein & Cruz-Uribe 2000, Halkett *et al.* 2004). Variations in tortoise from the Holocene record at Elands Bay Cave, indicate that human population was the densest at 10 000 BP (Klein & Cruz-Uribe 2016). Possible alternative explanations for variation in tortoise size, such as climatic shifts, have not been well explored.

Archaeologists consider tortoises to be a low cost-high gain resource, that does not require substantial quantities of energy and resources to acquire. In addition to their food value, skeletal elements have been used for bowls, musical instruments and for the manufacture of decorative items (e.g. Klein & Cruz-Uribe, 1983, 1987, 2000, Henshilwood 2008). A recent study by Thompson & Henshilwood (2014b) calculates the nutritional value of angulate tortoises to determine how important tortoises are among gathered items. The study showed that the average angulate tortoise (weighing ±560g, excluding the shell) can constitute 20-30% of a human's daily caloric dietary requirement.

2.6 Previous isotopic work on tortoises

Stable light isotope studies of animal tissues are heavily biased towards endotherms *i.e.* mammals and birds, as well as some fish (Murray & Wolf 2012). Only a few papers focus on reptiles and even fewer on *Testudines*. Most of the current literature on *Testudines* focuses on sea turtles, attempting to understand their diets and habitats. Isotopes have been used to determine dietary differences between juveniles and adults, differences in trophic levels and habitats (e.g Seminoff *et al.* 2006; Reich & Bjorndal 2008; Murray & Wolf 2012). The tissues most commonly analysed were red blood cells, plasma, keratinous scutes and skin (e.g. Seminoff *et al.* 2006; Reich & Bjorndal 2008). These tissues were preferred over bone and muscle as they do not require the sacrifice of the animal in the wild. However, there have been some studies of $\delta^{13}C$ and $\delta^{15}N$ in skeletal bone collagen of Mediterranean green turtles (*Chelonia mydas*) (Godley *et al.* 1998; Seminoff *et al.* 2006). A few papers have used feeding studies to determine diet-tissue discrimination in *Testudines*. These studies focus on diet discrimination in blood, muscles, skin and keratinous scutes and calculated fractionation as $\Delta = \delta_{tissue} - \delta_{diet}$ (Seminoff *et al.* 2007, Reich *et al.* 2008; Murray & Wolf 2012).

Murray & Wolf (2012) performed a feeding study on juvenile desert tortoises (*Gopherus agassizi*), to determine $\Delta^{13}C_{diet\ to\ tissue}$. This species, like angulate tortoises, occupies arid environments and is known to be herbivorous. However, this study analysed collagen in scutes rather than bone. Tortoises were fed a known isotopic diet for 371 days, before being switched to another known isotopic diet for another 371 days. Scute samples that were taken on day 371 of the second diet were considered at equilibrium and used to calculate $\Delta^{13}C_{diet\ to\ tissue}$ of 0.8±0.1 ‰. It was also seen that the growth of new keratin in the scutes influenced the isotopic values in previously formed scute rings. Blood plasma showed $\Delta^{13}C_{diet\ to\ tissue} = 1.0 \pm 0.2$ ‰ (Murray & Wolf 2012). Reich *et al.* (2008) looked at $\Delta^{13}C_{diet\ to\ tissue}$ and $\Delta^{15}N_{diet\ to\ tissue}$ for loggerhead turtles (*Caretta caretta*). Unlike angulate tortoises, these are omnivorous

marine turtles. $\Delta^{13}C_{diet\ to\ tissue}$ in juvenile loggerhead scutes was calculated 232 days after starting an isotopically known diet. $\Delta^{13}C_{diet\ to\ tissue}$ was 1.8 ± 0.6‰ and $\Delta^{15}N_{diet\ to\ tissue}$= -0.6 ± 0.1‰ (Reich *et al*. 2008).

Whilst $\Delta = \delta_{tissue} - \delta_{diet}$ is simple method to determine the fractionation between consumer and diet, it leads to deviations from the mathematically correct value if there is more than a 10‰ change in diet (Passey *et al.* 2005). Calculation of the enrichment factor (ε), whilst more technical, is sounder (Cerling and Harris 1999):

$\alpha_{diet\text{-}tissue} = 1000 + \delta diet / 1000 + \delta tissue$

&

$\varepsilon = (\alpha_{diet\text{-}tissue} - 1)1000$

The most detailed stable isotope study of angulate tortoises to date is Weeber (2013). In which $\delta^{13}C$ and $\delta^{15}N$ within the collagen of bone carapace and plastron of angulate tortoises from the Elands Bay region was analysed. A large part of the study focused on modern samples to create a base line. The remains of 61 modern angulate tortoises were collected from two sites, 26 from below a black eagle nest at Diepkloof and 35 from Steenbokfontein koppie. These two localities are 25 km apart.

First, Weeber (2013) tested within-animal inter- and intra-plate isotopic variability. To test inter-plate variability, 17 entire plates from a single animal were decalcified and the collagen homogenised by gelatinisation (see Chapter 4: Methods). Inter-plate variability was low, with a maximum difference of 0.4‰ in $\delta^{13}C$ and $\delta^{15}N$. To test intra-plate variability, three left femoral plates were cut into 2mm strips, following visible lines of growth, and each strip analysed separately. There was a range of up to 1.05‰ in $\delta^{13}C$ values and 1.85‰ in $\delta^{15}N$ values within a single plate. This is unsurprising as tortoise carapace and plastron are known to grow in increments and not be homogenized (Germano 1998). Thus, while any plate within

the carapace or plastron is suitable for isotopic analysis, a small fragment of a plate may not yield isotope values that are representative of the whole. Entire plates, or representative samples thereof should be analysed.

$\delta^{13}C$ values of the animals collected at Diepkloof and Steenbokfontein koppie were not significantly different. The mean $\delta^{13}C$ of all specimens (from both sites) was -22.1 ± 0.6 ‰, indicating a predominantly C_3 diet, although a slight intake of either C_4 or CAM plants cannot be ruled out. $\delta^{15}N$ values were significantly more positive in the tortoises from Steenbokfontein koppie (mean = 11.6 ± 1.4 ‰) when compared with those from Diepkloof (mean = 9.5 ± 1.7 ‰), $p < 0.01$. This was attributed to the proximity of Steenbokfontein koppie to very sandy soils where the nitrogen cycle is probably more open, leading to elevated $\delta^{15}N$. It is also closer to the coast than Diepkloof, so that nearby soils may be more saline (Heaton 1987).

Weeber (2013) also analysed 18 archaeological specimens: 14 nuchal plates from Dune Field Midden and one plate and three limb bones from archaeological excavations at Diepkloof Rock Shelter. The samples from Dune Field Midden date from 547 to 669 cal. BP and were significantly ^{13}C-enriched (mean = -20.7 ± 1.1 ‰, $p < 0.1$) compared with modern samples (after 2‰ had been added to the modern samples to correct for the fossil fuel effect [Schmitt *et.al* 2012]). The more positive $\delta^{13}C$ values were interpreted as indicating a period of aridity at Dune Field Midden during the Medieval Climate Anomaly. However, there was no observed difference in $\delta^{15}N$ between archaeological and modern specimens. Unfortunately, the small number (n=4) of archaeological specimens from Diepkloof (547-669 cal. BP), made it impossible to interpret these results with confidence.

Sealy (1984) reported $\delta^{13}C_{collagen}$ values for 12 modern angulate tortoises from the Western Cape and two from the Northern Cape. The results are summarized in Table 1.1.

Table 1.1: $\delta^{13}C$ values of Angulate tortoise skeletal collagen, 1.5‰ was added to modern values to account for the Fossil Fuel Effect [Schmitt *et.al* 2012] (Adapted from Sealy 1984)

Province	Region	N	$\bar{X}\delta^{13}C$	SD
Western Cape	Coastal Plain	5	-20.4	1.3
Western Cape	Fold Mountains	2	-21.6	1.2
Western Cape	Jonkershoek	6	-20.9	1.4
Northern Cape	Bushmanland Karoo	1	-21.3	–
Northern Cape	Karoo margins	1	-21.8	–

The specimens in Table 1 are once again indicative of tortoises consuming a predominantly C_3 diet with the possible inclusion of a small amount of C_4/CAM vegetation.

The variation in carbon and nitrogen isotopes in modern tortoises seen by Weeber (2013) indicate that tortoise isotopes present a localized signal. This is important as it means that archaeological specimens should demonstrate a local signal. In Weeber's study, the difference in $\delta^{13}C$ between modern and archaeological tortoises indicates that tortoises can demonstrate changes over time.

Chapter Three

3. Site Background

3.1 Environment of the Elands Bay Region today

This study is situated in the Elands Bay region, along the West Coast of South Africa (Figure 3.1). This region has a considerable number of preserved tortoise bone at archaeological sites (Klein & Cruz-Uribe 1989). As described in the previous chapter, a modern isotopic base line for angulate tortoises has already been established in the area by Weeber (2013). In addition, there have been several paleoenvironmental studies in the area based on fauna, isotopes, charcoal and pollen analysis. Comparisons of the data produced in this study with those from other proxy sources will indicate to what extent tortoise carapace usefully reflects environmental changes. The two archaeological sites that were chosen for this study are Elands Bay Cave (EBC) and Tortoise Cave (TC). These sites were chosen as foraging trips from each site would overlap (Lee 1968). Hence, tortoises dating to same period represent the same population, even if they are from different sites.

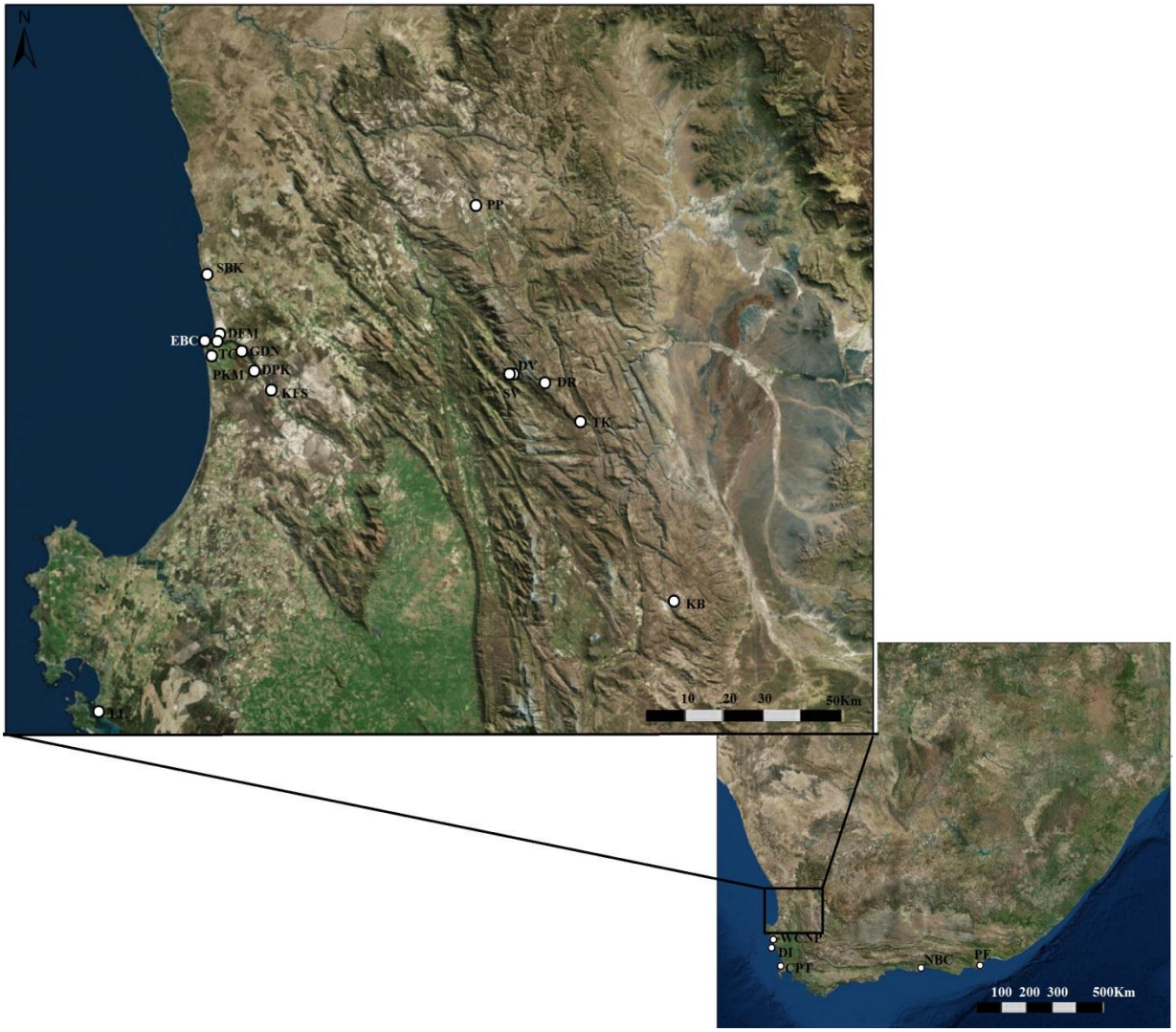

Fig 3.1: *Geographical location of the cities of Cape Town (CPT) & Port Elizabeth (PE), the West Coast National Park (WCNP), Dassen Island (DI), and the archaeological site of Nelson Bay Cave (NBC). Inset map shows the position of Elands Bay Cave (EBC), Tortoise Cave (TC), Pancho's Kitchen Midden (PKM), Dune Field Midden (DFM) and Diepkloof (DPK). Paleo proxy sites include: Grootdrift (GDN) and Klaarfontein Springs (KFS), Driekhoek and Sneeuberg Vlei, Pakhuis Pass (PP), De Rif (DR), Truitjies Kraal (TK), Katbakkies (KB) and Langebaan Lagoon.*

Elands Bay Cave and Tortoise Cave are approximately 180 km north-west of the city of Cape Town. Both sites are in the Southern African Mediterranean climate system, with warm dry, summers and cool, wet winters (Chase & Meadows 2007).

The Mediterranean climate system at the Cape is due to the South Atlantic High Pressure system responding to the pressure system in the interior of the country. During the summer months, the heat causes a low-pressure system to develop in the interior of the country. In response to this low-pressure cell, the South Atlantic high ridges eastward (Laing & Fritsch 1993), preventing moisture-bearing cold fronts from reaching the western region of the country. However, during winter the low-pressure cell over the interior of South Africa dissipates and the South Atlantic High Pressure shifts slightly north (Laing & Fritsch 1993). The shift in the South Atlantic High Pressure allows for the passage of rain bearing frontal systems over the western part of southern Africa during winter. The region that receives rain from this system is aptly referred to as the Winter Rainfall Zone (WRZ) and receives 66% of its rainfall between the months of April to September (Chase & Meadows 2007).

The frontal systems that provide the winter rains do not extend across the whole country. Thus, the eastern portion of southern Africa which receives 66% of its rainfall in summer is known as the Summer Rainfall Zone (SRZ). The region where the SRZ and WRZ overlap receives rainfall throughout the year (Year-round Rainfall Zone) (Chase & Meadows 2007). Figure 3.2 shows the three rainfall zones within South Africa.

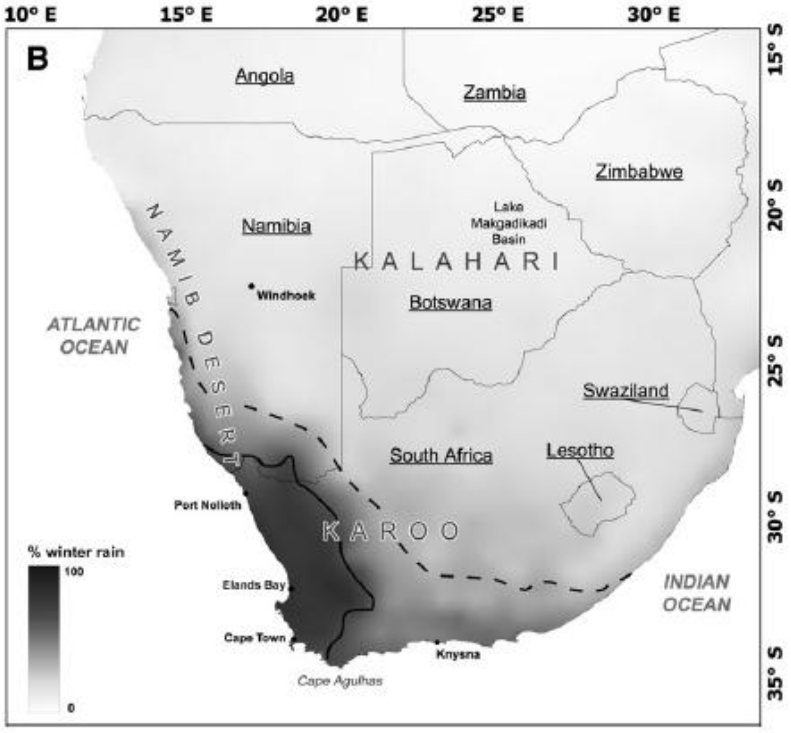

Fig 3.2: *Map charting Southern Africa's three rainfall zones. Winter rainfall is demarcated by the solid line, summer rainfall by the dashed line and year-round rainfall is found in the region between the two. From Chase & Meadows (2007).*

EBC and TC receive less than 300 mm of rainfall per annum (Baxter & Meadows 1999), which means that the area is classified as a xeric to sub-xeric zone (Munch *et al*. 2007). Nonetheless, it boasts considerable floral diversity. The sites fall into the fynbos biome, which is the smallest and one of the most diverse biomes in the world. The diversity is largely influenced by the geological substrates, with different soil types favouring different vegetation types (Meadows *et al*. 1996, Cartwright & Parkington 1997). The substrates in the area include calcareous sands, Malmesbury Shale, Table Mountain Sandstone and shales from the Klipheuwel Formation (Meadows *et al*. 1996). Thus, it is not surprising that four different vegetation types exist within the Elands Bay area: fynbos, strandveld, sea shore and freshwater wetland vegetation, with sub-types as shown in Figure 3.3.

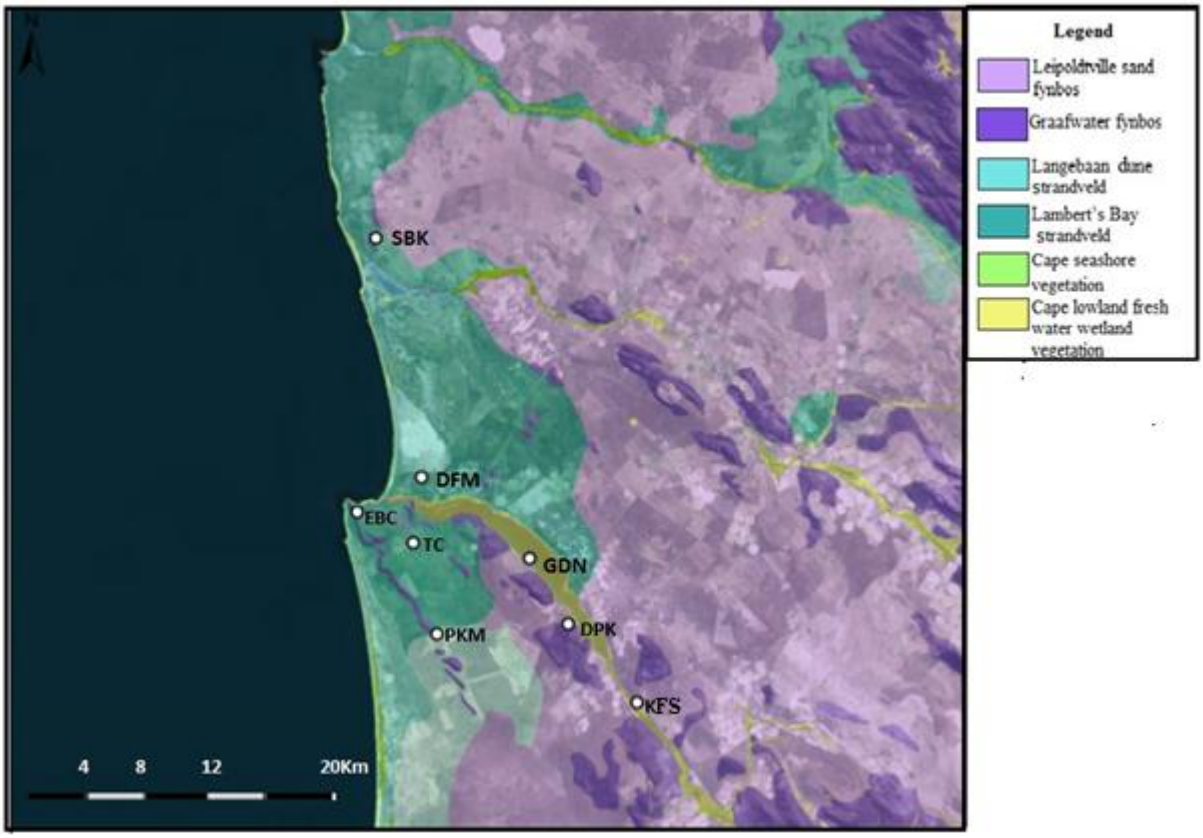

Fig. 3.3: *Vegetation map of the Elands Bay region showing the archaeological sites of DFM, DPK, EBC, PKM, SBK & TC and the GDN & KFS pollen site.* (Vegetation cover from Mucina & Rutherford 2010).

On Figure 3.3, fynbos vegetation is indicated by purple (Leipoldtville sand fynbos) and lilac (Graafwater fynbos). These groups of fynbos are characterised by low-lying, tightly clustered shrubs and by the frequency of plants in the families *Asteraceae* and *Restionaceae*. Proteoid families are also seen in Graafwater fynbos (Rebelo *et al*. 2006).

The aqua colour (Fig. 3.3) is representative of Langebaan Dune Strandveld, whilst the teal colour represents Lambert's Bay Strandveld vegetation. These types of strandveld vegetation are typified by evergreen, hard-leafed plants, ranging between 1.2 to 2 metres in height, beneath which smaller shrubs and annual herbs can be found (Mucina & Rutherford 2006).

Cape seashore vegetation is demarcated by light green colour on Fig. 3.3. This vegetation is often dominated by one species and is known for grasses, herbs, succulents and dwarf shrubs (Mucina *et al*. 2006).

Lastly the yellow region on Fig.3.3 represents Cape lowland fresh water wetland vegetation. Plants found here include trees, low shrubs, sedges, reeds and herbs (Rebelo *et al*. 2006).

3.2 Archaeological sites of Elands Bay Cave and Tortoise Cave

3.2.1 Elands Bay Cave

Elands Bay Cave is a large archaeological site that preserves Middle and Later Stone Age deposits. It is situated on the sea facing cliff of Baboon Point, south of the mouth of Verlorenvlei (see Fig. 3.1). This cave is comprised of quartzite and was formed through wave erosion along shear zones and bedding discontinuities (Butzer 1979). It has a surface area of 120m^2, is 13 meters wide with an entrance height of 10m, with rock art adorning the back wall (Parkington 1992). EBC was first excavated in late 1970 by Professor John Parkington, Cedric Poggenpoel and Peter Robertshaw to investigate the seasonal mobility hypothesis (Cartwright & Parkington 1997). This hypothesis proposed that people in the pre-colonial past travelled between the coast and the interior Cederberg Mountains on a seasonal basis pursuing favourable conditions (Parkington 1972, 1976). By the time excavations ended in February 1978 new questions, such as how EBC fitted into the economy of the region, were being investigated (Cartwright & Parkington 1997).

Fig 3.4: *Photographs of Elands Bay Cave A) the cave mouth B) rock art of eland and finger dots on the rear wall of the cave C) view from the cave onto the shoreline. Photos taken by N. Naidoo.*

Material from EBC was excavated in 1 x 1m squares and stratigraphic units distinguished according to changes in colour, texture and archaeological content (Parkington 2016). Three hundred and fifty units were excavated, covering an area of 96m^2 and reaching a maximum depth of 3.5m (Poggenpoel 1996). Radiocarbon dating shows that deposit extends from 300 bp (uncalibrated radiocarbon years before present) to over 40 000 bp (Parkington 1999). However, the sequence is not continuous as there are five breaks in occupation (hiatuses) (Parkington 1992). There are seven major pulses of occupation labelled A-G and further sub-divided into 25 “packages”, based on material culture, stratigraphic association and radiocarbon date (Poggenpoel 1996). Fig. 3.5 is a schematic section through EBC depicting different stratigraphic units and illustrating the hiatuses.

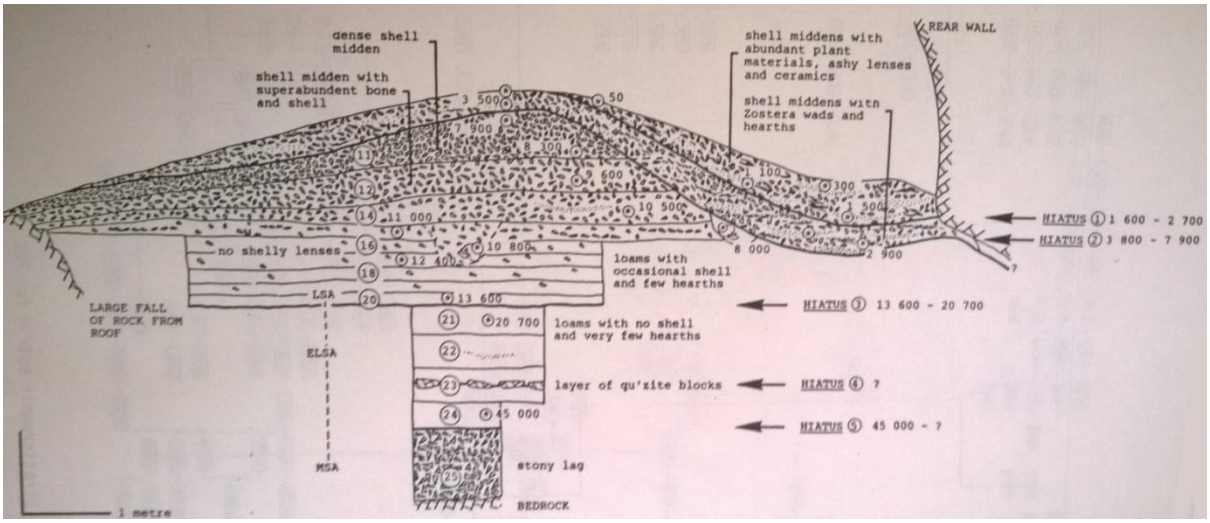

Fig. 3.5: *Stratigraphy of EBC, showing major hiatuses*. *From (Parkington 1992)*

As this study focuses on terminal Pleistocene and Holocene material, only pulses A to D will be discussed. Pulse D is sandwiched between hiatuses 3 and 2 (Parkington 1992). This pulse is represented by packages twenty to ten and dates from 13 600 to 7 900 radiocarbon years bp (Parkington 1992). Forty-five percent of excavated material is from this period and includes abundant fauna, especially ostrich egg shell (oes) and tortoise bone (Parkington 1992). Besides the spike in tortoise remains and oes, there is an increase in burials and broken and unfinished artefacts. This has led researchers to suggest that the cave was used more frequently during the late Pleistocene and early Holocene, than other periods of occupation (Poggenpoel 1996).

Packages twenty to sixteen represent the Pleistocene to Holocene transition, i.e. 13 600 to 10 800 bp (Parkington 1992). The sediments in these packages have been described as a mixed mineral-cultural deposit with very little mollusc or rubble elements, but rich in charcoal (Butzer 1979). Several human burials have also been found within these packages as well as large game such as quagga, wild pig, and eland (Parkington 1992).

Packages fifteen to ten represent the early Holocene, dating from 10 500 to 7 900 bp. The sediment in these packages consists of a thin upper shell midden and is interstratified with

cultural material (Butzer 1979). This period has yielded the most abundant ostrich eggshell and tortoise bone, with units 13 and 14 having at least 900 individual tortoises (Klein & Cruz-Uribe 1987). However, when compared with packages 20 to 16, large game species such as wild pig, eland, and quagga are less numerous, whilst the Cape horse disappears from the record (Klein & Cruz-Uribe 1987). The reduction in large game is thought to be a product of habitat loss because of the sea-level rising at 11 000 years ago due to deglaciation (Miller 1995). The sea-level moved from 30km west of EBC to only 200m away, leading to the flooding of the grasslands. This in turn led to the extinction of grazing fauna and perhaps the necessity for humans to turn to other food sources such as tortoises and ostrich eggs (Klein & Cruz-Uribe 1987).

The change from open grasslands to bushier environments during the early Holocene has been documented not only at EBC but across the south coast at sites such as Nelson Bay Cave and Klasies River (Klein 1983). As in EBC, when researching these sites, a change in fauna from grazers to browsers is used as proxy evidence for the shift in environment. Interestingly, after 9 000 bp the amount of tortoise bone at EBC plummets and small browsing bovids such as grysbok and steenbok increase (Klein & Cruz-Uribe 1987). There is also a huge increase in the quantities of marine resources found at the site during this period. The increase in marine exploitation is believed to be due to an increase in sea-level, as exploitation is more viable with a decrease in distance to the coast (Klein & Cruz-Uribe 1987).

Between pulses D and C there is a hiatus (2) in the depositional record, from 7 910 to 4 320 bp (Parkington 1992). During this time, the sea-level is believed to have risen three meters above present level (Miller *et al*. 1993), opening Verlorenvlei permanently to the sea and creating an estuary where the vlei is today.

Pulse C occurs between 4 300 to 2 900 bp and includes packages 8 to 13 (Parkington 1992). The stratigraphic units are composed of a smaller body of interstratified shell, hearths and ash lenses (Butzer 1979). Pulse C indicates a reuse of space with people moving towards the back of the cave and digging basins (Poggenpoel 1996). It is possible that large units in this pulse such as SHAK, NEFE and LBED are disturbed units that were dug out by new occupants of the cave (Parkington 1992). This theory is based on the *in situ* JOFR units which are in the middle of the cave. The JOFR units are not displaced as occupation at later stages hugged the back wall of the cave (Parkington 1992). This pulse accounts for approximately 20% of excavated material and has the lowest recorded densities of both marine and terrestrial bone at the site (Parkington 1992). However, the material within the pulse is dominated by mussels. Parkington (2016) states that this indicates a dependency on inter-tidal foraging. *Zostera capensis* is also present in copious quantities and is believed to have been used for bedding (Poggenpoel 1996).

Pulse C is separated from Pulse B by another hiatus (1) in human occupation. Hiatus 1 spans the period between 3 200-1 700 bp (Parkington 1999). This hiatus is observed not only at EBC, but also at Pancho's Kitchen Midden (PKM), Tortoise Cave (TC) and Spring Cave (SC) (Parkington 2016). Interestingly, large heaps of interstratified marine mollusc shell and stone tools, known as megamiddens, located along the coast line date to this period. This is believed to indicate a move in occupation from closed to open air sites, during the period spanned by hiatus 1 (Henshilwood *et al*.1994).

Pulse B dates from 1 700 to between 1 550 - 1 150 bp and contains the earliest pottery found at EBC (Parkington 1999). The presence of pottery within the record is indicative of a lifestyle change, which is a significant archaeological break. This pulse has high densities of fish bone, black mussel shell, terrestrial bone and ceramic pieces yet the quantities of *Zostera* are lower than in pulse C (Parkington 1992). Black mussels are also dominant within this

pulse, which is believed to represent a strong dependency on the intertidal zone (Parkington 2016).

There is no break in the deposit between Pulses B and A, making the distinction between the two ambiguous. As with Pulse B a distinction is made on an archaeological basis. Pulse A is defined by subsistence shift from black mussels to limpets (Parkington 1992). Differences in plant remains are also visible between Pulse A & B, where A has more woody fragments and less *Zostera* than B. Whilst this patterning may be the result of preservation, Parkington (1992) interprets it as human choice. Poggenpoel (1999) suggests that replacement of *Zostera* by terrestrial grass is evidence of the vlei becoming closed. The start date of Pulse A has been proposed to be between 1 550 and 1 150 bp and it terminates at 300 bp (Parkington 1992). Pulse A holds packages 1-6 and the quantities of crayfish, seal and bird remains approach and in some units even exceed those recorded in Pulse D (Parkington 1992). The pulse also contains string, brass and pottery (Parkington 1992). It should be noted that deposits in this pulse were the only ones to be coated by halite crystals, indicating an aridity that was not present in earlier deposits (Parkington 1992).

Table 3.1 below lists those units with calibrated radiocarbon dates, excluding dates the author considered possibly unreliable such as those on estuarine bedding grass or ostrich egg shell. Date from the Gakushin laboratory were also excluded as these were considerably younger than the dates produced in other labs.

Table 3.1: Calibrated radiocarbon dates from EBC. Dates calibrated on Oxcal version 4.2, using the SHcal13 calibration curve.

Pulse	Package	Strat unit	14C BP	95.4% (2sigma) cal age BP	median cal. BP	Lab identifier	Material dated
A	2	NKOM	320±50	487–154	373	Pta 1815	Charcoal
A	3	JECH	1310±40	1275–1075	1202	Pta 5595	Charcoal
A	3	KEPL	2100±20	2094–1934	2029	Pta 5611	Charcoal
A	3	CCLA	1040±50	1047–774	888	Pta 5822	Charcoal
A	3	POTA Sq. X2	1790 ± 50	1810–1542	1657	Pta 5820	Charcoal
A	3	BARR Sq. C3	1350 ±20	1280–1183	1223	Pta 6138	shell,corrected
A	3	BUTH Sq. A3	1400 ± 50	1357–1180	1275	Pta 6132	shell,corrected
A	3	BUTH Sq. A5	2790 ± 50	2960–2755	2845	Pta 5816	charcoal
A	4	BRST Sq. C8	1280 ± 50	1275–999	1154	Pta 5819	charcoal
B	5	GADD Sq. B9	1680 ± 40	1693–1418	1537	Pta 5815	charcoal
C	5	LARM Sq. E9	2190 ± 25	2305–2050	2141	Pta 5810	charcoal
C		MAUR	3835±50	4405–3990	4180	Pta 1754	Burial, rib collagen
C	6	GSFB	3590±60	4064–3644	3835	Pta 5594	Charcoal
C	7	RETS Sq. YB	3290± 60	3632–3358	3477	Pta 5811	Charcoal
C	8	JOFR	3780 ± 60	4419–4005	4234	Pta 5806	Charcoal
C	9	BARH	3490±60	3876–3564	3713	Pta 5317	Charcoal
C	9	SHAK	4370±60	5270–4660	4918	Pta 5313	Charcoal
D	10	MARO	7910±85	8993–8477	8707	Pta 1830	Charcoal
D	10	MARO	8340±80	9475–9033	9293	Pta 1817	Charcoal
D	10	LIRO	8860±90	10178–9565	9880	Pta 5305	Charcoal
D	11	Soil Sq. Y6	8920 ± 90	10225–9675	9971	Pta 5808	Charcoal
D	11	ALBA	10860±180	13104–12162	12735	OxA 478	Burial, limb collagen
D	12	Gnome Sq. Z4	9510 ± 90	11071–10571	10718	Pta 5824	Charcoal
D	13	BSBP	9600±90	11181–10601	10909	Pta 0686	Charcoal
D	13	NEPT	9640±90	11201–10690	10940	Pta 5306	Charcoal
D		YMFD	9800±160	11748–10668	11150	Oxa 456	Burial, limb collagen
D		URSU	9800±160	11748–10668	11150	Pta 3086	Burial, rib collagen
D	14	CRAY	10000±90	11772–11206	11451	Pta 2481	Charcoal
D	15	FOAM	10460±80	12555–11999	12269	Pta 5336	Charcoal
D	15	SMOK	10660±100	12734–12125	12569	Pta 5369	Charcoal
D	15	PBGB	10640±110	12725–12103	12538	Pta 0732	Charcoal
D	15	GBAN	10700±100	12752–12180	12598	Pta 0737	Charcoal
D	15	ASHE	10560±100	12675–12060	12447	Pta 5361	Charcoal
D	16	PLGB	10090±65	11924–11271	11564	UW 0193	Charcoal
D	16	KAMA	11070±140	13137–12698	12906	UW 0192	Charcoal

3.2.2 Tortoise Cave

Tortoise Cave is a Later Stone Age site located three kilometres from the mouth of Verlorenvlei. The cave formed between the interface of Table Mountain Sandstone conglomerate and quartzitic sandstone (Robey 1987). The mouth faces east and is five metres across, with approximately seven meters between the mouth and the rear wall (Robey 1987). Rock shelves ranging from 30-60cm have been created through weathering in front of the cave (Robey 1987).

The site was first excavated in 1978 by John Parkington, in hopes of understanding the archaeological economy within the Elands Bay region. Excavations were situated at the

northern half of the site, on either side of the dripline (Robey 1987). Excavation was then continued by Tim Robey from 1981 to 1983 (Robey 1987). Robey's excavations focused on the stratified deposits at the back of the cave, which he attempted to link to the poorly stratified units at the front (Robey 1987). Robey also extended excavations onto the talus slope. Thus, in total $35m^2$ of deposit was excavated (Robey 1987).

Material was excavated in 1x1m squares. Since stratigraphic units could not be recognised, most of the deposits were removed as 5cm spits (Robey 1987). $35m^2$ of deposit was excavated and more than 163 spits were removed. These spits were later amalgamated into 14 layers, which were further compiled into three units (Robey 1987). Figure 3.6 is a schematic section of TC showing the various groups of layers, with radiocarbon dates bp.

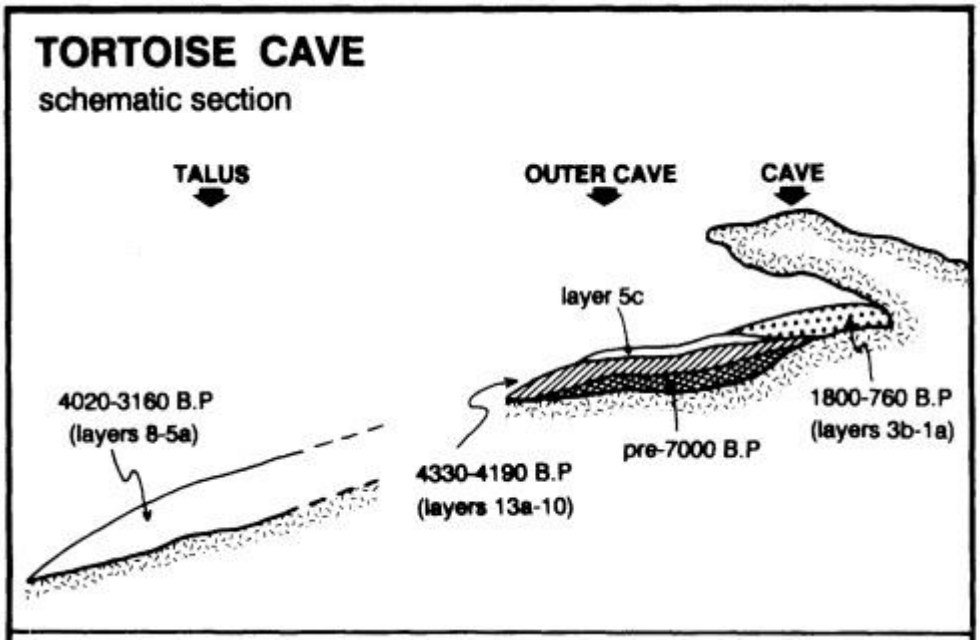

Figure 3.6: *A schematic section of Tortoise Cave. (Jerardino* 1995*).*

The oldest of these units are known as the outer cave deposits, housing layers 10 and 11 and 13-14 (Robey 1987). As the name suggests, these layers were excavated from the front of the shelter and extended over the rock shelf and across the drip line (Robey 1987). This unit

consists of poorly stratified layers of ash, soil and shell and much of it is thought to be disturbed, however, some primary deposits do remain (Robey 1987).

Layers 13 and 14 are thought to be slightly less than eight thousand years old and are separated from layers 10 and 11 by a hiatus of approximately 2 500 radiocarbon years (Robey 1987). This hiatus coincides with the hiatus between Pulses D and C at EBC. However, stone tools from layers 13 and 14 are more similar to tools found at 4 000 years ago from other sites in the Elands Bay area (Jerardino 1995). Layer 14 has also produced an uncalibrated radiocarbon date of 5530±50 (shell, Pta-5981). This leads researchers to believe that layers 13 and 14 have been mixed with later units (Jerardino 1995). For this reason, no samples from layer 13 or 14 will be analysed in the study.

The lower talus deposits, which include layers 5-8, date between 3 160 to 4 020 bp (Robey 1987). This unit was situated outside the shelter and mostly comprised of undifferentiated shell (Robey 1987). It is thought to be a secondary deposit from the occupants of the shelter removing material to increase living space (Robey 1987). Layer 5c is believed to be compromised with older deposit (Jerardino 1995) and will not be included in this study. Once again, there is a hiatus between the lower talus deposit and the next section. This coincides with Hiatus 1 observed at EBC and is believed to represent a shift from closed to open site use (Henshilwood *et al.* 1994).

The bulk of the material recovered from TC dates between 760 to 1780 bp. These layers (1-3) formed the fill in a basin excavated by the occupants to increase living space within the shelter (Robey 1987). They are clearly stratified, consisting of shell middens and ash heaps (Robey 1987). It should be noted that layer 1 is subdivided into 1a and 1b, with 1a being surface deposit (Robey 1987).

The location of layers 4, 9 and 12 are uncertain, and their radiocarbon dates ambiguous (Jerardino 1995, Robey 1987). Material from these layers has been excluded from this study.

Table 3.2: Calibrated radiocarbon dates for Tortoise Cave. Dates calibrated on Oxcal version 4.2, using the SHcal13 calibration curve.

Layer	14C BP	95.4% (2sigma) cal age BP	median cal. BP	Lab identifier	Material dated
1a	760±50	734–560	662	Pta 3600	Wood
2a	1660±45	1611–1378	1507	Pta 5855	Charcoal
2b	1580±50	1533–1320	1428	Pta 3309	Charcoal
3a	1590±50	1539–1520	1440	Pta 5817	Charcoal
3a	1610±50	1568–1352	1459	Pta 3311	Charcoal
3a	1620±50	1574–1360	1467	Pta 3310	Charcoal
3a	1680±50	1700–1409	1536	Pta 3312	Charcoal
3b	1780±50	1803–1537	1650	Pta 5615	Charcoal
3b	1800±60	1824–1541	1670	Pta 5616	Charcoal
5a,b	3560±60	3972–3638	3790	Pta 5498	Shell,corrected
6	3520±60	3900–3582	3751	Pta 3604	Charcoal
8	4020±60	4788–4235	4444	Pta 3595	Charcoal
10	4190±60	4840–4453	4681	Pta 3608	Charcoal

At TC, faunal remains consist of bird, fish, mammal and reptile bones, but the most common species throughout the sequence is *C. angulata* (Robey 1987, Klein 1987). From minimum numbers of individual (MNI) based on humeri counts, it was determined that the largest number of tortoise remains occurred at the site between 4 330 – 4 490 bp (Klein 1987).

3.3 Paleoenvironmental research in the Elands Bay Region and surrounds

The Elands Bay region has one of the best late Quaternary paleoclimate records in southern Africa. The estuary of Verlorenvlei and the depositional sequence of Elands Bay Cave both provide long, deep sequences, lending themselves to analysis. Verlorenvlei has produced many sediment cores that have allowed for pollen and diatom analysis, leading to insights into climate as well as past vegetation communities, sea-level and hydrological fluctuations (Meadows *et al*. 1996; Baxter and Meadows 1999; Meadows and Baxter 2001; Stager *et al*. 2012). Elands Bay Cave has also provided researchers with many proxy sources including fauna, micro-fauna, charcoal, pollen, and sediment analysis. This has allowed for research to

be conducted on past vegetation communities, climate and sea-surface temperatures (Klein and Cruz-Uribe 1987; Avery 1990; Cohen *et al*. 1992; Meadows and Baxter 1999; Cowling 1999; Stowe & Sealy 2016; Cartwright *et al*. 2016; Klein and Cruz-Uribe 2016). Hyrax middens and pollen cores from the eastern Cederberg provides information on rainfall, temperature and vegetation changes (Meadows & Sugden 1993; Scott & Woodborne 2007a; Scott & Woodborne 2007b; Meadows *et al*. 2010; Chase *et al*. 2011; Quick *et al*. 2011; Chase *et al*. 2015). The geological record from Langebaan Lagoon provides information about sea-level change (Compton 2001).

Though the Cederberg and Langebaan records are approximately 100km away from Elands Bay and may experience slightly different environmental stimuli, they will provide a good comparative record. Thus, this section will highlight differences and similarities within the records during the last 13 000 years. Findings will be grouped into three periods, namely the Younger Dryas (13 000 to 11 500 calibrated years before present) and early Holocene (11 500 to 8 200 calibrated years before present), the mid Holocene (8 200 to 4 200 calibrated years before present) and the late Holocene (4 200 calibrated years before present to present).

3.3.1 Younger Dryas & Early Holocene

The Younger Dryas (YD) is a cold interval within the global climate record, dated to between 13 000 to 11 500 calibrated years before present (cal. BP) (Dansgaard 1993). The early Holocene follows on from the Younger Dryas and is seen to end at the 8200 cal. BP bond event, which marks a brief cooling in global temperatures.

Evidence of the Younger Dryas in the Elands Bay region can be seen in sea surface temperature (SSTs) derived from $\delta^{18}O$ of aragonite in limpet shells from EBC, showing a period of cooling between 12700-11500 BP (Cohen *et al.* 1992). Faunal evidence from EBC shows that vegetation during the YD was quite different from the scrubland of today. The presence of large grazing game such as *Equus capensis*, *Syncerus antiquus* and *Redunca* spp.

at 13 000 bp is indicative of an open grassland system (Klein & Cruz-Uribe 1987). After 12 000 bp some grazing fauna such as *Equus capensis* disappear and the increase of browsing fauna such as *Raphicerus* spp indicates the presence of grasslands with a bushier component into the early Holocene (Klein & Cruz-Uribe 1987). Charcoal and pollen from EBC during the YD, is that of mesic thicket, indicating greater moisture availability and a larger grassland component than seen today (Parkington *et al.* 2000, Meadows & Baxter 2001). Stowe & Sealy (2016) have demonstrated, through isotopic study of tooth enamel from archaeological bovids excavated from EBC, that these grasslands were predominately C_3. From this they infer that winter rainfall was stronger during the Younger Dryas.

Pollen cores from Driehoek vlei in the Cederberg show very limited change within the environmental record (Meadows & Sugden 1993). However, increases in restioid fynbos are believed to indicate moister conditions during the Younger Dryas (Meadows & Sugden 1993). Isotope analysis of the De Rif hyrax middens in the Cederberg show less negative $\delta^{13}C$ and more positive $\delta^{15}N$ values between 12 700 to 11 500 cal. BP. This is indicative of less moisture during the Younger Dryas (Chase *et al*. 2011). However, pollen records from the De Rif midden are inconsistent with the interpretations of the isotope record, as the period of the YD is marked by lower proportions of pollen from taxa that favour more xeric conditions (Quick *et al.* 2011). Restioid and scrub pollen dating between 13 000 to 12 000 cal. BP from the Pakhuis Pass hyrax midden also indicate drier conditions during the YD (Scott & Woodborne 2007a). It must be noted that the mountain fynbos surrounding De Rif, Driehoek and Sneuuberg vlei acts as a constraint on climate interpretations from pollen analysis. That is that, the strong adaption of fynbos to their underlying substrates allows these plants to persevere through different environmental stresses. This remarkable preservation means that pollen records in areas dominated by fynbos will reflect periods of stability, even if there was climatic change (Quick *et al*. 2011).

Faunal evidence suggests that vegetation in the early Holocene would have been more like fynbos than the strandveld that is seen at present in Elands Bay (Klein & Cruz-Uribe 1987). This was inferred from the observation that in the early Holocene, *Raphicerus melanotis*, which prefers closed bushy environments, outnumbers *Raphicerus campestris*, which prefers more open, grassy environments (Klein & Cruz-Uribe 1987; Klein & Cruz-Uribe 2016). The presence of hedgehogs and the comparatively large size of dune mole rat distal humeri at EBC during the early Holocene is suggestive of greater moisture availability during the period (Klein & Cruz-Uribe 1987, Klein 1991). Charcoal and pollen from EBC is that of mesic thicket, indicative of greater moisture availability (Parkington *et al.* 2000, Meadows & Baxter 2001).

Low $\delta^{13}C$ and $\delta^{15}N$ values and increases in arboreal pollen in hyrax middens indicate cooler and moister conditions between 11 000 to 10 000 cal. BP at De Rif (Chase *et al.* 2011, Quick *et al.* 2011). Pollen cores from Sneeuberg vlei also indicate limited change during the Holocene, although cool and moist conditions are inferred from proteoid pollen at 9 600 cal. BP (Meadows & Sugden 1993). Evidence for a cool and moist early Holocene is also seen in the Truitjes Kraal hyrax midden. This is indicated by low $\delta^{13}C$ and $\delta^{15}N$ values, along with higher proportions of arboreal and *Proteacea* pollen at 9 500 cal. BP (Meadows *et al*. 2010). The presence of *Olea* and *Cyperaceae* from the Pakhuis Pass midden are thought to indicate cooler and moister conditions at 9 000 cal. B (Scott & Woodborne 2007a).

3.3.2 The mid-Holocene

The mid-Holocene is defined from the 8 200 cal. BP bond event to the 4 200 cal. BP bond event. It is a period of aridity in the southern hemisphere, commonly referred to as the Holocene Altithermal (HA) (Walker *et al.* 2012).

Very little paleoclimatic information is available from EBC for this period due to a hiatus within the record. Pollen from the Grootdrift core at Verlorenvlei has a high abundance of

Asteraceae and *Chenopodiaceae,* indicative of a more arid environment at 6300 cal. BP (Meadows 1996). These pollen types are abundant in the Klaarfontein springs, approximately 18 km inland of Elands Bay, between 7500-4000 cal. BP, again indicating aridity (Meadows & Baxter 2001). Miller *et al.* (1995) reports sea-level to be 2.8 metres higher than present at 4 200 bp, matching evidence for a rise in sea-level in the Grootdrift core, which shows a +3 metres transgression between 5 000 and 4 000 cal. BP (Baxter & Meadows 1999). Pollen from Klaarfontein Springs records an estuarine environment from this time, with saline tolerant plants such as *Chenopodiaceae*, being present until 3700 cal. BP (Meadows & Baxter 2001). Evidence from Langebaan Lagoon also suggests an increase in sea level between 4 000-6 000 cal. BP (Compton 2001).

Both the Driehoek and Sneeubergvlei pollen cores show a period of stability during the mid-Holocene (Meadows & Sugden 1993). However, *Asteraceae* pollen from the Pakhuis Pass midden record indicate drier conditions from 8 500 to 5 600 cal. BP (Scott & Woodborne 2007a). High $\delta^{13}C$ and $\delta^{15}N$ values from 8 000 to 3 000 cal. BP from the Truitjes Kraal midden also indicate dry and warm conditions during the HA. The dominance of *Asteraceae* elements from 7 000 to 3 000 cal. BP in the Truitjes Kraal midden are a further indication of aridity (Meadows *et al*. 2010). Unfortunately, no isotopic data exists for the De Rif midden between 8 000 to 6 000 cal. BP. Low $\delta^{13}C$ and $\delta^{15}N$ values in the hyrax midden at Katbakkies implies an increase in moisture between 6 900 to 5 600 cal. BP (Chase *et al.* 2015). Chase *et al.* (2015) reason that whilst the Katbakkies site falls into the WRZ. The site's position along the boundary of the WRZ and SRZ makes it a valuable site to track the influence of tropical easterlies in the WRZ. CREST analysis–a climate reconstruction model based on pollen probability density functions– indicates an increase in summer rainfall (of approximately 50 mm) between 6 900 to 5 500 cal. BP (Chase *et al.* 2015). The prominence of karroid shrub elements at the Pakhuis Pass midden is also suggestive of an increase in received summer

rainfall at 5 600 cal. BP (Scott & Woodborne 2007a). Sharp increases in ^{13}C and ^{15}N at the Katbakkies midden between 5 600 to 4 700 cal. BP signify a period of aridity (Chase *et al.* 2015). CREST analysis from Katbakkies shows that from 5 600 to 4 900 cal. BP there is a gradual decrease in summer rainfall (Chase *et al.* 2015). Decreases in summer rainfall are also indicated by low $\delta^{13}C$ values after 5 600 to 4 900 cal. BP at Pakhuis Pass midden (Scott & Woodborne 2007a). Changes in the pollen principal component analysis also indicate more C_3 plants and less summer rainfall after 5 600 to 4 900 cal. BP at Pakhuis Pass midden (Scott & Woodborne 2007a). Principal components analysis of pollen data also indicates a slight cooling at 5 000 cal. BP (Scott & Woodborne 2007a). Unfortunately, there is no reliable reconstruction from the Pakhuis Pass midden from 4 900 cal. BP to 2 800 cal. BP (Scott & Woodborne 2007a).

3.3.3 The late Holocene

The late Holocene can be described as beginning at the 4 200 cal. BP cooling event and extending up to the present.

Percentage aragonite and $\delta^{18}O$ from molluscs show that SST is approximately 2ºC lower between 3 000-2 000 bp, compared with 4000 bp at Elands Bay (Cohen 1992). Charcoal from 4 000 to 3 000 bp at EBC points to a drier environment, with a strong strandveld component (Parkington *et al.* 2000). From the pollen record at Verlorenvlei, Meadows & Baxter (1999) suggest a one metre drop in sea level between 3 700 to 2 800 cal. BP, leading to a depositional hiatus in the core from Grootdrift (Meadows & Baxter 2001). Pollen from the Klaarfontein record shows a fresh water system at 1 800 cal. BP, with increases in salt intolerant plants such as *Cyperus* sp. and *Typha* sp. (Meadows & Baxter 2001). Pollen from this record is also indicative of moister conditions, with arboreal and fynbos elements appearing at 1 800 cal. BP. However, after 1 800 cal. BP the Klaarfontein record shows more estuarine conditions, resulting from sea level increase. Pollen from *Chenopodiaceae* and

Mesmbryanthemum is seen once again, while *Typha* sp. declines (Meadows & Baxter 2001). Diatom and sedimentological evidence from Verlorenvlei point to more winter rainfall between 1 400 to 1 200 cal. BP (Stager *et al*. 2012). However, between 1100 to 960 cal. BP epiphytic diatoms increase within the record. Stager *et al.* (2012) interpret this to represent decreasing lake levels and precipitation. This would indicate that the Medieval Climate Anomaly (MCA), 1 050-550 cal. BP (Mayewski *et al*. 2004), was marked by drier conditions in the Elands Bay Region. The diatom record at Verlorenvlei points to enhanced rainfall during the last 700 years, with rainfall peaks occurring at ~600, 530, 470, 330, 200, 90 and 20 cal. BP (Stager *et al.* 2012). SSTs derived from mollusc %aragonite and $\delta^{18}O$, show a marked temperature drop at 500 bp (Cohen *et al.* 1992). The charcoal evidence from EBC does not distinguish either the MCA or the LIA and suggests that the period between 1400 to 320 bp was stable, with asteraceous shrubland and xeric thicket (Cowling *et al.* 1999). Unfortunately, there is no record from EBC after 320 bp as evidence of occupation in the cave (if any) is not preserved. The pollen and diatom record from this period are difficult to interpret to due to heavy presence of farming and colonial occupation (Baxter & Meadows 1994).

Evidence from Langebaan Lagoon shows a sea-level regression of -1 to -2 m.a.m.s.l. from 2 500 to 1 800 cal. BP, followed by a rise of between +0.5 and +1 m.a.m.s.l.at 1 300 cal. BP (Compton 2001).

Interpretations of ^{13}C and ^{15}N at Katbakkies indicate a period of aridity between 4 000 to 2 700 cal. BP (Chase *et al*. 2015). CREST software also indicates low summer rainfall rain between 3200 to 2700 cal. BP (Chase *et al*. 2015). Succulent and shrub pollens are dominant between 3 000-700 cal. BP in the De Rif hyrax midden, indicative of a stable but arid late Holocene (Quick *et al.* 2011). High $\delta^{13}C$ and $\delta^{15}N$ values, as well as, decreases in arboreal pollen from 3 000 to cal. BP also indicate aridity at Truitjies Kraal (Meadows *et al*. 2010)

However, increases in *Ericaceae* pollen in the Driehoek core at 3 230 cal. BP and in the Sneeuberg core at 3 310 to 1 990 cal. BP signify cooler and moister conditions (Meadows & Sugden 1993). The presence of *Cyperaceae* pollen in the Pakhuis Pass hyrax midden between 2 800 to 2000 cal. BP signals a period of increased moisture availability (Scott & Woodborne 2007a). Pollen analysis at Katbakkies indicates that summer rainfall increases to 90 mm between 2500 and 2600 cal. BP, after stabilising at 60 mm till the end of the record (Chase *et al*. 2015). Increases in *Cyperaceae* pollen and low $\delta^{13}C$ and $\delta^{15}N$ values between 2 400 to 1 300 cal. BP at the Katbakkies dassie midden indicates a cool and moist period (Meadows *et al.* 2010). Increases in *Asteraceae* pollen and a decline in $\delta^{13}C$ values between 2 000 to 1 000 cal. BP indicates a period of aridity at Pakhuis Pass (Scott & Woodborne 2007a). High $\delta^{13}C$ and $\delta^{15}N$ values after 800 cal. BP till the base of the sequence at 570 cal. BP at Katbakkies indicates arid conditions (Meadows *et al*. 2010). The presence of *Cyperaceae* pollen at 500 cal. BP indicates a return to cool and moist conditions at Pakhuis Pass (Scott & Woodborne 2007a).

3.3.4 Summary

Table 3.3 below provides a summary of the key trends in temperature and moisture availability during different periods for the Elands Bay and Cederberg regions. In general, there is a consensus between proxy records from the two regions. The exception is the Younger Dryas period, when temperatures were cool and moist on the coast but dry in the eastern Cederberg. Meadows *et al*. (2010) believes this difference to indicate that various parts of the WRZ are under different climatic controls during different periods. Given that the Cederberg sites of Pakhuis Pass, Katbakkies and De Rif benefit from and are influenced by summer rainfall (Scott & Woodborne 2007a, Scott & Woodborne 2007b, Chase *et al.* 2015), it is possible that the dry conditions seen in the eastern Cederberg during the YD are due to a

weakening of the summer rainfall system causing reductions in received summer rain (Chase *et al*. 2015).

Table 3.3: Comparison of key trends in temperature and moisture between Elands Bay and the Cederberg

	Region	
Period	Elands Bay	Cederberg
500 cal. BP	cool & moist	cool & moist
600-1 000 cal. BP	warm & dry	warm & dry
1 500-2 500 cal. BP	cool & moist	cool & moist
4 200- 8 000 cal. BP	warm & dry	warm & dry
9 000- 11 000 cal. BP	cool & moist	cool & moist
11 500- 13 000 cal. BP	cool & moist	dry

Chapter Four

4. Methods

4.1 Sample Preparation and Pre-treatment

165 tortoise bones from EBC and TC were selected for analysis from the collections curated at the Iziko South African Museum. 120 samples came from EBC, 60 from the late Holocene and 60 from the early Holocene. Initially, it was the intention to sample only one skeletal element throughout the study, in order to avoid possible repeat sampling of the same animal. The nuchal bone from the carapace was preferred as these can be easily identified, and there is only one nuchal per animal. This approach worked well for the early Holocene at EBC and for TC, where there were large numbers of nuchal bones in the collection. In the late Holocene levels of EBC, 45 nuchal bones were supplemented with 30 right femoral plates from the plastron. This was necessary because, especially for the period 0-1000 BP at EBC, there were insufficient nuchal bones to provide an adequate sample.

As mentioned in section 1.2.2, each plate within a tortoise shell grows in concentric increments (Germano 1998). This means that bone within plates is not homogeneous. Weeber (2013) showed that within-plate variation could be as large as 1.1‰ in the $\delta^{13}C$ values and 1.9‰ in the $\delta^{15}N$ values. This means that an entire plate (or a representative sample thereof) must be homogenised in order to obtain an average isotope value for the lifetime of the animal. Nuchal bones are symmetrical, allowing for half the plate to be analysed and the rest preserved for further study. Unfortunately, the femoral plate is asymmetrical so the whole bone must undergo treatment. Plates were selected on the following basis: a) They should not have been burnt or treated with glue or consolidant, and b) they were unbroken or if symmetrical one half was preserved. If conditions a) and b) were met and a unit had more suitable plates than were required, those with the least discolouration were selected. Plates

selected for analysis were catalogued and maximum dimensions and sample weights recorded.

All laboratory work was performed at the Stable Light Isotope laboratory in the Department of Archaeology at the University of Cape Town. Initially, samples were processed according to the methods described by Sealy *et al*. (2014), with minor modifications. At a later stage, some samples were decalcified using EDTA, as described below.

Plates were initially dry-brushed with a toothbrush and the surfaces lightly sanded with 0.5mm sandpaper to remove surface contaminants. Nuchal bones underwent an additional step, being halved lengthwise, using a Dremel drill equipped with an emery disc cutting wheel. Half of the bone was processed for analysis, while the other half was returned to the collection.

4.1.1 HCl method

Half of each nuchal bone or the entire femoral plate were placed into pre-weighed glass beakers and demineralized in 0.1 to 0.2M hydrochloric acid (HCl) at room temperature (Ambrose 1990). HCl was changed daily until bone became flexible and soft, whilst still retaining its original shape *i.e.* a pseudomorph of the bone was obtained. The concentration of HCl depended on the age of the bone. 0.2M HCl was used for samples between 300 to 2000 years of age, whilst samples between 2000 to 4000 years of age were treated with 0.1M. Samples 8000-12000 years old were treated with 0.1M HCl at 4°C. The concentration of acid within this range has been shown not to affect the quality of collagen extracted nor the resultant isotope ratios (Pestle 2010). Decalcification took between several days and five weeks. Visible macroscopic bodies such as rootlets, if present, were removed with tweezers. Samples were then rinsed three times in distilled water and then left in distilled water until the water remained neutral when tested using pH paper. Samples were then treated with 0.1M sodium hydroxide (NaOH) for twelve hours in order to remove base soluble contaminants

(Ambrose 1990). Again, samples were rinsed 3X in distilled water and then soaked in distilled water, changed daily, until the pH remained at 7. At this stage, the extracted collagen was dissolved ('gelatinized') in water acidified with HCl to pH 3. This was done on a hot-plate at 70°C, stirring continuously with a magnetic stirrer. This step causes the collagen chains to disassociate, forming a gelatinous solution and effectively homogenising the carapace or plastron plate. No visible particles of undissolved material were present in any of the samples after gelatinization. It should be noted that this gelatinized sample is mostly made up of collagen, however, small traces of non-collagenous proteins (NCPs) may be included (Schwarcz & Schoeninger 1991). The beakers were then placed in a freezer at -4°C until the gelatin solutions were frozen solid, or were at least very viscous. Finally, they were freeze dried for twelve hours. The mass of the extracted gelatin was measured and the % gelatin yield calculated by dividing the weight of the gelatin by the original starting weight of bone, and multiplying by 100.

4.1.2 EDTA Method

Previous experience in the UCT laboratory had been that it is difficult to extract collagen from terminal Pleistocene or early Holocene samples from coastal caves in South Africa using HCl. In this study, a few samples between 8000-12000 years old were treated with HCl, but they dissolved in the HCl so that collagen could not be isolated. Older samples were therefore decalcified using EDTA (ethylenediaminetetraacetic acid) which is less aggressive (Cleland *et al*. 2012). Tuross (2012) showed that decalcification using the HCl and EDTA methods produces collagen that yields identical stable carbon and nitrogen isotope and radiocarbon measurements, within analytical error. In this study, six plates from TC that yielded collagen using the HCl method were also decalcified using EDTA, and both collagen preparations were analysed. EDTA was used for the older samples and for a small number of more recent ones that had failed to yield usable collagen using HCl.

Half a nuchal plate was placed into a pre-weighed glass beaker and treated with 0.5M EDTA at room temperature. EDTA was replaced every six days until a pseudomorph was achieved. Samples were then rinsed seven times with distilled water and once with 0.1M NaOH, after which they were placed in distilled water in a fridge overnight. Next the pseudomorph was 'gelatinized' in water acidified with HCl to pH 3. Finally, they were freeze dried for twelve hours. The mass of the extracted gelatin was measured and the % gelatin yield calculated as above.

4.2 Mass Spectrometry

Approximately 0.5 mg of each freeze-dried gelatin was weighed into a tin capsule, then combusted at 1020°C in a Flash 2000 organic elemental analyser coupled to a Delta V Plus isotope ratio mass spectrometer. In the elemental analyser the sample is combusted in the presence of a chromium oxide (with an excess of oxygen), producing carbon dioxide and various nitrogen containing gases. These gases are then introduced into a reducing environment in the presence of copper at 650 ºC, to remove excess oxygen and convert nitrogen oxides into pure nitrogen gas (Brenna 2007). Gases are then passed through a manganese chlorite trap and water is removed from the system by a drying tube. Gases are transported in a stream of helium carrier gas through a gas chromatographic column to separate CO_2 and N_2, then passed through a Conflo IV gas unit and into the mass spectrometer (IRMS).

4.3 Calibration & Data Analysis

Along with samples, in-house standards were run in the IRMS in order to assess analytical precision, and in order to correct the measured values to the international standards PDB and AIR. In-house standards used in this study were Choc, MG, Seal and Valine. The external precision calculated from the standard deviations of over 12 standards per run was better than

0.2‰ (n=182) for δ^{13}C and δ^{15}N. Weight %C, weight %N and C: N ratios were also recorded as indicators of collagen quality.

For samples with well-preserved collagen, δ^{13}C and δ^{15}N were then analysed using descriptive statistics including means, standard deviations and ranges. Pearson's R tests were used to test if δ^{13}C and δ^{15}N vary according to similar controls. Kruskal-Wallis tests were performed to test for statistically significant variations between different time periods and Mann–Whitney tests used to explore these differences. These results will be discussed in the next chapter.

Chapter Five

5. Results

This chapter presents the collagen quality indicators, $\delta^{13}C$ and $\delta^{15}N$ values for 86 *C.angulata* specimens. All results are presented in Table 5. 1. Ten specimens have been excluded from the statistical analysis and interpretation of results as the collagen they yielded did not meet the collagen quality requirements set out by Ambrose (1990) and Van Klinken (1999). These requirements are that samples produce a collagen yield greater than 1%. %C should fall in the range from 15.3% to 47%, and %N from 5.3% to 17.3% and lastly, the C: N ratio should be in the range 2.9 to 3.6. Sample #18776 has a %C value of 48.7%, which is just over Ambrose's recommended maximum; however, given that the %N is within the acceptable range at 16.3%, as is the C: N ratio (3.5) the isotope measurements will be included in this analysis. Sample #18020 has low %C and %N values but a good C:N ratio. %C and %N values can be low when collagen yield is low as is the case of #18020 (Ambrose 1990). Therefore, sample #18020 will be included in this analysis.

Table 5.1: $\delta^{13}C$, $\delta^{15}N$, %C, %N, C:N ratio, % collagen yield, stratigraphic unit and chronological unit for all samples from which collagen was extracted. Analyses were done in duplicate and values averaged. UCT IDs in bold indicate collagen extracted using the EDTA method. Asterisks indicate samples that do not meet collagen quality criteria; these were excluded from further consideration. Samples with numeric values under stratigraphic/sedimentary unit are from Tortoise Cave.

UCT ID	$\delta^{13}C_{collagen}$(‰)	$\delta^{15}N_{collagen}$(‰)	%C	%N	C:N ratio	Collagen yield (%)	Stratigraphic/Sedimentary unit	Chronological unit
16450	-21.5	9.1	40.8	14.6	3.3	22	SENG	1
16451	-21.9	5.3	42.7	15.6	3.2	20	ELCH	1
16452	-20.4	10.2	41.7	15.3	3.2	22	ELCH	1
16454	-21.5	9.0	44.7	16.3	3.2	25	POTA	1
16455	-20.4	7.7	43.9	15.7	3.3	19	SITH	1
16563	-21.3	8.2	40.8	14.4	3.3	26	SITH	1
16564	-20.7	8.7	39.4	14.7	3.1	22	IANS	1
18070	-20.5	3.1	40.1	14.9	3.1	23	NKOM	1
18071	-21.4	7.5	43.2	15.6	3.2	24	NKOM	1
18774	-21.7	10.3	46.4	16.1	3.4	21	SITH	1
18775	-21.6	12.1	39.7	14.3	3.2	25	SITH	1
18776	-21.5	11.2	48.7	16.3	3.5	23	SITH	1
18777	-20.1	2.8	44.0	15.0	3.4	20	SITH	1
18778*	-20.5	10.1	13.1	4.6	3.3	21	SITH	1
18782	-21.2	11.1	45.5	16.0	3.3	19	SITH	1
18066	-19.1	10.9	40.9	14.8	3.2	20	DOLL	2
18068	-21.1	11.2	29.7	11.6	3.0	26	DOLL	2
18069	-19.9	4.3	37.9	15.4	2.9	26	DOLL	2
18771	-23.5	8.1	43.0	15.1	3.3	23	DOLL	2
18772	-21.2	11.2	35.4	12.3	3.4	21	DOLL	2
18773	-20.5	11.4	43.6	15.7	3.2	23	DOLL	2
18783	-20.1	10.2	46.5	16.5	3.3	21	EDDI	2
18784	-20.1	10.3	45.9	16.3	3.3	23	EDDI	2
18785	-20.6	12.2	44.9	15.8	3.3	19	EDDI	2
18788	-20.3	11.7	45.5	16.3	3.3	23	EDDI	2
16456	-21.4	5.6	42.8	15.6	3.2	26	JECH	3
16457	-21.4	9.7	42.5	15.7	3.2	23	JECH	3
16458	-20.7	9.2	43.2	16.0	3.1	20	TCHA	3
18163	-20.9	8.6	41.9	15.2	3.2	25	DOLA	3
18164	-20.4	9.2	41.2	14.7	3.3	23	DOLA	3
18166	-21.1	8.8	37.4	13.5	3.2	24	MIJA	3
18168	-21.8	11.9	42.4	15.0	3.3	24	RAYI	3
18170	-19.7	17.4	32.3	12.6	3.0	25	MRSN	3
18171	-20.7	8.7	37.7	12.9	3.4	25	BUTH	3
18172	-20.4	12.8	38.2	13.3	3.3	19	BUTH	3
18173	-21.4	9.7	40.0	14.7	3.2	23	ROBE	3
16566	-21.7	9.0	45.1	16.1	3.3	20	2	4
16567	-20.3	9.7	40.9	14.7	3.2	24	2	4
16568	-18.8	10.1	39.2	14.3	3.2	20	2	4
16569	-18.5	14.1	43.1	16.2	3.1	23	2	4
16570	-19.3	7.5	42.9	15.5	3.2	20	2	4
16571	-21.1	8.1	42.9	15.5	3.2	23	2	4
16572	-20.9	11.0	39.3	14.1	3.2	19	2	4
16573	-22.1	8.5	40.8	15.0	3.2	21	2	4
16574	-21.5	9.2	42.9	15.6	3.2	19	3	4
16576	-20.2	7.6	43.3	15.5	3.3	19	3	4
16577*	-22.0	9.6	4.7	1.2	4.6	14	3	4
16580	-21.8	8.3	45.0	16.2	3.2	20	3	4
16581	-21.8	10.4	38.5	14.0	3.2	18	3	4
16459	-19.0	10.3	46.3	16.1	3.3	23	LARM	5
20106	-20.4	11.4	40.7	14.3	3.3	25	LARM	5

UCT ID	$\delta^{13}C_{collagen}$(‰)	$\delta^{15}N_{collagen}$(‰)	%C	%N	C:N ratio	Collagen yield (%)	Stratigraphic/Sedimentary unit	Chronological unit
16460	-20.3	9.3	42.3	15.8	3.1	24	JOFR	6
16461	-20.6	9.1	39.8	14.7	3.2	13	JOFR	6
16462	-20.3	7.4	41.1	15.1	3.2	15	JOFR	6
16463	-19.9	7.0	42.8	15.7	3.2	12	JOFR	6
16464	-17.3	9.9	42.2	15.6	3.1	23	JOFR	6
16466	-19.7	7.0	37.4	13.5	3.2	15	OBOT	6
16467	-21.5	8.9	40.2	14.7	3.2	20	OBOT	6
16469	-19.1	10.0	41.5	14.0	3.5	24	SASO	6
16471	-21.5	9.1	41.7	15.1	3.2	21	SASO	6
16465	-21.3	8.1	41.0	14.8	3.2	17	JOFR	6
18019*	-24.5	4.8	40.8	7.1	6.7	7	7	6
18020	-22.4	9.2	9.9	3.2	3.6	8	8	6
16474	-21.1	9.1	42.8	14.8	3.4	12	NEFE	7
16475	-22.4	7.2	41.0	14.3	3.3	15	NEFE	7
18382	-19.4	9.7	29.4	10.4	3.3	17	UITT	7
18385	-22.4	8.0	39.6	13.7	3.4	16	SHAK	7
18386	-22.4	5.8	43.6	14.4	3.5	12	SHAK	7
18387	-21.7	8.0	43.7	14.8	3.4	15	SHAK	7
18388	-23.0	5.8	33.7	11.7	3.4	22	SHAK	7
18389	-20.3	10.7	35.4	12.6	3.3	22	WAYA	7
18390	-20.0	8.8	32.5	11.3	3.4	12	WAYA	7
18392	-19.9	16.6	34.6	13.2	3.4	14	WAYA	7
20158	-21.7	11.8	37.3	12.7	3.4	6	10	7
16477	-21.7	11.7	31.6	10.6	3.5	5	EUSE	8
16478	-22.1	6.7	43.1	15.6	3.2	4	HOCO	8
16482*	-20.6	11.0	22.5	7.2	4.0	9	PELE	8
16487*	-22.6	13.8	23.6	7.2	4.9	5	PELE	8
16488*	-20.3	28.8	10.3	2.4	5.0	6	PELE	8
16490	-18.9	9.9	42.4	14.1	3.5	6	PELE	8
20163	-19.1	9.9	41.9	14.1	3.5	8	PELE	8
17432*	-27.2	2.8	26.7	6.3	5.0	3	LIMP	9
17436	-20.8	11.7	43.8	14.9	3.4	8	OXYG	10
17444*	-22.0	5.9	39.2	12.4	3.7	7	SLAG	10
17440*	-27.9	1.2	28.0	6.9	4.7	10	PBGB	10
17445*	-25.8	6.6	9.4	1.8	6.0	9	SLAG	10

5.1 HCL vs. EDTA method

Six samples from Tortoise Cave were demineralized using both HCl and EDTA. This was done to investigate whether there might be differences in the isotopic ratios due to differing methods of preparation. Following demineralization, all samples were gelatinized using dilute HCl as described in Chapter 4. The results are presented in Table 5.2. Figures 5.1 and 5.2 show the differences in $\delta^{13}C_{EDTA}$- $\delta^{13}C_{HCL}$ and $\delta^{15}N_{EDTA}$- $\delta^{15}N_{HCl}$ respectively.

Table 5.2: $\delta^{13}C$, $\delta^{15}N$, %C, %N, C: N ratio, % collagen yield, and provenance for collagen extracted using both acid demineralization and EDTA. The latter have UCT ID numbers in bold.

UCT ID	$\delta^{13}C_{collagen}$(‰)	$\delta^{15}N_{collagen}$(‰)	%C	%N	C:N ratio	Collagen yield (%)	Sedimentary unit
16566	-22.0	9.3	32.0	10.9	3.4	21	2
16566	-21.7	9.0	45.1	16.1	3.3	20	2
16568	-18.9	10.0	41.5	14.8	3.3	19	2
16568	-18.8	10.1	39.2	14.3	3.2	20	2
16570	-19.5	7.7	35.7	12.4	3.4	22	2
16570	-19.3	7.5	42.9	15.5	3.2	20	2
16571	-21.4	10.0	28.6	8.5	3.9	20	2
16571	-21.1	8.1	42.9	15.5	3.2	23	2
16572	-21.7	10.4	18.5	6.2	3.5	16	2
16572	-20.9	11.0	39.3	14.1	3.2	19	2
16573	-22.5	8.5	35.8	12.2	3.4	19	2
16573	-22.1	8.5	40.8	15.0	3.2	21	2

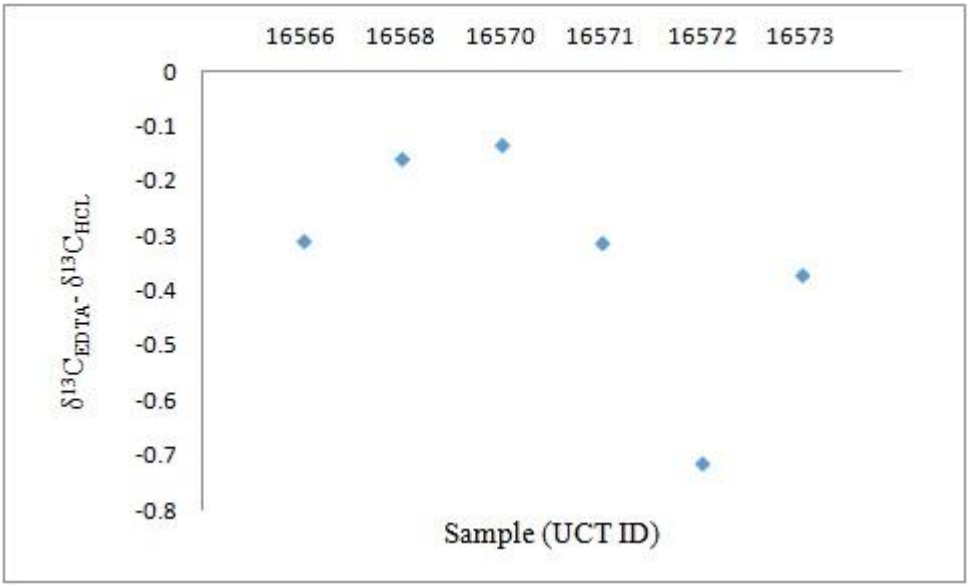

Fig. 5.1: *Scatterplot depicting* $\delta^{13}C_{EDTA}$- $\delta^{13}C_{HCL}$

As can be seen from Fig. 5.1 the differences in $\delta^{13}C$ between collagen produced by EDTA and HCL demineralization are less than 1‰, with mean $\delta^{13}C_{EDTA}$- $\delta^{13}C_{HCL}$ of 0.3±0.2‰. Thus, there is negligible variation in $\delta^{13}C$ produced by the two methods.

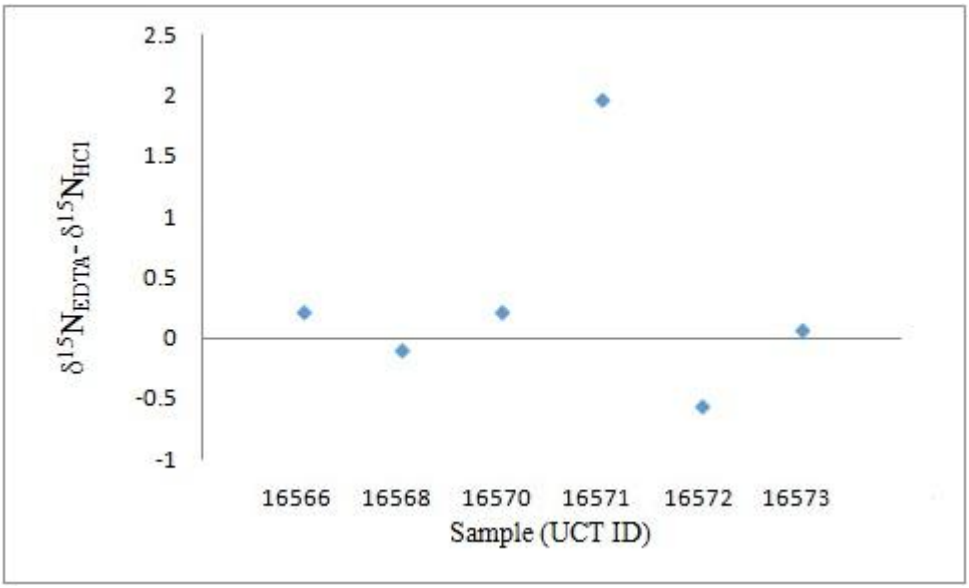

Fig. 5.2: *Scatterplot depicting* $\delta^{15}N_{EDTA}$- $\delta^{15}N_{HCl}$

For all samples except 16571, the difference in $\delta^{15}N$ between the EDTA and HCL method is less than 1‰. Sample #16571 is an outlier, exhibiting a difference of 2‰, but it should be

noted that the collagen from this sample produced by EDTA demineralization had a C:N ratio of 3.9, outside the acceptable range. Results for the comparison of the two methods for this sample should therefore be discounted. Excluding this outlier, mean $\delta^{15}N_{EDTA}$- $\delta^{15}N_{HCL}$ is 0.03±0.3‰. As for $\delta^{13}C$, there is negligible variation in the $\delta^{15}N$ values of collagen produced by the two methods.

Similar consistency between the results from the HCl and EDTA protocols has been demonstrated before (Tuross 2012). Therefore, data obtained from collagen produced using the EDTA method can be directly compared with data from collagen derived from the HCl method.

The range in $\delta^{13}C_{collagen}$ for all 76 specimens with good collagen preservation extends from -23.5 ‰ to -17.3 ‰ with a mean of -20.8±1.1 ‰. This is indicative of a predominantly C_3 diet with the possible inclusion of a small amount of C_4 or CAM plants. Given the large time range, the $\delta^{13}C_{collagen}$ values are tightly clustered. $\delta^{15}N_{collagen}$ for all 76 specimens ranges from 2.8 ‰ to 17.4‰ with a mean of 9.4±2.4‰. The $\delta^{15}N_{collagen}$ values are more varied yet, as seen in Fig. 5.3, most of the results cluster in the middle of the range.

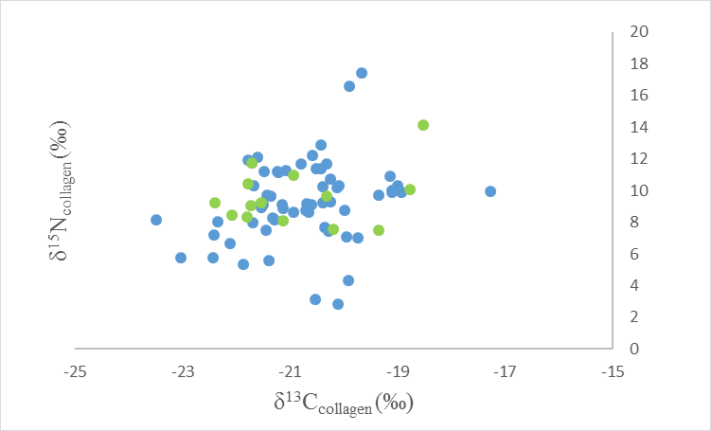

Fig. 5.3: *Scatterplot of $\delta^{13}C$ vs. $\delta^{15}N$ of the 76 specimens described in Table 5.2. Green markers represent tortoises found at EBC, whilst blue markers represent tortoises found at TC.*

5.2 Comparisons between EBC & TC

This section compares the isotopic results from EBC dating from 1180 to 1357 cal. BP and those from TC dating from 1320-1533 cal. BP. Samples from 1320-1533 cal. BP were selected for comparison as the largest sample size from TC is in this period. From EBC, samples from 1180 to 1357 cal. BP were selected as this period overlaps with the samples from TC. Figure 5.4 shows box plots comparing $\delta^{13}C$ and $\delta^{15}N$ results from the two sites during this period.

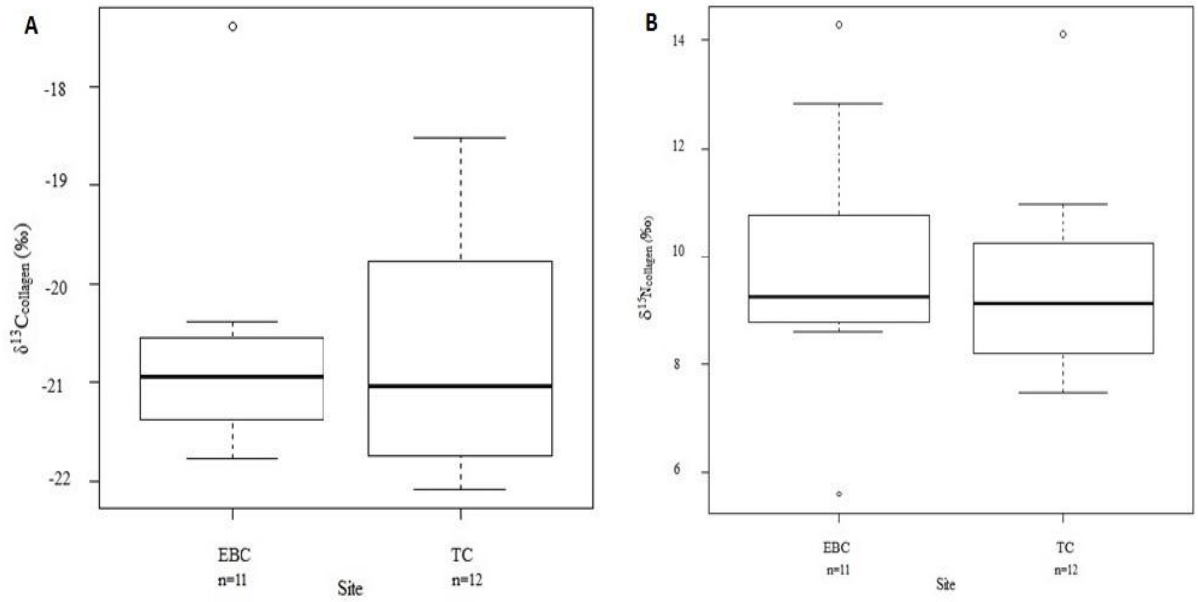

Fig 5.4: *Boxplot A compares $\delta^{13}C$ and B compares $\delta^{15}N$ from EBC and TC during overlapping time periods. The bold line in the middle of each box represents the median value. The lower quartile extends from the median line, down, to the end of the box. The upper quartile extends from the median line, up, to the end of the box. The whiskers represent the maximum and minimum endpoints of the continuously distributed data. The unfilled circles represent outlying data points. Outliers were defined as points falling outside the ranges: Quartile 1-(Interquartile range*1.5); Quartile 3+(Interquartile range*1.5).*

The $\delta^{13}C$ values from EBC during this period range from -21.8 to -19.7‰ with a mean of 20.9±0.6‰. Those from TC range from -22.1 to -18.5‰, with a mean of -20.6±1.3‰. These sets of values are not significantly different (Mann–Whitney Z-value = 0, p = 1).

The $\delta^{15}N$ values from EBC during this period range from 5.6 to 17.4‰, with a mean of 10.2±3.0‰. Those from TC range from 7.5 to 14.1‰ with a mean of 9.4±2.0‰. Once again, there is no significant difference between the two sites (Mann–Whitney Z-value = -0.68, p = 0.4965).

The lack of statistical difference between both isotopes at both sites was expected as the sites are only 4 km apart, meaning that the foraging ranges of people collecting tortoises would have overlapped. Thus, tortoises from both sites are in fact subsets of the same populations.

Therefore, samples from TC which fall into the same age bracket as samples from EBC can be grouped together. As such, this work analyses samples from 10 chronological periods – listed in Table 5.3 – in order to analyse the paleoenvironments of the Eland's Bay region.

Table 5.3: The calibrated age range of each chronological unit. Dates calibrated using Oxcal version 4.2, SHcal 13

Chronological Unit	Age cal. BP	Lab identifier
1	154-487	Pta 1815
2	744-1042	Pta 5822
3	1180-1357	Pta 6132
4	1320-1533	Pta 3309
5	2050-2305	Pta 5810
6	4005-4419	Pta 5806
7	4600-5270	Pta 5313; Pta 3595
8	8447-8993	Pta 1830
9	10690-11201	Pta 5306
10	12103-12725	Pta 0732

5.3 Comparison of $\delta^{13}C$ with $\delta^{15}N$ for Chronological Units

Chronological Unit 1 is dated to 154–487 cal. BP which is the time of the Little Ice Age. The LIA dates from 250 to 550 cal. BP, and although not continuous it is considered one of the most prominent cold periods since the YD (Tyson *et al.* 2000).

$\delta^{13}C_{collagen}$ for this unit ranges from -21.9‰ to -20.1‰ with a mean value of -21.1± 0.6‰, n=14. The range for $\delta^{15}N_{collagen}$ is 2.8‰ to 12.1‰ with a mean value of 8.3 ± 2.9‰, n=14. Figure 5.5 shows a plot of $\delta^{15}N_{collagen}$ against $\delta^{13}C_{collagen}$ for this unit.

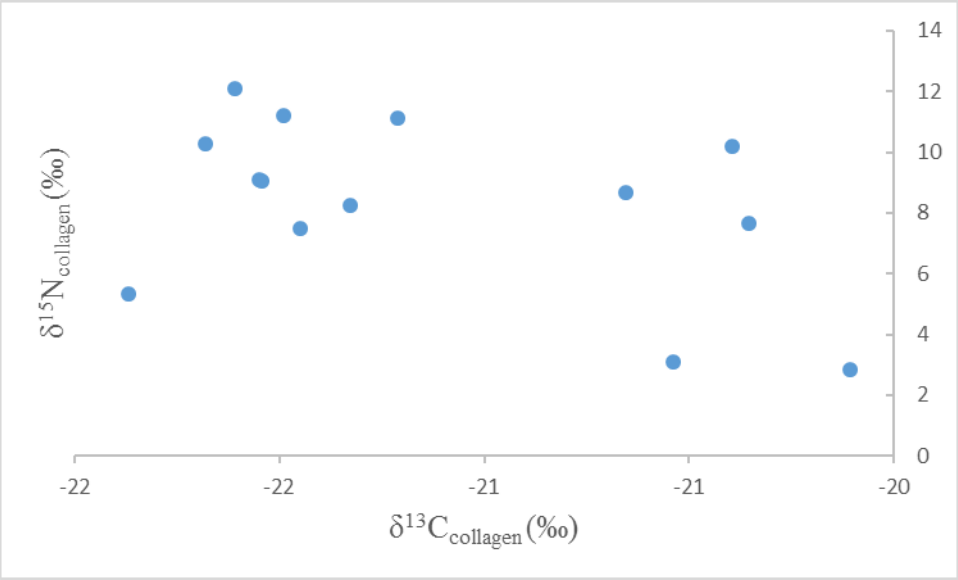

Fig. 5.5: *Scatterplot of $\delta^{13}C$ vs. $\delta^{15}N$ during Chronological Unit 1, from EBC, n=14.*

Fig. 5.5 depicts a weak relationship between $\delta^{13}C_{collagen}$ and $\delta^{15}N_{collagen}$. This is confirmed by a Pearson's R value of 0.44 and an R^2 co-efficient equal to 0.19. The Pearson's R test indicates a weak but positive relationship between $\delta^{13}C_{collagen}$ and $\delta^{15}N_{collagen}$ in Chronological Unit 1.

Chronological Unit 2 is dated to 744–1 042cal. BP which is the time of the Medieval Climate Anomaly (MCA). The MCA dates from 700 to 1 000 cal. BP and represents a period of increased temperature, however, it is not as globally extensive as the LIA (Tyson *et al*. 2000). $\delta^{13}C_{collagen}$ for this unit ranges from -23.5‰ to -19.2‰ with a mean value of -20.7± 1.2‰,

n=10. The range for $\delta^{15}N_{collagen}$ is 4.3‰ to 12.2‰ with a mean value of 10.2 ± 2.3‰, n=10. Figure 5.6 shows a plot of $\delta^{15}N_{collagen}$ against $\delta^{13}C_{collagen}$ for this unit.

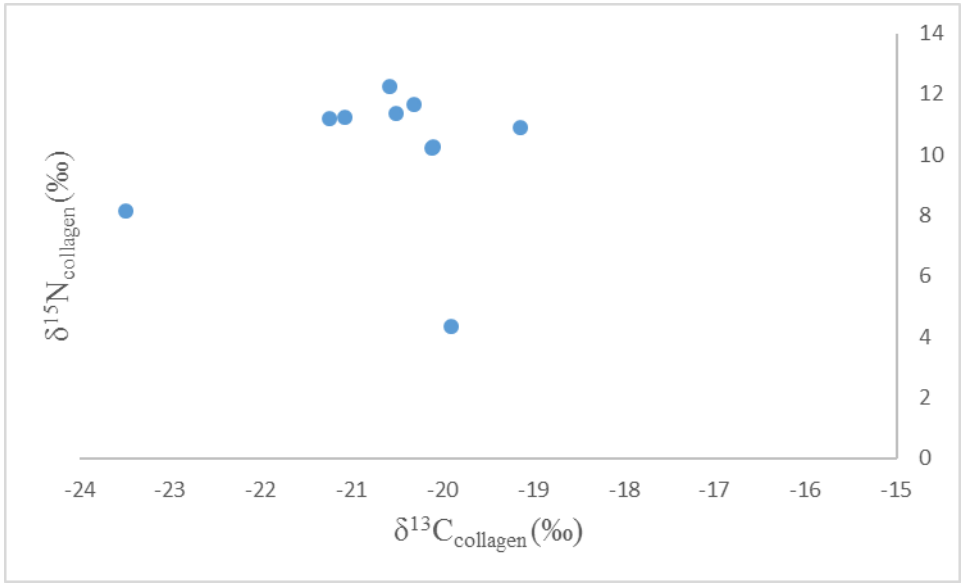

Fig. 5.6: *Scatterplot of $\delta^{13}C$ vs. $\delta^{15}N$ during Chronological Unit 2, from EBC, n=10.*

The results in Fig. 5.6 depict a weak relationship between $\delta^{13}C_{collagen}$ and $\delta^{15}N_{collagen}$. This is confirmed by a Pearson's R value of 0.46 and an R^2 co-efficient equal to 0.22. The Pearson's R test indicates a weak but positive relationship between $\delta^{13}C_{collagen}$ and $\delta^{15}N_{collagen}$ in Chronological Unit 2.

Chronological Unit 3 is dated to 1180–1357 cal. BP. $\delta^{13}C_{collagen}$ for this unit ranges from -21.8‰ to -19.7‰ with a mean value of -20.6± 0.6‰, n=11. The range for $\delta^{15}N_{collagen}$ is 5.6‰ to 17.4‰ with a mean value of 10.2 ± 3‰, n=11. Figure 5.7 shows a plot of $\delta^{15}N_{collagen}$ against $\delta^{13}C_{collagen}$ for this unit.

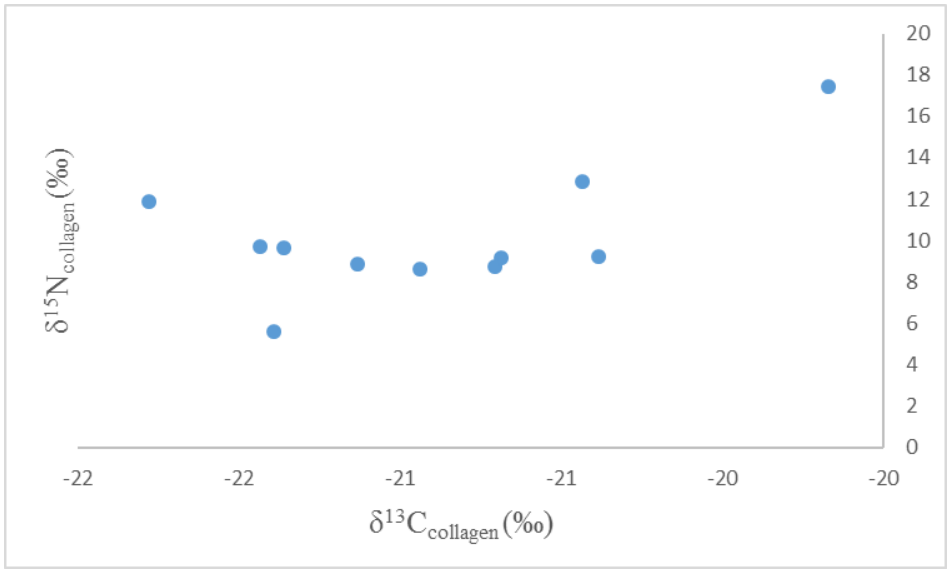

Fig. 5.7*: Scatterplot of $\delta^{13}C$ vs. $\delta^{15}N$ during Chronological Unit 3, from EBC, n=11.*

In general, the values in Fig 5.7 are strongly correlated, the Pearson's R value is equal to 0.74 and the R^2 co-efficient is equal to 0.55. This indicates a moderately strong and positive relationship between $\delta^{13}C_{collagen}$ and $\delta^{15}N_{collagen}$ in Chronological Unit 3.

Chronological Unit 4 is dated to 1410–1533 cal. BP. $\delta^{13}C_{collagen}$ for this unit ranges from -22.1‰ to -18.5‰ with a mean value of -20.7± 1.2‰, n=12. The range for $\delta^{15}N_{collagen}$ is 7.5‰ to 14.1‰ with a mean value of 9.5 ± 1.8‰, n=12. Figure 5.8 shows a plot of $\delta^{15}N_{collagen}$ against $\delta^{13}C_{collagen}$ for this unit.

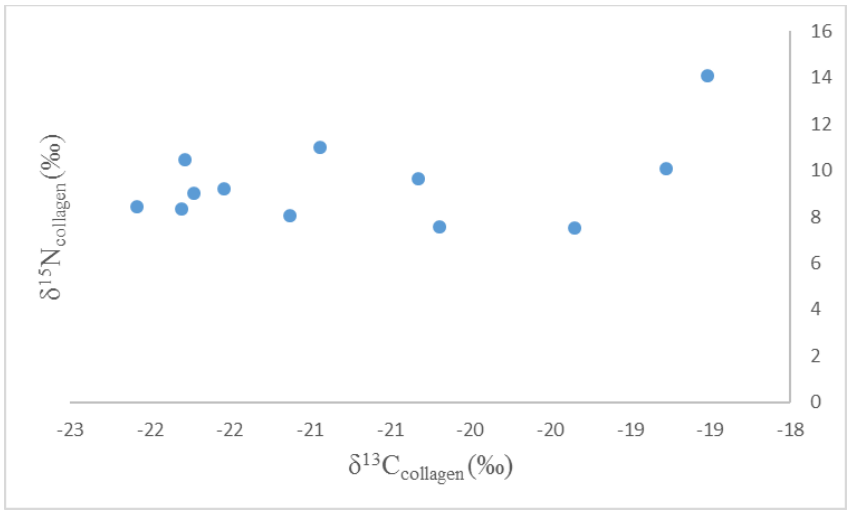

Fig. 5.8*: Scatterplot of $\delta^{13}C$ vs. $\delta^{15}N$ during Chronological Unit 4, from TC, n=12.*

Fig. 5.8 depicts a strong scatter of results; the Pearson's R value is equal to 0.52 and the R^2 co-efficient is equal to 0.27. This indicates a moderately positive relationship between $\delta^{13}C_{collagen}$ and $\delta^{15}N_{collagen}$ in Chronological Unit 4.

Chronological Unit 5 dates to 2050–2305 cal. BP and has only two samples. This is due to sparse occupation of EBC during this period. Both samples come from the LARM stratigraphic unit and the mean $\delta^{13}C_{collagen}$ is -19.7±1‰ and $\delta^{15}N_{collagen}$ is 10.8±0.8‰.

Chronological Unit 6 is dated to 5270-4660 cal. BP. $\delta^{13}C_{collagen}$ for this unit ranges from -22.4‰ to -17.3‰ with a mean value of -20.4± 1.4‰, n=11. The range for $\delta^{15}N_{collagen}$ is 7‰ to 10‰ with a mean value of 8.7 ± 1.1‰, n=11. Figure 5.9 shows a plot of $\delta^{15}N_{collagen}$ against $\delta^{13}C_{collagen}$ for this unit.

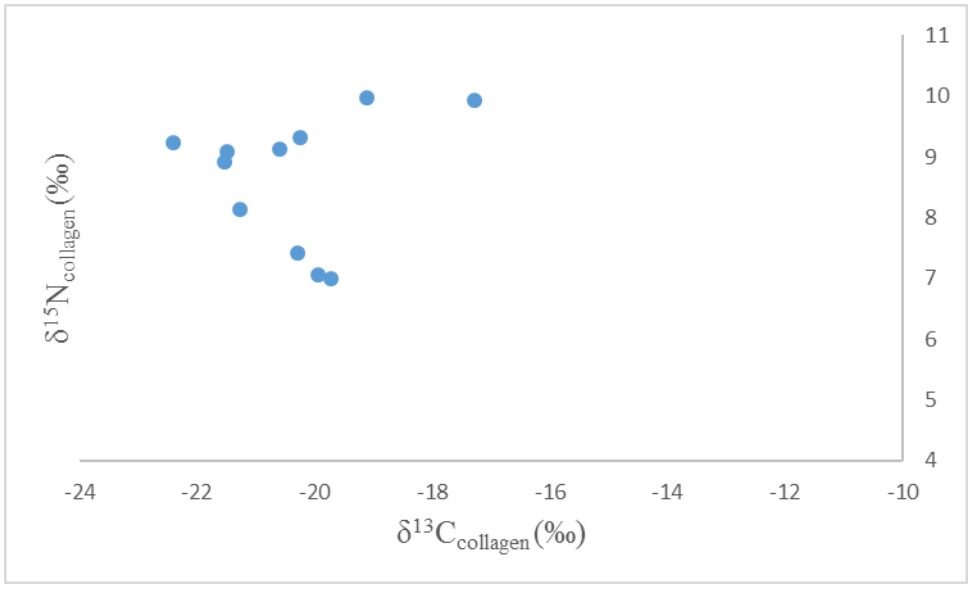

Fig. 5.9: *Scatterplot of $\delta^{13}C$ vs. $\delta^{15}N$ during Chronological Unit 6, from EBC & TC, n=11.*

The results depicted in Fig. 5.9 depict a weak relationship between $\delta^{13}C_{collagen}$ and $\delta^{15}N_{collagen}$. This is confirmed by a Pearson's R value of 0.23 and an R^2 co-efficient equal to 0.05. The Pearson's R test indicates a weak but positive relationship between $\delta^{13}C_{collagen}$ and $\delta^{15}N_{collagen}$ in Chronological Unit 1.

Chronological Unit 7 is dated to 4005–4419 cal. BP. $\delta^{13}C_{collagen}$ for this unit ranges from -23‰ to -19.4‰ with a mean value of -21.3± 1.2‰, n=11. The range for $\delta^{15}N_{collagen}$ is 5.8‰ to 16.6‰ with a mean value of 9.2 ± 3.1‰, n=11. Figure 5.10 shows a plot of $\delta^{15}N_{collagen}$ against $\delta^{13}C_{collagen}$ for this unit.

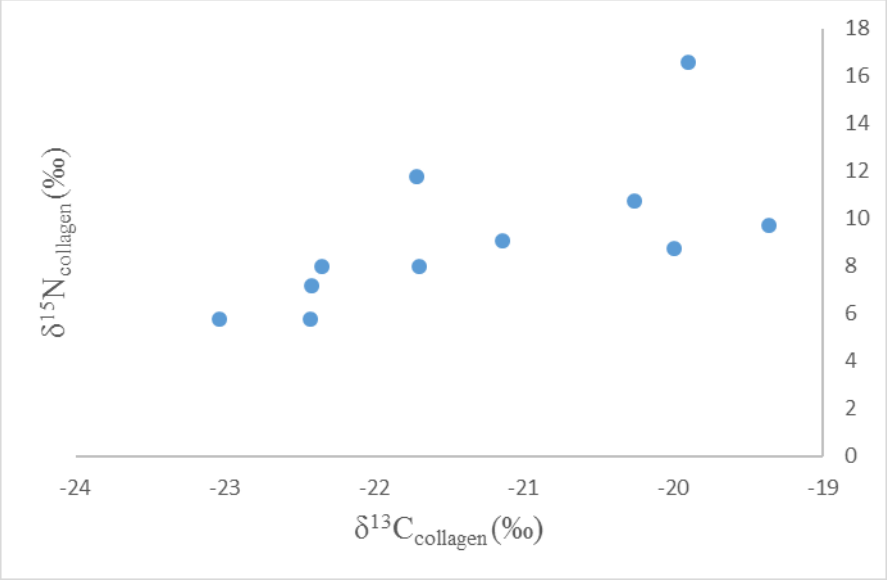

Fig. 5.10: *Scatterplot of $\delta^{13}C$ vs. $\delta^{15}N$ during Chronological Unit 7, from EBC & TC, n=11.*

Fig. 5.10 depicts a stronger relationship between $\delta^{13}C$ and $\delta^{15}N$; the Pearson's R value is equal to 0.72 and the R^2 co-efficient is equal to 0.5. This indicates a moderately positive relationship between $\delta^{13}C_{collagen}$ and $\delta^{15}N_{collagen}$ in Chronological Unit 7.

Chronological Unit 8 is dated to 8447–8993 cal. BP. $\delta^{13}C_{collagen}$ for this unit ranges from -22.1‰ to -18.9‰ with a mean value of -21.3± 1.2‰, n=4. The range for $\delta^{15}N_{collagen}$ is 5.8‰ to 16.6‰ with a mean value of 9.6 ± 2.1‰, n=4. Figure 5.11 shows a plot of $\delta^{15}N_{collagen}$ against $\delta^{13}C_{collagen}$ for this unit.

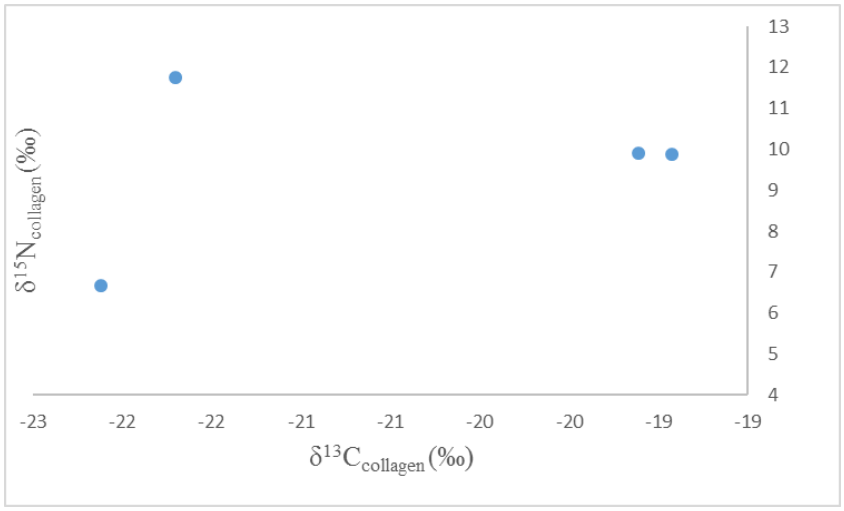

Fig. 5.11: *Scatterplot of $\delta^{13}C$ vs. $\delta^{15}N$ during Chronological Unit 8, from EBC, n=4.*

Fig. 5.11 depicts a strong scatter of results; the Pearson's R value is equal to 0.81 and the R^2 co-efficient is equal to 0.66. This indicates a strong positive relationship between $\delta^{13}C_{collagen}$ and $\delta^{15}N_{collagen}$ in Chronological Unit 8.

Only one sample from Chronological Unit 9, dating to 10690–11201 cal. BP, yielded collagen. The collagen extracted from this sample–#17432–, did not meet the collagen quality criteria outlined by Ambrose (1990) and van Klinken (1999). As such, no samples from Chronological Unit 9 will be discussed.

The tenth Chronological Unit dates to 12103–12725 cal. BP. Collagen was successfully extracted from only one sample, #17436, which has a $\delta^{13}C$ of -20.8‰ and $\delta^{15}N$ value of 11.7‰.

5.4 Changes in $\delta^{13}C$ through time

Figure 5.12 is a boxplot showing $\delta^{13}C_{collagen}$ in different Chronological Units.

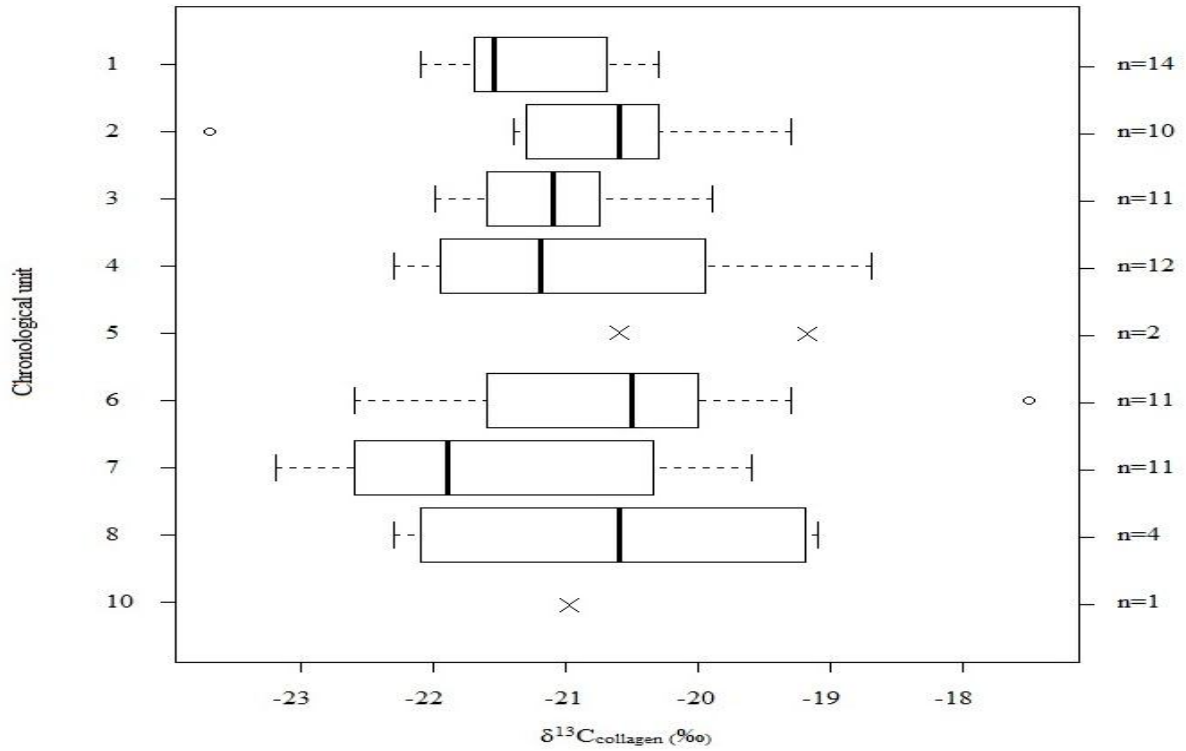

Fig. 5.12: *Boxplot showing $\delta^{13}C_{collagen}$ in different chronological units. The bold line in the middle of the box represents the median value. The lower quartile extends from the median line, left, to the end of the box. The upper quartile extends from the median line, right, to the end of the box. The whiskers represent the maximum and minimum endpoints of the data. The X represents individual data points. The unfilled circles represent outlying data points. Anything that fell out of the range calculated by the following two formulas, were considered outliers: Quartile 1-(Interquartile range*1.5); Quartile 3+(Interquartile range*1.5).*

Mann–Whitney tests were used to check for differences in distribution between pairs of units. $\delta^{13}C_{collagen}$ values from Chronological Unit 1 differ from those from Chronological Unit 2 (Mann–Whitney Z–value= -2.08, p= 0.0375). $\delta^{13}C_{collagen}$ values from Chronological Unit 2 do not differ from those of Chronological Unit 3 (Mann–Whitney Z–value= -1.44, p= 0.1499). If the outlier with a $\delta^{13}C_{collagen}$ value of -23.5‰ is removed from Chronological Unit 2 there is a statistical difference (Mann–Whitney Z–value= -1.98, p-value= 0.0477). $\delta^{13}C_{collagen}$ values from Chronological Unit 3 do not differ from those of Chronological Unit 4 (Mann–Whitney

Z–value= 0, p= 1). $\delta^{13}C_{collagen}$ values from Chronological Unit 4 do not differ from those of Chronological Unit 6 (Mann–Whitney Z–value= -0.36, p= 0.7188). If the outlier with a $\delta^{13}C_{collagen}$ value of -17.3‰ is removed from Chronological Unit 6, there is still no statistical difference (Mann–Whitney Z–value= -0.71, p= 0.4777). $\delta^{13}C_{collagen}$ values from Chronological Unit 6 do not differ from those of Chronological Unit 7 (Mann–Whitney Z–value= -1.48, p= 0.1389). If the outlier with a $\delta^{13}C_{collagen}$ value of -17.3‰ is removed from Chronological Unit 6 there is still no statistical difference (Mann–Whitney Z–value= -1.2, p= 0.2301). Sample counts from Chronological Units 5, 8 and 10 are too low for meaningful statistical analysis.

Table 5.4 gives the p–values of the pair–wise Mann–Whitney tests performed on $\delta^{13}C$ values from each Chronological Unit with a large enough sample size, once outliers had been removed. P–values that indicate significance have been highlighted in red. As can be read off the table there is significant difference between Chronological Units 1& 2 and 2 & 3, as already discussed above. There is also a significant difference between Chronological Units 1& 6, where Chronological Unit 1 has low $\delta^{13}C$ values in comparison to unit 6.

Table 5.4: P–values of the pair–wise Mann–Whitney tests performed on $\delta^{13}C$ values for different Chronological Units. Outliers from each unit were removed to calculate the p-values in this table.

p-value	Chronological Unit 2	Chronological Unit 3	Chronological Unit 4	Chronological Unit 6	Chronological Unit 7
Chronological Unit 1	0.0037	0.3371	0.6455	0.0193	0.5687
Chronological Unit 2	-	0.0477	0.2713	0.4902	0.1285
Chronological Unit 3	-	-	1	0.5029	0.3953
Chronological Unit 4	-	-	-	0.7188	0.2801
Chronological Unit 6	-	-	-	-	0.2301

5.5 Changes in $\delta^{15}N$ through time.

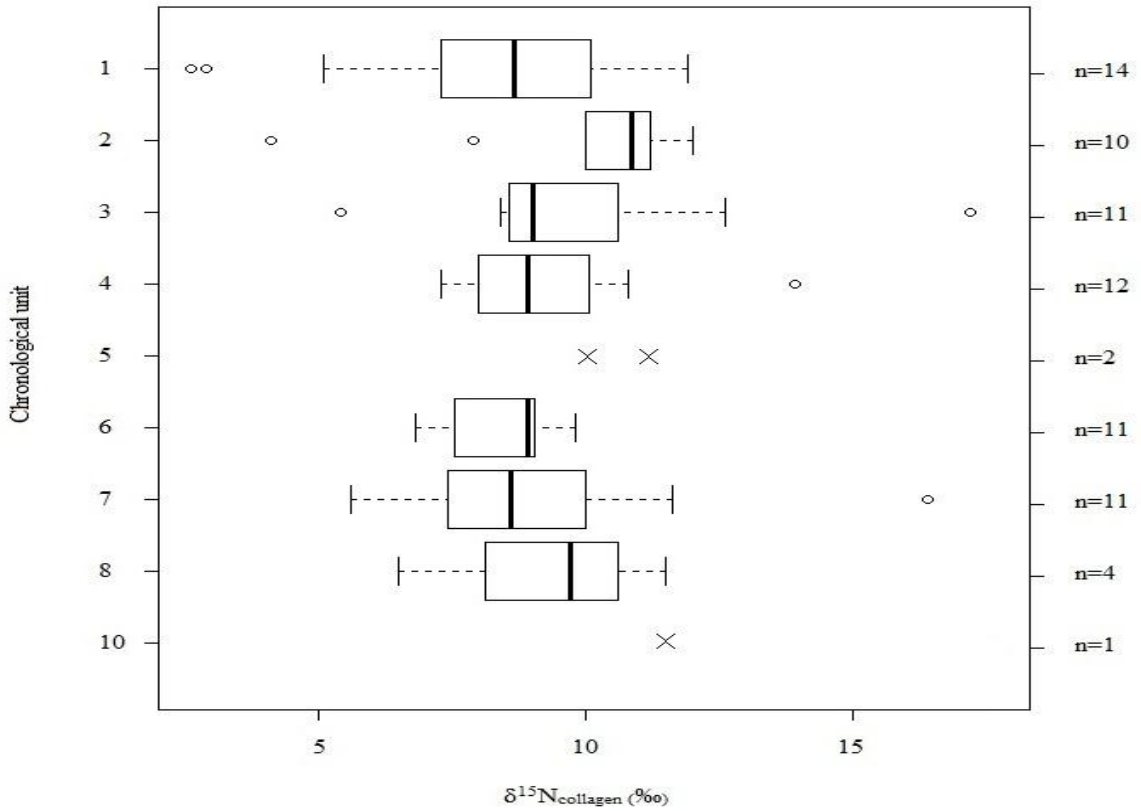

Fig. 5.13: *Boxplot showing $\delta^{15}N_{collagen}$ in different Chronological Units. For figure format refer to Fig. 5.12*

Figure 5.13 is a boxplot showing $\delta^{15}N_{collagen}$ in different chronological units. Mann–Whitney tests were used to check for difference in distribution between pairs of units.

$\delta^{15}N_{collagen}$ values from Chronological Unit 1 do not differ from those of Chronological Unit 2 (Mann–Whitney Z–value= -1.87, p= 0.0615). If the two outliers from Unit 1 with $\delta^{15}N_{collagen}$ values of 3.1 & 2.8‰ and the two outliers from Unit 2 with $\delta^{15}N_{collagen}$ values of 4.3 & 8.1‰ are removed, a difference is seen between the two units (Mann–Whitney Z–value= -2.39, p= 0.0168). $\delta^{15}N_{collagen}$ values from Chronological Unit 2 do not differ from those of Chronological Unit 3 (Mann–Whitney, Z–value= -0.74, p= 0.4593). If the two outliers from Unit 2 with $\delta^{15}N_{collagen}$ values of 4.3 & 8.1‰ and the two outliers from Unit 3 with $\delta^{15}N_{collagen}$ values of 5.6 & 17.4‰ are removed, a difference is seen between the two

units (Mann–Whitney Z–value= -1.97, p= 0.0488). $\delta^{15}N_{collagen}$ values from Chronological Unit 3 do not differ from those of Chronological Unit 4 (Mann–Whitney Z–value= -0.68, p= 0.4965). If the two outliers from Unit 3 with $\delta^{15}N_{collagen}$ values of 5.6 & 17.4‰ and the outlier from Unit 4 with $\delta^{15}N_{collagen}$ value of 14.1‰ are removed, there is still no difference between the two units (Mann–Whitney Z–value= -1.18, p= 0.238). $\delta^{15}N_{collagen}$ values from Chronological Unit 4 do not differ from those of Chronological Unit 6 (Mann–Whitney Z–value= 0.95, p= 0.3421). If the outlier from Unit 4 with a $\delta^{15}N_{collagen}$ value of 14.1‰ is removed, there is still no difference between the two units (Mann–Whitney Z–value= 0.66, p= 0.5093). $\delta^{15}N_{collagen}$ values from Chronological Unit 6 do not differ from those of Chronological Unit 7 (Mann–Whitney Z–value= 0.03, p= 0.9761). If the outlier from Unit 7 with a $\delta^{15}N_{collagen}$ value of 16.6‰ is removed, there is still no difference between the two units (Mann–Whitney Z–value= 0.42, p= 0.6745). Sample count from Chronological Units 8 and 10 are too low for meaningful statistics

Table 5.5 gives the p–values of the pair–wise Mann–Whitney tests performed on $\delta^{15}N$ values from each Chronological Unit with a large enough sample size, once outliers had been removed. P–values that indicate significance have been highlighted in red. All Chronological Units are statistically different from Chronological Unit 2, which has the highest $\delta^{15}N$ values amongst the units.

Table 5.5: P–values of the pair–wise Mann–Whitney tests performed on $\delta^{15}N$ values for different Chronological Units. Outliers from each unit were removed to calculate the p–values in this table.

p-value	Chronological Unit 2	Chronological Unit 3	Chronological Unit 4	Chronological Unit 6	Chronological Unit 7
Chronological Unit 1	0.0168	0.4533	0.6892	0.4065	0.4122
Chronological Unit 2	-	0.0488	0.0131	0.0003	0.0067
Chronological Unit 3	-	-	0.238	0.2113	0.131
Chronological Unit 4	-	-	-	0.5093	0.131
Chronological Unit 6	-	-	-	-	0.6745

5.6 Comparisons of $\delta^{13}C$ between the late, middle and early Holocene

Figure 5.14 is a boxplot comparing $\delta^{13}C_{collagen}$ in the late Holocene (LH) (Chronological Units 1 to 5) with the middle Holocene (MH) (Chronological Units 6 to 7) and early Holocene (EH) (Chronological units 8 to 10). The LH has 49 samples with $\delta^{13}C_{collagen}$ ranging from -23.5 to -18.5 and a mean of -20.8±0.9‰. If the outlying values of -23.5(UCT #18771) and -18.5 (UCT #16569) are removed, the range is from -22.1 to -18.8‰ with a mean of -20.8±0.8‰. The MH has 22 samples with a range from -23.0 to -17.3‰ and a mean of -20.8±1.4‰. The EH has 5 samples with $\delta^{13}C_{collagen}$ ranging from -21.7 to -18.9‰ and a mean of -20.5±1.5‰. $\delta^{13}C_{collagen}$ values in the LH, MH and EH are not significantly different from one another (Kruskal–Wallis H=0.09, DF=2, p= 0.956). This remains true if the outliers from the LH are removed (Kruskal–Wallis H=0.01, DF=2, p= 0.9512)

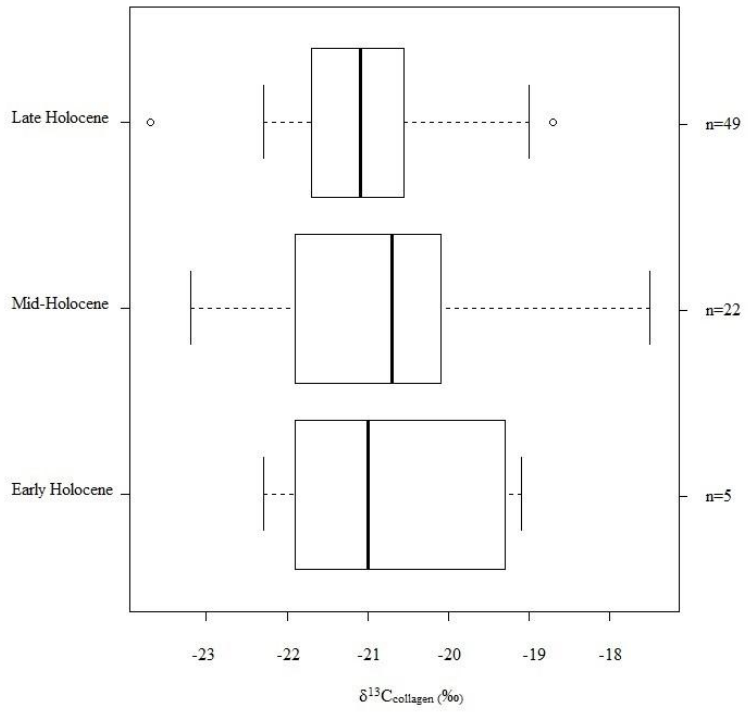

Fig 5.14: *Boxplot showing $\delta^{13}C_{collagen}$ at Elands Bay for different periods during the Holocene. For figure format refer to Fig. 5.12*

5.7 Comparisons of $\delta^{15}N$ between the late, middle and early Holocene

Figure 5.15 is a boxplot comparing $\delta^{15}N_{collagen}$ in the late Holocene (LH) with the middle Holocene (MH) and early Holocene (EH). The LH has 49 samples with $\delta^{15}N_{collagen}$ ranging from 2.8 to 17.4 and a mean of 9.5±2.6‰. If the outlying values of 2.8‰ (UCT #18777); 3.1‰ (UCT #18070) and -17.4‰ (UCT #18170) are removed, the range is from 4.1 to 14.1‰ with a mean of 9.6±2‰. The MH has 22 samples with a range from 5.8 to -16.6‰ and a mean of 9.1±2.3‰. If the outlying value of 16.6 (UCT #18392) is removed, the range is from 4.1 to 11.8‰ with a mean of 8.7±1.6‰. The EH has 5 samples with $\delta^{15}N_{collagen}$ ranging from 6.7 to 11.7‰ and a mean of 10±2‰. If the outlying value of 6.7‰ (UCT #18392) is removed, the range is from 9.9 to 11.7‰ with a mean of 10.8±1‰. $\delta^{15}N_{collagen}$ values in the LH, MH and EH are not significantly different from one another (Kruskal–Wallis H= 3.54, DF=2, p= 0.1703). However, difference is observed if the outliers from the late and mid–Holocene are removed (Kruskal–Wallis H= 8.35, DF=2, p= 0.0154). Outlying samples from the early Holocene were not removed to preserve sample size.

Mann–Whitney tests show statistical difference between the late Holocene and mid Holocene units (Mann–Whitney Z–value= 2.53, p= 0.0114). This means that $\delta^{15}N$ in the late Holocene period ($\overline{x}$=9.5±2.2, n=46) is statistically higher compared to mid–Holocene period ($\overline{x}$=8.6±1.5, n=21). No difference was observed between the early Holocene and late Holocene (Mann–Whitney Z–value= -0.62, p= 0.5353) or between the early Holocene and mid–Holocene (Mann–Whitney Z–value= -0.13, p= 0.8966)

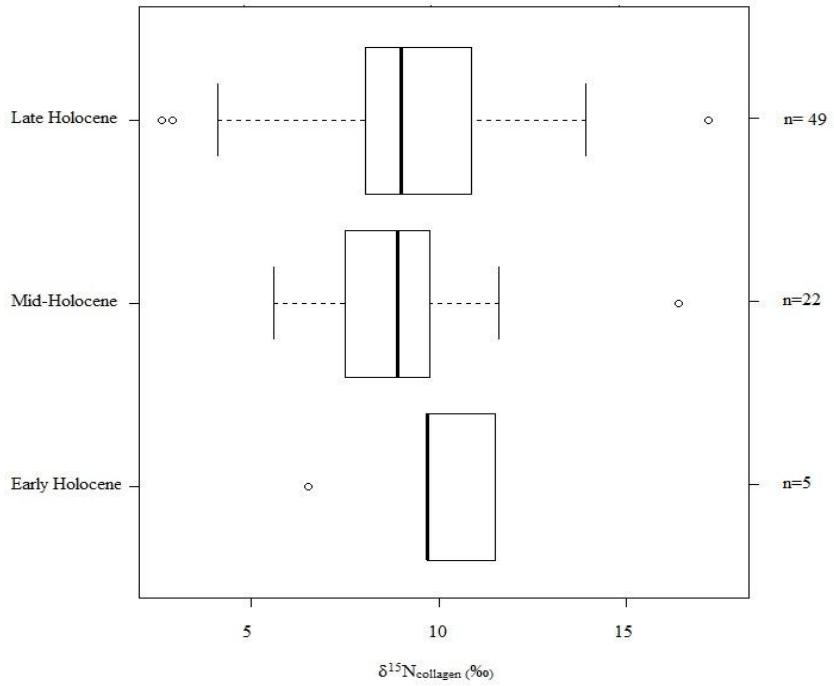

Fig 5.15: *Boxplot showing $\delta^{15}N_{collagen}$ at Elands Bay for different periods during the Holocene. For figure format refer to Fig. 5.12*

The significance of the correlation calculated in section 5.3 will be further discussed in Chapter 6. The climatic implications of significant variance in $\delta^{13}C$ and $\delta^{15}N$ between Chronological Units 1;2 and 3 will also be reviewed in Chapter 6. As will the variability in $\delta^{13}C$ between Chronological Units 1 and 6. The climatic implications will then be compared to the existing paleoenvironmental record for the region. Chapter 6 also compares modern results from Weeber (2013) to the results from the archaeological samples in this study.

Chapter Six

Discussion

The aim of Chapter 6 is, first, to compare the results reported in Chapter 5 with those of Weeber's 2013 pilot study. This comparison will be covered in section 6.1. Second, the chapter aims to discuss and interpret the results from Chapter 5 and section 6.1, and compare them with other climate proxy data from the West Coast in section 6.3

6.1 Comparison of results with Weeber (2013)

Weeber (2013) analysed 58 contemporary tortoises, 34 from Steenbokfontein and 24 from Diepkloof, and 14 archaeological animals from Dune Field Midden. Figure 6.1 is a boxplot comparing $\delta^{13}C$ in different time periods at Elands Bay Cave and Tortoise Cave with Weeber's values.

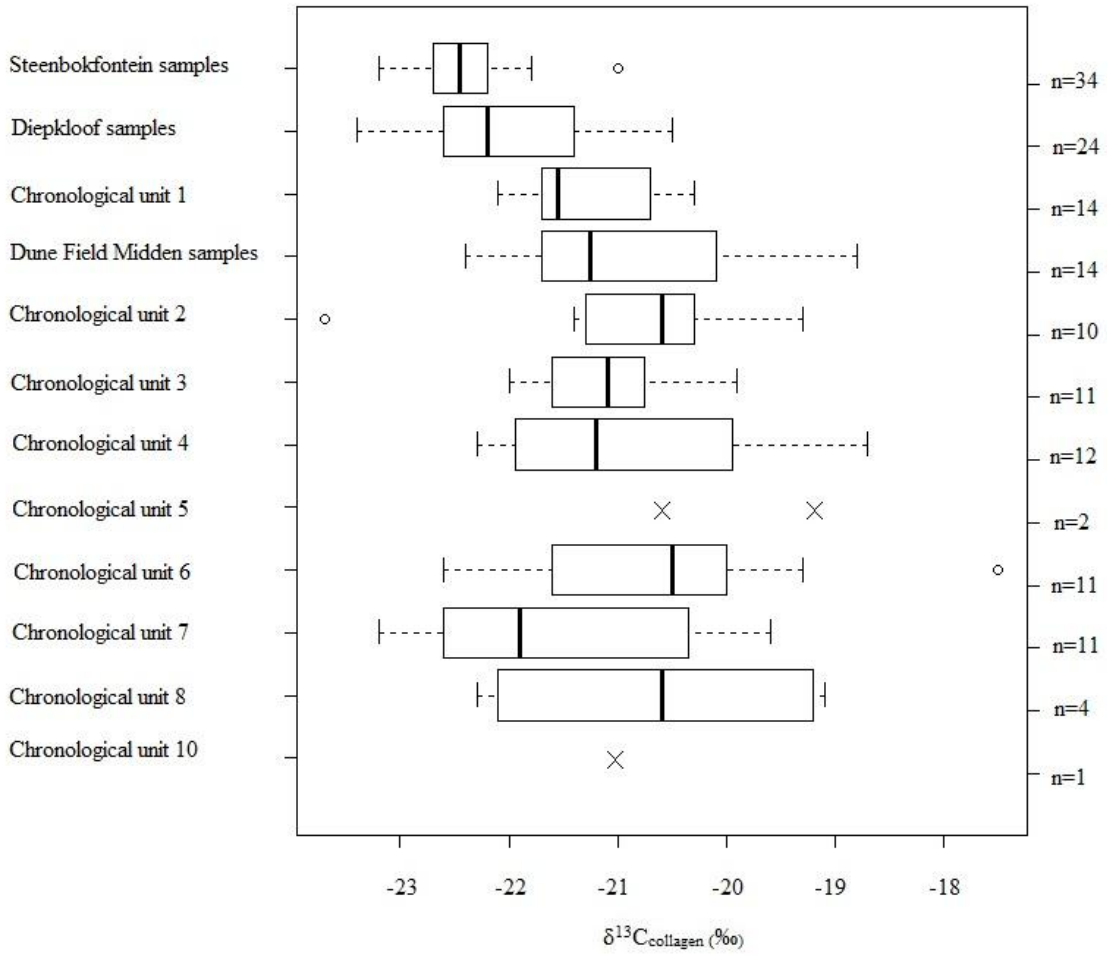

Fig. 6.1: *Boxplot showing $\delta^{13}C_{collagen}$ of modern tortoises from Steenbokfontein and Diepkloof, compared with archaeological samples from Dune Field Midden and different Chronological Units at Elands Bay Cave and Tortoise Cave. 2‰ has been added to values for modern samples to correct for the fossil fuel effect (Schmitt* et. al *2012). The bold line in the middle of the box represents the median value. The box encloses the middle half of the data. The whiskers represent the maximum and minimum endpoints of the continuous data. The Xs represent individual points. The unfilled circles represent outlying data points.*

There is no difference in the distribution of $\delta^{13}C$ values of samples from Steenbokfontein (mean = -22.2±0.4, n=34) and Diepkloof (mean=-21.8±0.8, n=24) (Mann–Whitney z value=-1.85, p value= 0.0643). However, Steenbokfontein differs from Chronological Unit 1 (487–

154 cal. BP, the period of the LIA) (Mann–Whitney z value=-5.07, p value= <.0001), as do samples from Diepkloof (Mann–Whitney z value=-2.62, p value= 0.0088). $\delta^{13}C$ in samples from Dune Field Midden (-20.7±1.1, n=14) dating to 669 to 547 cal. BP does not differ from Chronological Unit 1 (Mann–Whitney z value=1.03, p value= 0.303) or Chronological Unit 2 (Mann–Whitney z value=-0.59, p value= 0.5552).

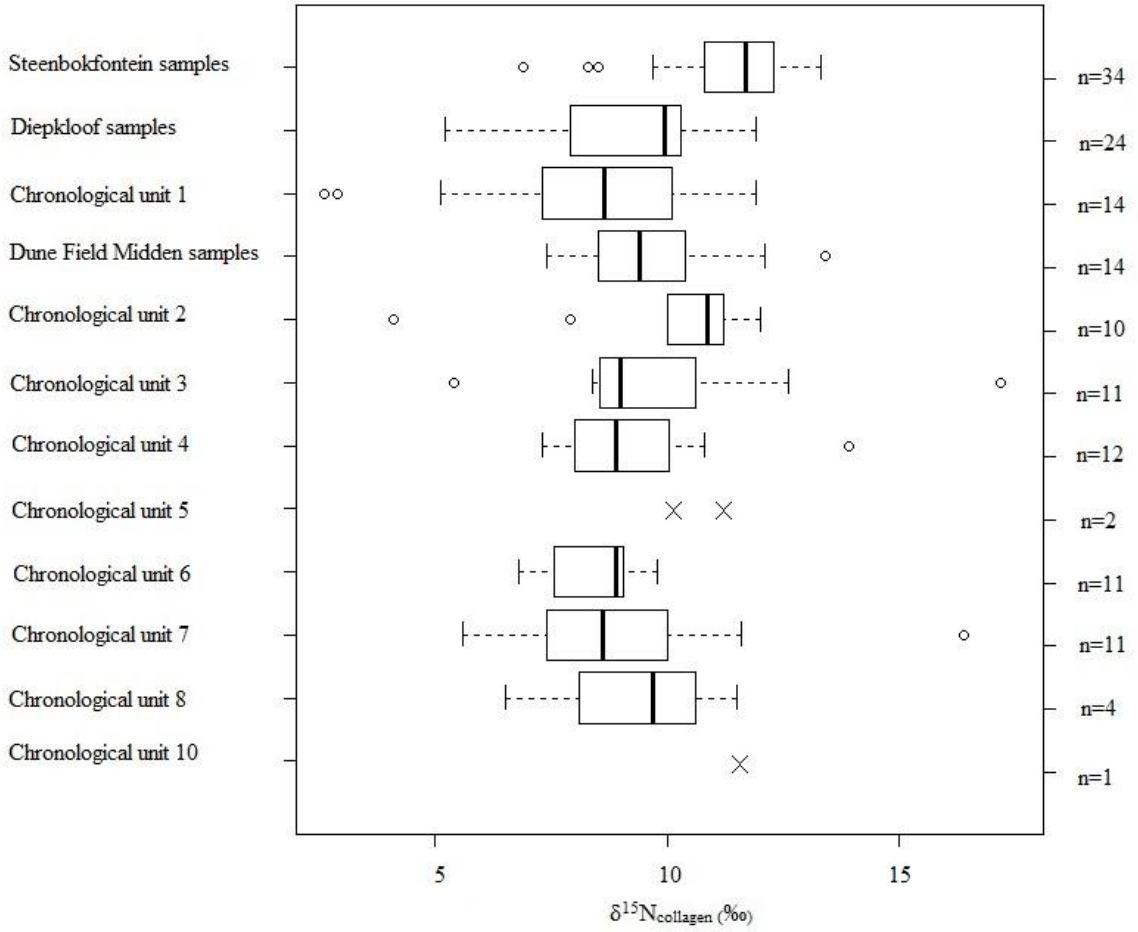

Fig. 6.2 *Boxplot showing $\delta^{15}N_{collagen}$ of modern tortoises from Steenbokfontein and Diepkloof, compared with archaeological samples from Dune Field Midden and different Chronological Units at Elands Bay Cave and Tortoise Cave. See Fig. 6.1 for plot description.*

The distribution of $\delta^{15}N$ in the contemporary samples from Steenbokfontein (mean = 11.6±1.4, n=34) differs from those from Diepkloof (mean = 9.5±1.7, n=24) (Mann–Whitney

z value= 4.48, p value=<.0001). Samples from Chronological Unit 1 differ from Steenbokfontein (Mann–Whitney z value=4.03, p value=0.0001) but not Diepkloof (Mann-Whitney z value=1.04, p value=0.2983). $\delta^{15}N$ in samples from Dune Field Midden (10±1.6, n=14) do not differ from Chronological Unit 1 (Mann–Whitney z value=1.4, p value=0.1615) or Chronological Unit 2 (Mann–Whitney z value=-1.02, p value=0.3077). If the outlying values are removed, DFM still does not differ from Chronological Unit 1 (Mann–Whitney z value=-0.63, p value=0.5287) but does differ from Chronological Unit 2 (Mann–Whitney z value=-2.43, p value=0.0151).

6.2 Interpretation of results

Based on the $\delta^{13}C$ and $\delta^{15}N$ correlations calculated in section 5.3, it is evident that there is no strong correlation between $\delta^{13}C$ and $\delta^{15}N$ in tortoise collagen-except for Unit 8 (R=0.81). $\delta^{13}C$ and $\delta^{15}N$ values in Units 3, 4 and 7 have moderately strong correlations (R between 0.52–0.74), indicating that some of the variation in $\delta^{13}C$ and $\delta^{15}N$ values respectively is caused by the same factor/s, though not to the extent that is seen in ungulates.

There is no statistical difference in ^{13}C between the contemporary samples from Steenbokfontein and Diepkloof. However, $\delta^{13}C$ is low at both contemporary sites when compared with Chronological Unit 1 (154–487 cal. BP, which spans the LIA). Lower ^{13}C in modern samples could indicate a decrease in temperature since 370 bp, meaning that the present period is cooler than the west coast during the LIA. However, this seems highly unlikely and is contrary to climate models based on proxy records. These models show the LIA on the west coast of South Africa to be at least 2ºC cooler than present (Mann *et al*. 2009). It is more likely that the low $\delta^{13}C$ values in the present are due to agricultural practices around the sites of Steenbokfontein and Diepkloof. Farms in the Elands Bay and Lamberts Bay area currently farm wheat, oats, berries and potatoes, all of which are C_3 plants. At least some crops are irrigated, which is likely to lead to lower $\delta^{13}C$ values. Contemporary samples

were accumulated through bird predation, meaning that tortoises would have come from further afield than the location of the sites. If tortoises were consuming crops from nearby farm lands, this would have affected their $\delta^{13}C$ values.

Modern tortoises from Steenbokfontein are higher in $\delta^{15}N$ than those from Diepkloof. Weeber (2013) attributed this to the nitrogen cycle near Steenbokfontein being more open. Steenbokfontein is also closer to the coast than Diepkloof, so nearby soils may be more saline (Heaton 1997). However, it should be noted that Steenbokfontein receives approximately 20mm less rain than Elands Bay annually (www.weathersa.co.za). Precipitation is known to affect ^{15}N where less rainfall tends to cause an increase in ^{15}N (Gröcke *et al*.1997). The high $\delta^{15}N$ values at Steenbokfontein compared to Diepkloof may result from the difference in rainfall.

This points to the importance of setting boundary zones in a paleoenvironmental analysis. Whilst Steenbokfontein is only 25km away from Diepkloof, differences in topography, rainfall and substrates can lead to microclimates. By analysing sites from different microclimates one may think that there is a temporal change in climate when in fact there is only a spatial change.

Samples from Steenbokfontein are higher in $\delta^{15}N$ compared with both the Diepkloof and Chronological Unit 1 (LIA) samples. Yet, samples from Diepkloof show no difference in ^{15}N compared with the LIA samples (Chronological unit 1). Thus, the factors that contribute to the differences in modern samples and between Steenbokfontein and Diepkloof are probably at play in the comparison between contemporary samples from Steenbokfontein and LIA samples from EBC.

Tortoises from Chronological Unit 1 (154–487 cal. BP, spanning the LIA) have low $\delta^{13}C$ values when compared with those from Chronological Unit 2 (744–1042 cal. BP, which

coincides with the MCA) (Mann–Whitney Z–value= -2.08, p= 0.0375). Given that angulate tortoises are preferential C_3 feeders (Joshua *et al.* 2010), this probably reflects a decrease in the ^{13}C values of C_3 plants in Chronological Unit 1, as expected in the cooler, wetter conditions of the LIA (Stager *et al* 2012; Cohen *et al.* 1992).

Tortoises from Chronological Unit 1 also have significantly lower $\delta^{15}N$ values when compared with Chronological Unit 2 (Mann–Whitney Z–value= -2.39, p= 0.0168) Variation in ^{15}N is difficult to interpret due to the complexity of both the nitrogen cycle and nitrogen metabolism within animals. However, as explained in Chapter 2, $\delta^{15}N$ varies inversely with moisture availability. As for the $\delta^{13}C$ values, this pattern is consistent with higher rainfall/moister conditions during Chronological Unit 1 compared with Chronological Unit 2.

Interestingly, samples from Chronological Unit 1/the LIA show no difference in both isotopes to samples from DFM (547 to 669 cal. BP, spans the late MCA). Yet, DFM samples have low $\delta^{15}N$ values when compared with samples from Chronological Unit 2 (744-1 042 cal. BP, spans the early MCA). This indicates that there is more precipitation/moisture available in the late MCA than the early MCA. The isotope results indicate that Chronological Unit 1, which is representative of the LIA, is cooler and moister than Chronological Unit 2, which is representative of the early MCA. In addition, the period from 547 to 669 cal. BP experienced more moisture/precipitation than the early MCA.

Tortoises from Chronological Unit 2 are significantly higher in $\delta^{13}C$ compared with Chronological Unit 3 (1 180–1 357 cal. BP) (Mann–Whitney Z–value= -1.98, p = 0.0477). Since values for both units fall into the C_3 range the increase in ^{13}C is probably due to an increase in temperature and aridity from Chronological Unit 3 to 2. A statistically significant variation is also seen in $\delta^{15}N$, where values from Unit 2 are higher than those from Unit 3 (Mann–Whitney Z–value= -1.97, p= 0.0488). This points to lower levels of precipitation or

available moisture in Unit 2 (the early MCA) when compared with Unit 3 (which immediately pre–dates the MCA). Interestingly, $\delta^{15}N$ is higher in samples from Chronological Unit 2 than any other unit between 154–5 270 cal. BP (refer to Table 5.5). This implies that the greatest aridity experienced in the region between 154–5 270 cal. BP is in the period 744–1 042 cal. BP.

There are only two samples from Chronological Unit 5 (2005–2305 cal. BP). These appear to be somewhat higher in both $\delta^{13}C$ and $\delta^{15}N$ when compared with Unit 4 (1320–1533 cal. BP), but the sample size is too small to draw any conclusions. Future studies could obtain clearer results by including material from additional sites to increase the sample size. For example, the site of Pancho's Kitchen Midden (PKM), which is only three kilometres away from EBC and has material dating from 2 600–2 900 bp, would be very useful in this study.

Chronological Unit 6 (4 005–4 419 cal. BP) shows no statistical difference in $\delta^{13}C$ and $\delta^{15}N$ when compared to Chronological Unit 7 (4 660–5 720 cal. BP). This implies a period of stability in climate between the two units. Chronological Unit 6, however, has higher $\delta^{13}C$ values than Chronological Unit 1 (Mann–Whitney Z–value= -2.34, p= 0.0193). Since values for both units fall into the C_3 range the increase in ^{13}C is probably due to increased temperatures in Chronological Unit 6 compared to 1.

At a macro-scale, differences emerge in ^{15}N between samples from the late Holocene (154–2 305 cal. BP) and the mid Holocene (4 005–5 720 cal. BP) (Mann–Whitney Z–value= 2.53, p= 0.0114). Samples from the late Holocene are higher in $\delta^{15}N$, indicating less moisture availability in this period. However, it is likely that the extremely high $\delta^{15}N$ values in Chronological Unit 2 are skewing the results, making the late Holocene as a whole seem more arid than it is. No statistical change was seen between the early Holocene units and

either the late or mid Holocene units. This is most likely due to the small sample size within the early Holocene (n=5, mean=10.8±1‰.).

Thus, the tortoise isotopic record demonstrates anthropogenic changes in modern samples, with different environmental effects near Elands Bay and Steenbokfontein. The climate data generated from tortoises indicate a cool and moist LIA and a warm and dry MCA, specifically the early MCA. The record also reflects a cooler and moister period between 1 180–1 357 cal. BP. A period of climatic stability is reflected in the tortoise isotope record between 4 005–5 270 cal. BP. Higher $\delta^{13}C$ values at 4 005–4 419 cal. BP compared with values at 154–487 cal. BP indicate warmer conditions at the start of the middle Holocene.

6.3 Comparison of tortoise paleorecord with other proxy records

This section compares the paleorecord derived from tortoise shell with other records from proxy sources in the Elands Bay and Cederberg region. Cool and moist conditions are seen in the tortoise record between 154–487 cal. BP, corresponding to the LIA event. A period of aridity between 744–1042 cal. BP coincides with the MCA.

A cool, moist LIA and warm dry MCA are also reflected in other proxy records within a 10 kilometre radius from the study sites. Marine mollusc shells from a number of archaeological sites around Elands Bay reflect a 1–2°C drop in sea surface temperatures during the LIA when compared with the MCA (Cohen *et al* 1992). Diatom studies based on cores from Verlorenvlei show an increase in winter rainfall after 600 cal. BP and less precipitation between 960 to 1100 cal. BP (MCA) (Stager *et al.* 2012). However, charcoal pollen from Elands Bay Cave itself reflects apparently stable environmental conditions from the MCA to the LIA (Cowling *et al.* 1999). It must be pointed out that the charcoal record from within the cave is likely to be biased by an anthropogenic effect. Particular types of plants were probably selected over others (for example, as good firewood), leading to a skewed sample.

The presence of *Cyperaceae* pollen at the Pakhuis Pass hyrax middens are indicative of an increase in moisture availability at 500 cal. BP (Scott & Woodborne 2007a). Although these authors are hesitant to associate this change in climate with the LIA, the increase in moisture availability does correspond with the pattern seen at Elands Bay and attributed here to the LIA.

Unfortunately, no other proxies in the Cederberg provide a record of the period between 154–487 cal. BP. However, higher $\delta^{13}C$ and $\delta^{15}N$ in the hyrax midden at Katbakkies indicate aridity between 800 cal. BP and 570 cal. BP (Meadows *et al*. 2010) This overlaps with the warm and dry period seen within the tortoise record between 744–1 042 cal. BP. The MCA is not as defined at De Rif as the arid periods seen at Pakhuis Pass and Katbakkies. Increases in succulent and shrub pollens in the De Rif hyrax midden are indicative of a stable but arid late Holocene between 3 000–700 cal. BP (Quick *et al.* 2011). It must be noted the Katbakkies, Truitjies Kraal and De Rif hyrax midden records rely on a limited number of radiocarbon dates (two each for Katbakkies and Truitjies Kraal [Meadows *et al*. 2010]. While the De Rif middens have seven radiocarbon dates for the entire Holocene [Quick *et al*. 2011]). By assuming constant accumulation rates authors can interpolate between these dates to fill in the gaps. If there were changes in accumulation rates or hiatuses in the midden that are not visible, the interpolated dates may be erroneous (Meadows *et al*. 2010, Quick *et al*. 2011).

The tortoise isotope record indicates cool and moist conditions prior to the MCA, between 1 180–1 357 cal. BP. It also indicates more variability in climate during this period than the Klaarfontein pollen, EBC charcoal and Elands Bay marine mollusc records (Meadows & Baxter 2001; Cowling *et al.* 1999; Cohen *et al.* 1992). However, the presence of diatoms from the Verlorenvlei cores that reflect moderately brackish conditions indicate a slight increase in precipitation between 1190–1340 cal. BP (Stager *et al.* 2012).

In general, a drying trend is observed during this period at the Cederberg. The presence of *Asteraceae* pollens and increases in ^{13}C isotope values between 2 000 to 1 000 cal. BP indicate an arid environment at Pakhuis Pass (Scott & Woodborne 2007a). As stated previously, shrub and succulent pollens between 3 000–700 cal. BP at De Rif highlight a dry but stable period (Quick *et al.* 2011). Higher $\delta^{13}C$ and $\delta^{15}N$ values and decreases in arboreal pollen from 3 000 to cal. BP to 1275 cal. BP also indicate aridity at Truitjies Kraal (Meadows *et al*. 2010). Moist and cool conditions are seen at Katbakkies hyrax midden between 2 400 to 1 300 cal. BP, indicated by increases in *Cyperaceae* pollen and low $\delta^{13}C$ and $\delta^{15}N$ values (Meadows *et al*. 2010). However, these conditions are likely due to the strong influence of summer rainfall at Katbakkies during this period (Chase *et al.* 2015).

Though the Cederberg records do not reflect a cool and moist period between 1 180–1 357 cal. BP, it does not necessarily mean that the event was not present in the Cederberg. Meadows *et al*. 2010 cautions that changes within centuries, as is the case during 1 180–1 357 cal. BP, may not be reflected in Hyrax middens. This is because samples extracted for analysis from the middens span a hundred–year period (Meadows *et al*. 2010). Therefore, environmental changes within a century may not be seen in analysis of Hyrax middens.

The last noteworthy period identified in the tortoise record is a dry and stable period from 4 005–5 270 cal. BP. Proxy records from Elands Bay are sparse for this period. Charcoal and pollen records from EBC support a stable, though dry, environment throughout the middle Holocene (Cowling *et al*. 1999). Pollen from Grootdrift and Klaarfontein indicate dry conditions between 4000 to 6000 cal. BP (Meadows & Baxter 2001).

Carbon isotope data from hyrax middens in the Cederberg spanning the period between 4 005 to 5 270 cal. BP also indicate drier conditions (Scott & Woodborne 2007; Chase *et al*. 2015), although the pollen records from cores from Driehoek and Sneeubergvlei show little variation

during this period (Meadows & Sugden 1993), perhaps because of the resilience of mountain fynbos (Quick *et al*. 2011).

In the Pakhuis Pass hyrax midden, low $\delta^{13}C$ values and changes in the pollen principal component 2 indicate decreased summer rainfall between 5 600 to 4 900 cal. BP (Scott & Woodborne 2007a). Unfortunately, poor resolution within this midden between 4 900–2 800 cal. BP means that it is not possible to make comparisons with the tortoise record between 4 005–4 419 cal. BP. Evidence from several sites suggests drier conditions during the mid-Holocene, although the dates do not precisely match those of the chronological units employed in this study. High $\delta^{13}C$ and $\delta^{15}N$ values, and the dominance of *Asteraceae* pollen indicate a drying trend between 8 000 to 3 000 cal. BP at Truitjes Kraal (Meadows *et al*. 2010). Sharp increases in ^{13}C and ^{15}N between 5 600 to 4 700 cal. BP also indicate a dry period at Katbakkies (Chase *et al.* 2015).

Table 6.1 summarises the general trends observed in proxies from Elands Bay, the Cederberg and the tortoise isotope record. As seen in Table 6.1, the results from angulate tortoise bone are generally in agreement with previous paleoenvironmental studies from the west coast. The tortoise record does pick up a slight increase in moisture availability between 1 180-1 357 cal. BP, which is generally not recorded in other proxies. However, it is noted in the diatom record from Verlorenvlei (Stager *et al.* 2012). This indicates that the tortoise record is quite sensitive to change. Given the agreement seen between different proxies in this region and the sensitivity shown in the tortoise record, it is clear that Angulate tortoise shell from archaeological sites can be used as a proxy for paleoenvironmental reconstruction.

Table 6.1: Comparing general trends in proxies with trends in the tortoise record.

	Region		
Period	Elands Bay	Cederberg	Tortoise record
500 cal. BP	cool & moist	cool & moist	cool & moist
600-1 000 cal. BP	warm & dry	warm & dry	warm & dry
1 180-1 357 cal. BP	warm & dry	warm & dry	cool & moist
4 200- 5 000 cal. BP	warm & dry	warm & dry	warm & dry

Chapter Seven

Conclusions, critiques and future research

This study shows that stable carbon and nitrogen isotope values of tortoises, specifically angulate tortoises, can be used as a paleoenvironmental proxy. $\delta^{13}C$ and $\delta^{15}N$ values for angulate tortoise collagen show changes through time which match predictions based on palaeoclimatic changes inferred from existing proxies. The tortoise isotope record shows a cool and wet LIA, and an extreme arid event during the MCA. It also shows a cool moist period just before the MCA and a temperature increase between 4 005–5 270 cal. BP, at the start of the middle Holocene.

This adds significantly to the Holocene palaeoenvironmental proxy record. The presence of the LIA and unequivocal indication of the MCA seen in the tortoise record, is the first terrestrial indication for the two events in the archaeological record. Although the marine mollusc record indicates the presence of the LIA in the Elands Bay region, this is a proxy for sea surface temperature, rather than terrestrial temperature. Thus, the tortoise record adds to the existing record of paleoenvironmental conditions based on archaeological evidence from EBC, and provides a finer level of detail. The use of isotopes from tortoise shell will help in developing new paleorecords at other archaeological sites, or improving existing records.

However, the use of $\delta^{13}C$ and $\delta^{15}N$ of tortoise collagen in palaeoenvironmental reconstructions is limited by the same general constraints as in all studies based on collagen. That is, in hot and arid environments collagen degradation begins to occur quite soon after death and by 10 000 years little or none remains. Unfortunately, this was the case in this study: of the 59 samples taken from the early Holocene and terminal Pleistocene, only twelve yielded collagen. Seven of the twelve collagen extracts had C:N ratios outside the accepted

range of values, so that only five samples yielded usable results. Bone collagen is therefore not an ideal material for analysis of samples from the early Holocene and older.

One way of overcoming this problem would be to analyse bone apatite. Bone apatite has the advantage of surviving much longer into the archaeological record than collagen, although it has the disadvantage of being more susceptible to diagenetic changes. However, methods have been developed to remove the diagenetically altered components of bone apatite (Lee-Thorp *et al.*1989; Krueger, 1991). Whilst these treatments are not always successful, their effectiveness can be monitored e.g. by Fourier transform infrared spectroscopy (Wright & Schwarcz 1996). Thus, using bone apatite would be a possible avenue to explore in future research.

Another avenue for future research that has already been mentioned is to include more material from additional sites in the study area. This will enlarge the sample sizes in periods where these are limited, and allow better chronological coverage of the Holocene. This will enable us to achieve a finer scale reconstruction of past climate change. For example, both the sites of Spring Cave and Mike Taylors Midden have large tortoise assemblages that can be used to generate a proxy record for to 2 000 to 4 000 cal. BP (Jerardino 1997). Addition of these two sites to the study would be beneficial as there is a hiatus in the material at EBC and TC from 2 000 to 3000 cal. BP.

To conclude, $\delta^{13}C$ and $\delta^{15}N$ measured in collagen in tortoise shell make for an excellent late and middle Holocene paleoenvironmental proxy, that can and should be used at other archaeological sites. The tortoise record for the Elands Bay region shows clear evidence of climate change between 147–5 270 cal. BP, recording the presence of both the LIA and MCA. Lastly, this study could be improved by incorporating material from surrounding sites and future studies may benefit by using bone apatite as a source material.

References

Alexander, G. and Marais, J. 2007. *A guide to the reptiles of southern Africa*. Cape Town: Struik Publishers.

Ambrose, S.H.,1990. Preparation and characterization of bone and tooth collagen for isotopic analysis. *Journal of archaeological science*, 17(4): 431–451.

Ambrose, S.H. 1991. Effects of diet, climate and physiology on nitrogen isotope abundances in terrestrial foodwebs. *Journal of archaeological science*, 18(3): 293–317.

Ambrose SH (1993) Isotopic analysis of palaeodiets: methodological and interpretive considerations. In: Sanford MK (ed) Investigations of ancient human tissue: 59–130. Gordon and Breach, Langhorn.

Ambrose S.H., Norr L. (1993) Experimental Evidence for the Relationship of the Carbon Isotope Ratios of Whole Diet and Dietary Protein to Those of Bone Collagen and Carbonate. In: Lambert J.B., Grupe G. (eds). *Prehistoric Human Bon*e. Springer, Berlin, Heidelberg

Auffenberg, W. and Weaver, W.G. 1969. *Gopherus berlandieri in southeastern Texas*. Bull. Florida State Museum, 13: 141–203.

Avery, D.M. 1990. Holocene climatic change in Southern Africa: the contribution of micromammals to its study. *South African Journal of Science*, 86, 407–412.

Avery, G., Kandel, A.W., Klein, R.G., Conard, N.J., Cruz-Uribe, K. 2004. Tortoises as food and taphonomic elements in palaeo 'landscapes' In: Brugal, J-P and Desse, J. (eds). Petits *Animaux et Sociétés Humaines: du Complément Alimentaire aux Ressources Utilitaires*: 147–162. Antibes: Association Pour la Promotion et la Diffusion des Connaissances Archéologiques (APDCA).

Balasse, M., Smith, A.B., Ambrose, S.H. and Leigh, S.R. 2003. Determining sheep birth seasonality by analysis of tooth enamel oxygen isotope ratios: the Late Stone Age site of Kasteelberg (South Africa). *Journal of Archaeological Science*, 30(2): 205–215.

Balsamo, R.A., Hofmeyr, M.D., Henen, B.T. and Bauer, A.M. 2004. Leaf biomechanics as a potential tool to predict feeding preferences of the geometric tortoise Psammobates geometricus. *African Zoology*, 39(2): 175–181.

Bar-Matthews, M., Marean, C.W., Jacobs, Z., Karkanas, P., Fisher, E.C., Herries, A.I., Brown, K., Williams, H.M., Bernatchez, J., Ayalon, A. and Nilssen, P.J. 2010. A high resolution and continuous isotopic speleothem record of paleoclimate and paleoenvironment from 90 to 53 ka from Pinnacle Point on the south coast of South Africa. *Quaternary Science Reviews*, 29(17): 2131-2145.

Baxter, A.J. and Meadows, M.E. 1994. Palynological evidence for the impact of colonial settlement within lowland fynbos: A high- resolution study from the Verlorenvlei, southwestern Cape Province, South Africa. *Historical Biology*, 9(1-2): 61-70.

Baxter, A.J. and Meadows, M.E. 1999. Evidence for Holocene sea level change at verlorenvlei, western cape, South Africa. *Quaternary International*, 56(1): 65–79.

Bocherens, H. and Drucker, D. 2003. Trophic level isotopic enrichment of carbon and nitrogen in bone collagen: case studies from recent and ancient terrestrial ecosystems. *International Journal of Osteoarchaeology*, 13(1- 2): 46–53.

Boskey, A.L. 2013. Bone composition: relationship to bone fragility and antiosteoporotic drug effects. *BoneKEY reports*, 2: 477–502

Boycott, R.C. and Bourquin, O. 2000. The southern African tortoise book. *A Guide to southern African Tortoises, Terrapins and Turtles.* Hilton: O. Bourquin

Branch, W.R. 1984. Preliminary observations on the ecology of the angulate tortoise (*Chersina angulata*) in the Eastern Cape Province, South Africa. *Amphibia-Reptilia*, 5(1): 43–55.

Branch, W.R., Benn, G.A. and Lombard, A.T. 1995. The tortoises (*Testudinidae*) and terrapins (*Pelomedusidae*) of southern Africa: their diversity, distribution and conservation. *South African Journal of Zoology*, 30(3): 91–102.

Branch, W.R. 1998. *Field guide to snakes and other reptiles of southern Africa.* Cape Town: Struik Publishers.

Buffrénil, V. 1982. Morphogenesis of bone ornamentation in extant and extinct crocodilians. *Zoomorphology*, 99(2): 155–166.

Butzer, K.W. 1979. Geomorphology and geo-archeology at Elandsbaai Western Cape, South Africa. *Catena*, 6(2): 157–166.

Calvin, M. and Benson, A.A. 1948. *The path of carbon in photosynthesis*. Science 107: 476–480

Cartwright, C. and Parkington, J. 1997. The wood charcoal assemblages from Elands Bay Cave, southwestern Cape: principles, procedures and preliminary interpretation. *The South African Archaeological Bulletin*, 52: pp.59–72.

Cartwright, C.R., Porraz, G. and Parkington, J. 2016. The wood charcoal evidence from renewed excavations at Elands Bay Cave, South Africa. *Southern African Humanities*, 29(1): 249–258.

Caughley, G. and Sinclair, A.R.E. 1994. *Wildlife ecology and management*. Cambridge: Blackwell Science.

Caut, S., Angulo, E. and Courchamp, F. 2009. Variation in discrimination factors (Δ^{15}N and Δ^{13}C): the effect of diet isotopic values and applications for diet reconstruction. *Journal of Applied Ecology*, 46(2): 443–453.

Cebra- Thomas, J.A., Betters, E., Yin, M., Plafkin, C., McDow, K. and Gilbert, S.F. 2007. Evidence that a late- emerging population of trunk neural crest cells forms the plastron bones in the turtle Trachemys scripta. *Evolution & development*, 9(3): 267–277.

Cerling, T.E., Harris, J.M., MacFadden, B.J., Leakey, M.G., Quade, J., Eisenmann, V. and Ehleringer, J.R. 1997. Global vegetation change through the Miocene/Pliocene boundary. *Nature*, 389(6647): 153–158.

Cerling, T.E., Ehleringer, J.R. and Harris, J.M. 1998. Carbon dioxide starvation, the development of C4 ecosystems, and mammalian evolution. Philosophical Transactions of the Royal Society of London B: *Biological Sciences*, 353(1365): 159–171.

Cerling, T.E. and Harris, J.M. 1999. Carbon isotope fractionation between diet and bioapatite in ungulate mammals and implications for ecological and paleoecological studies. *Oecologia*, 120(3): 347–363.

Cerling, T.E., Harris, J.M. and Passey, B.H. 2003. Diets of East African *Bovidae* based on stable isotope analysis. *Journal of Mammalogy*, 84(2): 456–470.

Chase, B.M. and Meadows, M.E. 2007. Late Quaternary dynamics of southern Africa's winter rainfall zone. *Earth-Science Reviews*, 84(3): 103–138.

Chase, B.M., Quick, L.J., Meadows, M.E., Scott, L., Thomas, D.S. and Reimer, P.J. 2011. Late glacial interhemispheric climate dynamics revealed in South African hyrax middens. *Geology*, 39(1): 19–22.

Chase, B.M., Scott, L., Meadows, M.E., Gil-Romera, G., Boom, A., Carr, A.S., Reimer, P.J., Truc, L., Valsecchi, V. and Quick, L.J. 2012. Rock hyrax middens: a palaeoenvironmental archive for southern African drylands. *Quaternary Science Reviews*, 56: 107–125.

Chase, B.M., Lim, S., Chevalier, M., Boom, A., Carr, A.S., Meadows, M.E. and Reimer, P.J. 2015. Influence of tropical easterlies in southern Africa's winter rainfall zone during the Holocene. Quaternary Science Reviews, 107: 138–148.

Clark, K., Bender, G., Murray, B.P., Panfilio, K., Cook, S., Davis, R., Murnen, K., Tuan, R.S. and Gilbert, S.F. 2001. Evidence for the neural crest origin of turtle plastron bones. *Genesis*, 31(3): 111–117.

Cleland, T.P., Voegele, K. and Schweitzer, M.H. 2012. Empirical evaluation of bone extraction protocols. *PLoS One*, 7(2): 31443.

Cohen, A.L., Parkington, J.E., Brundrit, G.B. and van der Merwe, N.J. 1992. A Holocene marine climate record in mollusc shells from the southwest African coast. Quaternary Research, 38(3): 379–385.

Compton, J.S. 2001. Holocene sea-level fluctuations inferred from the evolution of depositional environments of the southern Langebaan Lagoon salt marsh, South Africa. *The Holocene*, 11(4): 395–405.

Cowling, R.M., Cartwright, C.R., Parkington, J.E. and Allsopp, J.C. 1999. Fossil wood charcoal assemblages from Elands Bay Cave, South Africa: implications for Late Quaternary vegetation and climates in the winter- rainfall fynbos biome. *Journal of Biogeography*, 26(2): 367–378.

Dansgaard, W., Johnsen, S.J., Clausen, H.B., Dahl-Jensen, D., Gundestrup, N.S., Hammer, C.U., Hvidberg, C.S., Steffensen, J.P., Sveinbjörnsdottir, A.E., Jouzel, J. and Bond, G. 1993. Evidence for general instability of past climate from a 250-kyr ice-core record. *Nature*, 364(6434): 218–220.

DeNiro, M.J. and Epstein, S. 1981. Influence of diet on the distribution of nitrogen isotopes in animals. *Geochimica et cosmochimica acta*, 45(3): 341–351.

DeNiro, M.J., 1985. Postmortem preservation and alteration of in vivo bone collagen isotope ratios in relation to palaeodietary reconstruction. *Nature*, 317(6040): 806–809.

Diefendorf, A.F., Mueller, K.E., Wing, S.L., Koch, P.L. and Freeman, K.H. 2010. Global patterns in leaf ^{13}C discrimination and implications for studies of past and future climate. *Proceedings of the National Academy of Sciences*, 107(13): 5738–5743.

Dinacauze, D.F. 2000. *Environmental Archaeology, Principales and Practice*. Cambridge: Cambridge University.

Ehleringer, J.R., Cerling, T.E. and Helliker, B.R. 1997. C4 photosynthesis, atmospheric CO2, and climate. *Oecologia*, 112(3): 285–299.

Ehleringer, J.R., Sage, R.F., Flanagan, L.B. and Pearcy, R.W. 1991. Climate change and the evolution of C_4 photosynthesis. *Trends in Ecology & Evolution*, 6(3): 95–99.

Ehleringer, J.R. and Cerling, T.E. 2002. C_3 and C_4 photosynthesis. *Encyclopedia of global environmental change*, 2: 186–190.

Germano, D.J. 1998. Scutes and age determination of desert tortoises revisited. *Copeia*, 1998(2): 482–484.

Gilbert, S.F., Cebra–Thomas, J.A., Burke, A. 2007a. How the turtle gets its Shell In: Wyneken, J., Godfrey, M.H. and Bels, V. (eds). 2007. *Biology of Turtles: From Structures to Strategies of Life*. Boca Raton: CRC Press.

Gilbert, S.F., Bender, G., Betters, E., Yin, M. and Cebra-Thomas, J.A. 2007b. The contribution of neural crest cells to the nuchal bone and plastron of the turtle shell. *Integrative and Comparative Biology*, 47(3): 401–408.

Godley, B.J., Thompson, D.R., Waldron, S. and Furness, R.W. 1998. The trophic status of marine turtles as determined by stable isotope analysis. *Marine Ecology Progress Series*, 166: 277–284.

Grieg, J.C and Burdett, P.D. 1976. Patterns in the distribution of southern African terrestrial tortoises (Cryptodira: Testudinidae). *Zool. Africana ll* (2): 249–273.

Gröcke, D.R., Bocherens, H. and Mariotti, A. 1997. Annual rainfall and nitrogen-isotope correlation in macropod collagen: application as a palaeoprecipitation indicator. *Earth and Planetary Science Letters*, 153(3–4): 279–285.

Halkett, D., Hart, T., Yates, R., Volman, T.P., Parkington, J.E., Orton, J., Klein, R.G., Cruz-Uribe, K. and Avery, G. 2003. First excavation of intact Middle Stone Age layers at Ysterfontein, Western Cape Province, South Africa: implications for Middle Stone Age ecology. *Journal of Archaeological Science*, 30(8): 955–971.

Handley, L.L., Austin, A.T., Stewart, G.R., Robinson, D., Scrimgeour, C.M., Raven, J.A. and Schmidt, S. 1999. The ^{15}N natural abundance ($\delta^{15}N$) of ecosystem samples reflects measures of water availability. *Functional Plant Biology*, 26(2):185–199.

Hartman, G. and Danin, A. 2010. Isotopic values of plants in relation to water availability in the Eastern Mediterranean region. *Oecologia*, 162(4): 837–852.

Heaton, T.H., Vogel, J.C., von La Chevallerie, G. and Collett, G. 1986. Climatic influence on the isotopic composition of bone nitrogen. *Nature*, 322(6082): 822–823.

Heaton, T.H. 1987. The $^{15}N/^{14}N$ ratios of plants in South Africa and Namibia: relationship to climate and coastal/saline environments. *Oecologia*, 74: 236–246.

Henshilwood, C., Nilssen, P. and Parkington, J. 1994. Mussel drying and food storage in the Late Holocene, SW Cape, South Africa. *Journal of Field Archaeology*, 21(1): 103–109.

Henshilwood, C.S. 2008. Winds of change: palaeoenvironments, material culture and human behaviour in the Late Pleistocene (c. 77 – 48 ka) in the Western Cape Province, South Africa. *South African Archaeological Society Goodwin Series* 10: 1–17

Henshilwood, C.S., Sealy, J.C., Yates, R., Cruz-Uribe, K., Goldberg, P., Grine, F.E., Klein, R.G., Poggenpoel, C., Van Niekerk, K. and Watts, I. 2001. Blombos Cave, southern Cape, South Africa: preliminary report on the 1992–1999 excavations of the Middle Stone Age levels. *Journal of Archaeological Science*, 28(4): 421–448.

Hobbie, E.A., Macko, S.A. and Williams, M. 2000. Correlations between foliar $\delta^{15}N$ and nitrogen concentrations may indicate plant-mycorrhizal interactions. *Oecologia*, 122(2): 273-283.

Hoefs, J. 2009. Theoretical and experimental principles. In: Hoefs, J. (eds). *Stable Isotope Geochemistry*: 1–33. Berlin: Springer.

Hofmeyr, M.D., 2009. Chersina angulata (Schweigger 1812) - angulate tortoise, South African bowsprit tortoise. In: Rhodin, A.G.J., Pritchard, P.C.H., van Dijk, P.P., Sumure, R.A., Buhlmann, K.A., Iverson, J.B., Mittermeier, R.A. (eds.). *Conservation Biology of Freshwater Turtles and Tortoises: a Compilation Project of the IUCN/SSC Tortoise and Freshwater*: 31-36. Turtle Specialist Group Chelonian Research Foundation.

Iglesias, A.A., González, D.H. and Andreo, C.S. 1986. The C_4 pathway of photosynthesis and its regulation. *Biochemical Education*, 14(3): 98–102.

Jerardino, A. 1995. The problem with density values in archaeological analysis: a case study from Tortoise Cave, Western Cape, South Africa. *The South African Archaeological Bulletin*, 60(161): 21–27.

Jerardino, A. and Yates, R., 1997. Excavations at Mike Taylor's Midden: a summary report and implications for a re-characterisation of megamiddens. *The South African Archaeological Bulletin*, 52(165): 43–51.

Johnson, M. 2011. *Archaeological theory: an introduction*. Chichester: John Wiley & Sons.

Jones, P.D. and Mann, M.E. 2004. Climate over past millennia. *Reviews of Geophysics*, 42(2): 1–42

Joshua, Q.I., Hofmeyr, M.D., Henen, B.T. and Weitz, F.M. 2005. Seasonal changes in the vegetation of island and mainland habitats of angulate tortoises in the Western Cape, South

Africa: NRF/Royal Society programme. *South African journal of science*, 101(9–10): 439–445.

Joshua, Q.I., Hofmeyr, M.D. and Henen, B.T. 2010. Seasonal and site variation in angulate tortoise diet and activity. *Journal of Herpetology*, 44(1): 124–134.

Klein, R.G. and Cruz-Uribe, K. 1983. Stone age population numbers and average tortoise size at Byneskranskop Cave 1 and Die Kelders Cave 1, southern Cape Province, South Africa. *The South African Archaeological Bulletin*, 38(137) 26–30.

Klein, R.G. and Cruz-Uribe, K. 1987. Large mammal and tortoise bones from Eland's Bay Cave and nearby sites, Western Cape Province, South Africa. *Papers in the prehistory of the western Cape, South Africa*, 1. International Series 332. Oxford: B.A.R.: 132–63

Klein, R.G. and Cruz-Uribe, K. 1989. Faunal evidence for prehistoric herder-forager activities at Kasteelberg, Western Cape Province, South Africa. *The South African Archaeological Bulletin*, 44: 82–97.

Klein, R.G. 1991. Size variation in the Cape dune molerat (*Bathyergus suillus*) and Late Quaternary climatic change in the southwestern Cape Province, South Africa. *Quaternary Research*, 36(3): 243–256.

Klein, R.G. and Cruz-Uribe, K., 2000. Middle and later stone age large mammal and tortoise remains from Die Kelders Cave 1, Western Cape Province, South Africa. *Journal of Human Evolution*, 38(1): 169–195.

Klein, R.G. and Cruz-Uribe, K. 2016. Large mammal and tortoise bones from Elands Bay Cave (South Africa): implications for Later Stone Age environment and ecology. *Southern African Humanities*, 29(1): 259–282.

Krueger, H.W. 1991. Exchange of carbon with biological apatite. *Journal of Archaeological Science*, 18(3): 355–361.

Laing, A.G. and Fritsch, J.M. 1993. Mesoscale convective complexes in Africa. *Monthly Weather Review*, 121(8): 2254–2263.

Larsen, C.S. 2015. *Bioarchaeology: interpreting behaviour from the human skeleton*: Cambridge: Cambridge University Press.

Lee, R.B. 1968. What hunters do for a living, or, how to make out on scarce resources. In: Lee, R.B. & DeVore, I. (eds) *Man the Hunter*: 30–48. Chicago: Aldine

Lee-Thorp, J. and Sponheimer, M. 2003. Three case studies used to reassess the reliability of fossil bone and enamel isotope signals for paleodietary studies. *Journal of Anthropological Archaeology*, 22(3): 208–216.

Lee-Thorp, J.A., Sealy, J.C. and van Der Merwe, N.J. 1989. Stable carbon isotope ratio differences between bone collagen and bone apatite, and their relationship to diet. *Journal of archaeological science*, 16(6): 585–599

Lee-Thorp, J.A. 2008. On isotopes and old bones. *Archaeometry*, 50(6): 925–950.

Luckman, B.H. 1997. Developing a proxy climate record for the last 300 years in the Canadian Rockies—some problems and opportunities. *Clim Change*, 36:455–476.

Luyt, J., Lee-Thorp, J.A. and Avery, G. 2000. New light on Middle Pleistocene west coast environments from Elandsfontein, Western Cape Province, South Africa. *South African Journal of Science, 96*(7): 399–403

Mann, M.E., Zhang, Z., Rutherford, S., Bradley, R.S., Hughes, M.K., Shindell, D., Ammann, C., Faluvegi, G. and Ni, F. 2009. Global signatures and dynamical origins of the Little Ice Age and Medieval Climate Anomaly. *Science,* 326(5957): 1256–1260.

Marshall, J.D., J. Brooks, R., and Lajtha, K. 2007. Sources of variation in the stable isotopic composition of plants. In: Michener, R. & Lajtha, K. (eds). *Stable Isotopes in Ecology and Environmental Science 2*: 22–60. Oxford: Blackwell Publishing.

Mayewski, P.A., Rohling, E.E., Stager, J.C., Karlén, W., Maasch, K.A., Meeker, L.D., Meyerson, E.A., Gasse, F., van Kreveld, S., Holmgren, K. and Lee-Thorp, J. 2004. Holocene climate variability. *Quaternary research*, 62(3): 243–255.

Meadows, M.E. and Sugden, J.M. 1993. The late Quaternary palaeoecology of a floristic kingdom: the southwestern Cape South Africa. *Palaeogeography, Palaeoclimatology, Palaeoecology*, 101(3): 271–281.

Meadows, M.E., Baxter, A.J. and Parkington, J. 1996. Late Holocene environments at Verlorenvlei, Western Cape Province, South Africa. *Quaternary International*, 33: 81–95.

Meadows, M.E. and Baxter, A.J. 1999. Late Quaternary palaeoenvironments of the southwestern Cape, South Africa: a regional synthesis. *Quaternary International*, 57: 193–206.

Meadows, M.E. and Baxter, A.J. 2001. Holocene vegetation history and palaeoenvironments at Klaarfontein Springs, Western Cape, South Africa. *The Holocene*, 11(6): 699-706.

Meadows, M.E., Chase, B.M. and Seliane, M. 2010. Holocene palaeoenvironments of the Cederberg and Swartruggens mountains, Western Cape, South Africa: pollen and stable isotope evidence from hyrax dung middens. Journal of arid environments, 74(7): 786–793.

Miller, D.E., Yates, R.J., Jerardino, A., Parkington, J.E. 1995. Late Holocene Coastal Change in the Southwestern Cape, South Africa. *Quaternary International*, 29/30: 3–10.

Mucina, L. & Rutherford, M.C. (eds) 2010. (CD Set). i. Pretoria: South African National Biodiversity Institute.

Mucina, L., Adams, J.B., Knevel, I.C., Rutherford, M.C., Powrie, L.W., Bolton, J.J., van der Merwe, J.H., Anderson, R.J., Bornman, T.G., le Roux, A. and Janssen, J.A. 2006. Coastal vegetation of South Africa. In: Mucina, L. and Rutherford, M.C (eds). *The vegetation of South Africa, Lesotho and Swaziland*: 658–583. Pretoria: South African National Biodiversity Institute

Münch, Z. and Conrad, J. 2007. Remote sensing and GIS based determination of groundwater dependent ecosystems in the Western Cape, South Africa. *Hydrogeology Journal*, 15(1): 19–28.

Murphy, B.P. and Bowman, D.M. 2006. Kangaroo metabolism does not cause the relationship between bone collagen $\delta^{15}N$ and water availability. *Functional Ecology*, 20(6): 1062–1069.

Murphy, B.P. and Bowman, D.M. 2009. The carbon and nitrogen isotope composition of Australian grasses in relation to climate. *Functional Ecology*, 23(6):1040–1049.

Murray, I.W. and Wolf, B.O. 2012. Tissue carbon incorporation rates and diet-to-tissue discrimination in ectotherms: tortoises are really slow. *Physiological and Biochemical Zoology*, 85(1): 96–105.

Nagy, K.A. and Medica, P.A. 1986. Physiological ecology of desert tortoises in southern Nevada. *Herpetologica*, 42(1): 73–92.

Nielsen-Marsh, C.M. and Hedges, R.E. 2000. Patterns of diagenesis in bone I: the effects of site environments. *Journal of Archaeological Science*, 27(12): 1139–1150.

National Oceanic and Atmospheric Administration.2016. Paleoclimatology data map. Available at: https://gis.ncdc.noaa.gov/maps/ncei/paleo?layers=0010101000101001

O'Leary, M.H. 1981. Carbon isotope fractionation in plants. *Phytochemistry*, 20(4): 553–567.

Parkington, J.E. 1972. Seasonal mobility in the late stone age. *African Studies*, 31(4): 223–244.

Parkington, J. 1976. Coastal settlement between the mouths of the Berg and Olifants Rivers, Cape Province. *The South African Archaeological Bulletin*, 31(123/124); 127–140.

Parkington, J.E. 1992. Making sense of sequence at the Elands Bay cave, western Cape, South Africa. *Guide to archaeological sites in the south-western Cape*, 6: 12–28.

Parkington, J., Cartwright, C., Cowling, R.M., Baxter, A. and Meadows, M. 2000. Palaeovegetation at the last glacial maximum in the western Cape, South Africa: wood charcoal and pollen evidence from Elands Bay Cave. *South African Journal of Science*, 96(11): 543–546.

Parkington, J. 2016. Elands Bay Cave: keeping an eye on the past. *Southern African Humanities*, 29(1): 17–32.

Passey, B.H., Robinson, T.F., Ayliffe, L.K., Cerling, T.E., Sponheimer, M., Dearing, M.D., Roeder, B.L. and Ehleringer, J.R. 2005. Carbon isotope fractionation between diet, breath CO_2, and bioapatite in different mammals. *Journal of Archaeological Science*, 32(10): 1459–1470.

Pate, F.D. and Anson, T.J. 2008. Stable nitrogen isotope values in arid- land kangaroos correlated with mean annual rainfall: Potential as a palaeoclimatic indicator. *International Journal of Osteoarchaeology*, 18(3): 317–326.

Pestle, W.J. 2010. Chemical, elemental, and isotopic effects of acid concentration and treatment duration on ancient bone collagen: an exploratory study. *Journal of Archaeological Science*, 37(12): 3124–3128.

Pidwirny, M. 2006. *The Nitrogen Cycle. Fundamentals of Physical Geography*. Okanagan: University of British Columbia.

Poggenpoel, C.A. 1996. The exploitation of fish during the Holocene in the South-Western Cape, South Africa. Unpublished PhD dissertation. Cape Town: University of Cape Town.

Quick, L.J., Chase, B.M., Meadows, M.E., Scott, L. and Reimer, P.J. 2011. A 19.5 kyr vegetation history from the central Cederberg Mountains, South Africa: palynological evidence from rock hyrax middens. *Palaeogeography, Palaeoclimatology, Palaeoecology*, 309(3): 253–270.

Ranson, S.L. and Thomas, M. 1960. Crassulacean acid metabolism. *Annual Review of Plant Physiology*, 11(1): 81–110.

Rebelo, A.G., Boucher, C., Helme, N., Mucina, L. and Rutherford, M.C. 2006. Fynbos Biome. In: Mucina, L. and Rutherford, M.C (eds). *The Vegetation of South Africa, Lesotho and Swaziland*: 55–206. Pretoria: South African National Biodiversity Institute.

Reich, K.J., Bjorndal, K.A. and Del Rio, C.M. 2008. Effects of growth and tissue type on the kinetics of ^{13}C and ^{15}N incorporation in a rapidly growing ectotherm. *Oecologia*, 155(4): 651–663.

Robey, T. 1987. The stratigraphic and cultural sequence at Tortoise Cave, Verlorenvlei. In Papers in the prehistory of the western Cape, South Africa, *Oxford: British Archaeological Reports*, 332: 294–325.

Sage, R.F. 2004. The evolution of C_4 photosynthesis. *New phytologist*, 161(2): 341–370.

Sampson, C.G. 2000. Taphonomy of tortoises deposited by birds and Bushmen. *Journal of Archaeological Science*, 27(9): 779–788.

Scheyer, T.M. and Sander, P.M. 2004. Histology of ankylosaur osteoderms: implications for systematics and function. *Journal of Vertebrate Paleontology*, 24(4): 874–893.

Scheyer, T.M. 2007. Skeletal histology of the dermal armor of Placodontia: the occurrence of 'postcranial fibro-cartilaginous bone'and its developmental implications. *Journal of Anatomy*, 211(6): 737–753.

Schmitt, J., Schneider, R., Elsig, J., Leuenberger, D., Lourantou, A., Chappellaz, J., Köhler, P., Joos, F., Stocker, T.F., Leuenberger, M. and Fischer, H. 2012. Carbon isotope constraints on the deglacial CO_2 rise from ice cores. *Science*, 336(6082): 711–714.

Schoeninger, M.J., Moore, K.M., Murray, M.L. and Kingston, J.D. 1989. Detection of bone preservation in archaeological and fossil samples. *Applied Geochemistry*, 4(3): 281–292.

Schwarcz, H.P. and Schoeninger, M.J. 1991. Stable isotope analyses in human nutritional ecology. *American Journal of Physical Anthropology*, 34(S13): 283–321.

Scott, L. and Woodborne, S. 2007a. Vegetation history inferred from pollen in Late Quaternary faecal deposits (hyraceum) in the Cape winter-rain region and its bearing on past climates in South Africa. Quaternary Science Reviews, 26(7); 941–953.

Scott, L. and Woodborne, S. 2000b. Pollen analysis and dating of Late Quaternary faecal deposits (hyraceum) in the Cederberg, Western Cape, South Africa. *Review of Palaeobotany and Palynology*, 144(3); 123–134.

Sealy, J.C., 1984. Stable carbon isotopic assessment of prehistoric diets in the south-western Cape, South Africa. Unpublished Masters degree. Cape Town: University of Cape Town.

Sealy, J.C., Van Der Merwe, N.J., Thorp, J.A.L. and Lanham, J.L. 1987. Nitrogen isotopic ecology in southern Africa: implications for environmental and dietary tracing. *Geochimica et Cosmochimica Acta*, 51(10): 2707–2717.

Sealy, J., Johnson, M., Richards, M. and Nehlich, O. 2014. Comparison of two methods of extracting bone collagen for stable carbon and nitrogen isotope analysis: comparing whole bone demineralization with gelatinization and ultrafiltration. *Journal of Archaeological Science*, 47: 64–69.

Seminoff, J.A., Jones, T.T., Eguchi, T., Jones, D.R. and Dutton, P.H. 2006. Stable isotope discrimination ($\delta^{13}C$ and $\delta^{15}N$) between soft tissues of the green sea turtle Chelonia mydas and its diet. *Marine Ecology Progress Series*, 308: 271–278.

Sponheimer, M., Robinson, T.F., Roeder, B.L., Passey, B.H., Ayliffe, L.K., Cerling, T.E., Dearing, M.D. and Ehleringer, J.R. 2003. An experimental study of nitrogen flux in llamas: is ^{14}N preferentially excreted? *Journal of Archaeological Science*, 30(12): 1649–1655.

Stager, J.C., Mayewski, P.A., White, J., Chase, B.M., Neumann, F.H., Meadows, M.E., King, C.D. and Dixon, D.A. 2012. Precipitation variability in the winter rainfall zone of South Africa during the last 1400 yr linked to the austral westerlies. *Climate of the Past*, 8(3): 877–887.

Steele, T.E. and Klein, R.G. 2013. The Middle and Later Stone Age faunal remains from Diepkloof Rock Shelter, Western Cape, South Africa. *Journal of Archaeological Science*, 40(9): 3453–3462.

Still, C.J., Berry, J.A., Collatz, G.J. and DeFries, R.S. 2003. Global distribution of C_3 and C_4 vegetation: carbon cycle implications. *Global Biogeochemical Cycles*, 17(1): 6–14.

Stowe, M.J. and Sealy, J. 2016. Terminal Pleistocene and Holocene dynamics of southern Africa's winter rainfall zone based on carbon and oxygen isotope analysis of bovid tooth enamel from Elands Bay Cave. *Quaternary International*, 404: 57–67.

Sulzman, E.W. 2007. Stable isotope chemistry and measurement: a primer. In: Michener, R. & Lajtha, K. (eds). *Stable Isotopes in Ecology and Environmental Science 2*: 1–18. Oxford: Blackwell Publishing

Swap, R.J., Aranibar, J.N., Dowty, P.R., Gilhooly, W.P. and Macko, S.A. 2004. Natural abundance of ^{13}C and ^{15}N in C_3 and C_4 vegetation of southern Africa: patterns and implications. *Global Change Biology*, 10(3): 350–358.

Talma, A.S. and Vogel, J.C. 1992. Late Quaternary paleotemperatures derived from a speleothem from Cango caves, Cape province, South Africa. *Quaternary Research*, 37(2): 203–213.

Thompson, J.C. and Henshilwood, C.S. 2014a. Tortoise taphonomy and tortoise butchery patterns at Blombos Cave, South Africa. *Journal of Archaeological Science*, 41: 214–229.

Thompson, J.C. and Henshilwood, C.S. 2014b. Nutritional values of tortoises relative to ungulates from the Middle Stone Age levels at Blombos Cave, South Africa: Implications for foraging and social behaviour. *Journal of human evolution*, 67: 33–47.

Thomson, J.S. 1932. *The anatomy of the tortoise*. Dublin: Royal Dublin Society.

Tuross, N. 2012. Comparative decalcification methods, radiocarbon dates, and stable isotopes of the VIRI bones. *Radiocarbon*, 54(3-4): 837–844.

Tuross, N., Behrensmeyer, A.K., Eanes, E.D., Fisher, L.W. and Hare, P.E. 1989. Molecular preservation and crystallographic alterations in a weathering sequence of wildebeest bones. *Applied Geochemistry*, 4(3): 261–270.

Tyson, P.D., Karlen, W., Holmgren, K. and Heiss, G.A., 2000. The Little Ice Age and medieval warming in South Africa. *South African Journal of Science*, *96*(3):121–126

van der Merwe, N.J. and Medina, E. 1991. The canopy effect, carbon isotope ratios and foodwebs in Amazonia. *Journal of Archaeological Science*, 18(3): 249–259.

van Klinken, G.J. 1999. Bone collagen quality indicators for palaeodietary and radiocarbon measurements. *Journal of Archaeological Science*, 26(6): 687–695.

Vogel, J.C., Fuls, A. and Ellis, R.P. 1978. Geographical distribution of Kranz grasses in South Africa. *South African Journal of Science*, 74: 209–215.

Walker, M.J., Berkelhammer, M., Björck, S., Cwynar, L.C., Fisher, D.A., Long, A.J., Lowe, J.J., Newnham, R.M., Rasmussen, S.O. and Weiss, H. 2012. Formal subdivision of the Holocene Series/Epoch: a Discussion Paper by a Working Group of INTIMATE (Integration of ice- core, marine and terrestrial records) and the Subcommission on Quaternary Stratigraphy (International Commission on Stratigraphy). *Journal of Quaternary Science*, *27*(7): 649–659.

Weeber, J. 2013. Investigating the potential of stable carbon and nitrogen isotopes in tortoise bones as a palaeoenvironmental proxy. Unpublished Honours degree. Cape Town: University of Cape Town.

Woodborne, S., Hall, G., Robertson, I., Patrut, A., Rouault, M., Loader, N.J. and Hofmeyr, M. 2015. A 1000-year carbon isotope rainfall proxy record from South African baobab trees (Adansonia digitata L.). *PloS one*, 10(5): 124–202.

Wright, L.E. and Schwarcz, H.P. 1996. Infrared and isotopic evidence for diagenesis of bone apatite at Dos Pilas, Guatemala: palaeodietary implications. *Journal of Archaeological Science*, 23(6): 933–944.